

# **Apoptosis and cell cycle regulation in a basal model system**

## **- Insights from the placozoan *Trichoplax adhaerens***

Von der Naturwissenschaftlichen Fakultät der  
Gottfried Wilhelm Leibniz Universität Hannover

zur Erlangung des Grades  
Doktorin der Naturwissenschaften (Dr. rer. nat.)

genehmigte Dissertation

von

Sarah Rolfes, M.Sc.

2020

Referent: Prof. Dr. Bernd Schierwater

Koreferent: Prof. Dr. Dieter Steinhagen

Tag der Promotion: 09.07.2020

*This thesis is dedicated to my parents, Bärbel and Georg Rolfes*

## Zusammenfassung

Masterkontrollgene sind essentiell für das Zusammenspiel und die Regulation grundlegender molekularer und zellulärer Prozesse in Metazoen. Da sie komplexe Gennetzwerke kontrollieren, hat ihre Fehlfunktion in vielen Fällen dramatische Auswirkungen auf den Organismus und wird mit Krankheiten wie Krebs assoziiert. Im Rahmen dieser Arbeit wurden die zwei Masterkontrollgene p53 und Myc in *Trichoplax adhaerens* (Tierstamm Placozoa) umfassend untersucht. Zusätzlich eröffnen sich mit der neu beschriebenen Art, *Polyplacotoma mediterranea*, weitere vielversprechende Möglichkeiten für funktionelle und vergleichende Studien.

Die wohl bekannteste Funktion des Tumorsuppressors p53, ist die Regulation des programmierten Zelltods (Apoptose). In dieser Arbeit wurden funktionelle und vergleichende genetische Studien an dem p53-Homolg tap53 in *T. adhaerens* durchgeführt. Sowohl die Anreicherung von tap53 *in vivo*, durch die Inhibition der tap53-taMdm2 Interaktion, als auch der tap53 Knockdown, führten zu einer Zunahme apoptotischer Zellen und war letal für die Versuchstiere. Nach dem tap53 Knockdown konnten durch Transkriptomanalysen Interaktionspartner von tap53 identifiziert werden, die auf einen alternativen, p53-unabhängigen Apoptosemechanismus hinweisen. Des Weiteren wurden differentiell exprimierte Gene gefunden, die zum angeborenen Immunsystem und zur zellulären Stressantwort gehören. Diese Ergebnisse unterstützen die Hypothese, dass tap53 entscheidende Funktionen in *Trichoplax* übernimmt und somit essentiell für das Überleben der Tiere ist.

Als Transkriptionsfaktoren regulieren Myc und sein wichtigster Interaktionspartner Max eine Vielzahl zellulärer Mechanismen. Dazu zählen Proliferation, Differenzierung und die Kontrolle des Zellzyklus. Die in dieser Arbeit durchgeführten Studien an den Volllängenproteinen taMyc und taMax von *T. adhaerens*, gaben erste Einblicke in die Proteinstruktur und ihre Interaktion. Die Dimerisierung der Volllängenproteine taMyc und taMax konnte mit unterschiedlichen Methoden gezeigt werden. Dies ist der erste Schritt, um funktional an DNA binden zu können. Die Ergebnisse lassen darauf

schließen, dass taMyc und taMax eine wesentliche Rolle als Transkriptionsfaktoren in *Trichoplax* zukommt und ihre Funktionen im Laufe der Evolution konserviert blieb.

Diese Arbeit liefert neue und wichtige Erkenntnisse bezüglich der Funktionen und Eigenschaften der regulatorischen Netzwerke von p53 und Myc/Max in dem einfachsten Mehrzeller. Damit bildet sie eine Grundlage für zukünftige medizinische Forschung an zellulären Regulationsprozessen.

Stichworte: Placozoa, p53, Myc/Max, Transkriptionsfaktoren, Apoptose, Zellzyklus

## Abstract

Complex gene networks regulated by master control genes are critical for the coordination of fundamental molecular and cellular processes in metazoans. Their malfunction might cause severe diseases like cancer. In this thesis, two evolutionary highly conserved master control genes, namely p53 and Myc, have been comprehensively analyzed in the simple metazoan model system *Trichoplax adhaerens* (phylum Placozoa). Additionally, the newly described species, *Polyplacotoma mediterranea*, will provide further promising possibilities for functional and comparative studies.

The tumor suppressor p53 is well known for the regulation of programmed cell death (apoptosis), but also controls the cell metabolism and cell cycle. In this work, functional and comparative genetic studies on the p53 homolog tap53 have been performed in *T. adhaerens*. The *in vivo* accumulation of tap53 by inhibiting the tap53-taMdm2 interaction as well as the tap53 knockdown resulted in a significant increase of apoptotic cells and an increased mortality. Furthermore, multiple tap53 interaction partners identified by transcriptomic analyses after tap53 knockdown suggest the existence of an alternative and tap53-independent apoptosis signaling pathway. Genes belonging to the innate immune system and the cellular stress response were likewise found differentially expressed in response to tap53 knockdown. These results suggest that tap53 fulfills multiple crucial functions in *Trichoplax* and is essential for the survival of the organism.

As transcription factors, Myc and its most important interaction partner Max regulate cellular processes and mechanisms such as differentiation, proliferation and the cell cycle. The biochemical studies carried out in the course of this thesis on the full-length proteins taMyc and taMax of *T. adhaerens* provided first insight on their protein structure and interaction. Using different methods, dimerization of full-length proteins was demonstrated which is a prerequisite for functional DNA binding capabilities. This suggests that taMyc and taMax play an essential role as transcription

factors in *Trichoplax* and support an evolutionary conserved function throughout metazoans.

This thesis provides new important insights on the function and characteristics of p53 and Myc/Max regulatory networks in a simple metazoan and is the base for future applied medical research on cellular regulation processes.

Keywords: Placozoa, p53, Myc/Max, transcription factors, apoptosis, cell cycle

# Contents

	List of Figures	ix
	List of Tables	x
	Abbreviations	xi
1	Introduction	14
2	Experimental studies	28
	Chapter I Inhibitors of the p53-Mdm2 interaction increase programmed cell death and produce abnormal phenotypes in the placozoan <i>Trichoplax adhaerens</i> (F.E. Schulze).	29
	Chapter II <i>Polyplacotoma mediterranea</i> is a new ramified placozoan species.	30
	Chapter III The role of p53 in the regulation of apoptosis in the placozoan <i>Trichoplax adhaerens</i> .	31
	Chapter IV New insights into the protein biochemistry of Myc and Max in the placozoan <i>Trichoplax adhaerens</i> .	51
3	Discussion	71
A	Appendix	78
A.1	The role of p53 in the regulation of apoptosis in the placozoan <i>Trichoplax adhaerens</i> . (Chapter III)	79
A.2	New insights into the protein biochemistry of Myc and Max in the placozoan <i>Trichoplax adhaerens</i> . (Chapter IV)	89
	Curriculum Vitae	99
	List of Publications	101
	Acknowledgements	102



## List of Figures

1.1	Placozoan morphology	15
1.2	p53-dependent apoptosis: the intrinsic and the extrinsic pathway	17
1.3	Structures of Myc/Max dimerization	19
2.1	Time course of population and body size after tap53 knockdown	38
2.2	Phenotypic variability in <i>Trichoplax</i> specimen after tap53 knockdown	39
2.3	TUNEL staining 21 h after tap53 knockdown	40
2.4	Comparison of differentially expressed genes	42
2.5	Alignment of amino acid sequences of <i>Trichoplax</i> taMyc and taMax proteins with their homologs from human, chicken and <i>Hydra</i>	58
2.6	Expression of taMyc and taMax proteins	59
2.7	Disorder probabilities of taMyc and taMax	61
2.8	Far-ultraviolet circular dichroism of 6His-YFP-taMyc.	63
2.9	Sedimentation of 6His-YFP-taMyc:6His-taMax heterodimers and 6His-YFP-taMyc and 6His-taMax monomers by analytical ultracentrifugation	64
2.10	6His-YFP-taMyc:6His-taMax interaction measured by microscale thermophoresis	65
A1.1	Live image of transfected animals	78
A1.2	Semi-quantitative PCR after tap53 knockdown	78

## List of Tables

2.1	Assembly and reference transcriptome statistics	41
2.2	Comparison of differentially expressed genes	42
2.3	Proteins belonging to the apoptosis pathway, innate immunity system and stress response were found DE after tap53 knockdown	45
2.4	Ratio of secondary structures within the 6His-YFP-taMyc protein	63
A1.1	Sequences of primer sets used in Chapter III	79
A1.2	Sequences of RNAi probes	79
A1.3	Raw data of animals' population sizes after tap53 knockdown	80
A1.4	Statistics of animals' body sizes after knockdown	81
A1.5	Raw data obtained from TUNEL staining after knockdown	82
A1.6	Statistics on all differentially expressed genes after tap53 knockdown in a tap53 vs IF comparison	83
A1.7	Statistics on all differentially expressed genes after tap53 knockdown in a tap53 vs ITS comparison	84
A1.8	All identified proteins from differentially expressed genes after tap53 knockdown	86
A2.1	Primer sequences for gene amplification and cloning into pET23a-YFP and pETDuet-1 plasmids	88
A2.2	6His-taMax and 6His-YFP-taMyc amino acid sequences and protein information	88
A2.3	Genetic distances of Myc and Max proteins and their conserved domains between human, chicken, <i>Hydra</i> and <i>Trichoplax</i>	89
A2.4	Disorder probabilities of taMyc	90
A2.5	Disorder probabilities of 6His-YFP-taMyc	92
A2.6	Disorder probabilities of taMax	95
A2.7	Disorder probabilities of 6His-taMax	96

## Abbreviations

5'	five prime
3'	three prime
A	adenine
Ala	alanine
Arg	arginine
Asn	asparagine
Asp	aspartate
ASW	artificial sea water
ATP	adenosine triphosphate
bHLHLZ	basic helix-loop-helix leucine zipper
BLAST	Basic Local Alignment Search Tool
bp	base pair
BrdU	bromdesoxyuridine
BSA	bovine serum albumin
C	cytosine
°C	degree Celcius
CDK	cycline dependent kinase
cDNA	complementary DNA
cf.	confer
Cys	cysteine
DAPI	4',6-diamindino-2-phenylindole
ddH <sub>2</sub> O	double distilled water
DEPC	diethylpyrocarbonate
DMSO	dimethyl sulfoxide
DNA	desoxyribonucleic acid
ds	double-stranded
dUTP	desoxyuridine triphosphate
DTT	dithiothreitol
e.g.	<i>exempli gratia</i>
EDTA	ethylenediaminetetraacetic acid
EtOH	ethanol
Fig.	figure
G	guanine
Glu	glutamate
Gln	glutamine
Gly	glycine
H	haplotype
h	hours
HCl	hydrochloric acid
HEPES	4-(2-hydroxyethyl)-1-piperazineethanesulfonic acid

His	histidine
i.e.	<i>id est</i>
Ile	isoleucine
IPTG	isopropyl- $\beta$ -D-thiogalactoside
JGI	Joint Genome Institute
kb	Kilobase (1000 base pairs)
KD	knockdown
LB	lysogeny broth
Leu	leucine
Lys	lysine
M	molar
MB	Myc box
Met	methionine
mg	milligram
min	minute
ml	milliliter
mM	milli molar
mm	millimeter
$\mu$ g	microgram
$\mu$ l	microliter
$\mu$ m	micrometer
N	normal (chemically)
NaCl	sodium chloride
NCBI	National Center for Biotechnology Information
ng	nanogram
nm	nanometer
no.	number
OD	optical density
PCR	polymerase chain reaction
Phe	phenylalanine
Pro	proline
rRNA	ribosomal ribonucleic acid
RNA	ribonucleic acid
rpm	rotations per minute
RT	room temperature
S	Svedberg unit
SDS	sodium dodecyl sulfate
sec	seconds
Ser	serine
T	thymine
TBS	tris buffered saline
TBSTT	tris buffered saline +0.1% Tween-20 +0.1% TritonX
TCEP	tris-(2-carboxyethyl)-phosphine
Thr	threonine
Tris	tris(hydroxymethyl)aminomethane

Trp	tryptophan
Tyr	tyrosine
TUNEL	terminal deoxynucleotidyl transferase-mediated deoxyuridine triphosphate nick end labeling
U	uracil
Val	valine

# ***1. Introduction***

---

*If there is magic on this planet, it is contained in water.*

*- Loren Eiseley*

### **Placozoa – an enigmatic phylum**

The first species of the phylum Placozoa was discovered in 1883 by the German zoologist Franz Eilhard Schulze [1] when he found a small inconspicuous creature in a sea water aquarium at the University of Graz (Austria). Due to its flat and round-like shape, that is covered with ciliae, he named the species *Trichoplax adhaerens* [1, 2] (see Fig. 1.1b). Shortly after its description, *Trichoplax* fell into oblivion for almost 70 years, as it was claimed to be a morphological abnormal hydrozoan larvae [3]. *Trichoplax* gained interest again, after intensive morphological studies of K. G. Grell. He described *Trichoplax* to be completely different from all known animals and also discovered evidence for sexual reproduction [4]. Following Bütschli's placula hypothesis about the origin of Metazoa [5], Grell introduced a new phylum named 'Placozoa' [6]. Finally, more than a century after its first discovery genetic evidence has been suggesting that *Trichoplax* is a suitable surrogate of the urmetazoan [7, 8].

*Trichoplax adhaerens* was the only described species within the phylum Placozoa for a long time, despite that increasing number of distinct genetic lineages has been described [9]. These so-called genetic 'haplotypes' are defined by differences in the mitochondrial 16S rDNA sequence and share common morphological features [9, 10]. Albeit their phylogenetic position is an ongoing discussion [11-14], placozoans are morphologically the most primitive animals (not secondarily reduced) with an average size of 3 mm. They harbor only two cell layers and six somatic cell types (but probably subpopulations of cell types [15, 16]), and have no defined body axis but show polarity i.e. a top to bottom orientation (Abb 1.1a) [2, 17, 18]. Muscle and nerve cells are absent as well as complex structures like sensory organs, and placozoans lack a basal lamina and extracellular matrix [19-21]. Nevertheless, they are able to perceive light and gravitation [19, 22]. Placozoans reproduce mainly vegetatively under laboratory conditions (by fission or budding of small swimmers) [23, 24], but genetic evidence for sexual reproduction was also reported [25]. Since embryonic development terminates at 128-cell state in the laboratory, the placozoan life cycle still remains unclear [26].

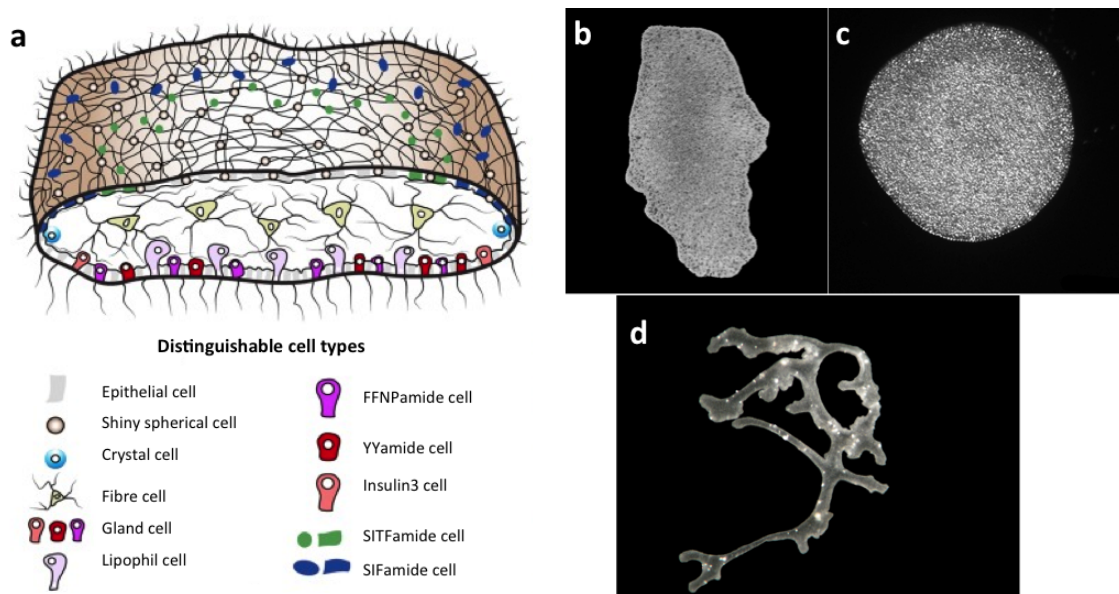


**Figure 1.1: Placozoan morphology**

(a) Schematic illustration of a placozoan cross-section (modified after [27]). Three species are described in the phylum Placozoa (b-c). *Trichoplax adhaerens* (b) and *Hoilungia hongkongensis* (c) show no morphological differences. *Polyplacotoma mediterranea* displays a stretched and ramified body which is clearly distinguishable from *Trichoplax* and *Hoilungia*. (c) was taken from [28], (d) photo credit: Osigus, H.J..

Although extensive sampling efforts uncovered a worldwide distribution of placozoans with diversity hot spots in tropical and subtropical oceans [10, 29, 30], very little is known about their habitat preferences and interactions with other organisms. The classification of placozoans by 16S rDNA has shown a variety of 20 different haplotypes [29, 31], yet the existence of more cryptic species is very likely [9, 10] and two new species were recently described [28, 31]. Like most placozoans, *Hoilungia hongkongensis* (formerly haplotype H13), does not show any morphological differences to *Trichoplax* (Fig. 1.1c), but comparison of its genome with *Trichoplax adhaerens* revealed remarkable structural genomic alterations [28]. The newly described species *Polyplacotoma mediterranea* (H0), however, differs intensely from all known placozoans in both, morphology and genetics (Fig 1.1d). Its extraordinary body is ramified and stretched, with a length of more than 10 mm. Furthermore, *Polyplacotoma* harbors the most compact mitochondrial genome and has been classified as a sister group to all other placozoans [31].

Despite their simple appearance, placozoans display a remarkable repertoire of genes, which are also present in morphologically much more complex animals. They



possess homologs of important signaling pathways, which play for instance a role in cell cycle regulation, immunity, stress responses and programmed cell death [19, 28, 32, 33]. Therefore, and because placozoans might present the potential surrogate to the 'urmetazoan' [12], they are promising model organisms to study complex regulatory signaling pathways in an evolutionary context.

### **p53 and the regulation of apoptosis**

Tumor virus research peaked in the late 1970s. During that time, p53 was discovered by different approaches by three groups, simultaneously. A 53 kDa host protein was found to bind simian virus 40 large T antigen in cells that were transformed by an avian virus [34-36]. Therefore, p53 was first assumed to act as an oncogene but was quickly re-classified, when its tumor suppressor potential was discovered [37]. Extended research on the tumor suppressor p53 did not only uncover its ability to eliminate damaged cells by apoptosis, but found evidence e.g. for its involvement in cell cycle regulation, metabolism, autophagy, cell fate determination or stress response (reviewed by [38]). p53 is a key player in the regulation of cellular mechanisms, which ensures the organism's integrity and has therefore been named 'guardian of the genome' [39]. However, this naming is somewhat misleading, as mutant p53 can be found in more than 50 % of human cancers, and other malignancies are also associated with p53 malfunction [40]. p53 is a short-lived protein that is tightly regulated under normal conditions. The most important p53 inhibitor is the ubiquitin ligase Mdm2, which inhibits p53's transcriptional activity and marks it for proteasomal degradation [41]. Thereby, p53 protein concentration is constantly kept at low concentrations [41, 42]. However, the inhibition of p53 is interrupted when a cell is exposed to stress (e.g. DNA damage, loss of normal cell contacts, oncogene activation) and p53 levels increase. Depending on severity level, p53 stimulates cell cycle arrest or apoptosis [42].

Apoptosis exhibits specific morphological and biochemical characteristics, including cell shrinkage, nuclear fragmentation, membrane blebbing, protein-cleavage and protein cross-linking [43, 44]. Two p53-mediated apoptosis pathways can be discriminated, ultimately resulting in caspase activation and cell death (cf. [45]) (Fig. 1.2). (i) The extrinsic apoptosis signaling pathway includes the involvement of

transmembrane receptors, which belong to the tumor necrosis factor (TNF) super gene family, also known as death receptors [46]. Upon ligand binding, the receptors transmit the ‘death signal’ into the cytoplasm where adapter proteins are recruited [47]. They in turn recruit further proteins, which are associated with Caspase-8. The formation of a death-inducing signaling complex (DISC) and further caspase activation finally result in cell death [48, 49]. (ii) The intrinsic apoptosis signaling pathway, however, is associated with the Bcl-2 family of regulatory genes [50]. They govern depolarization of the mitochondrial membrane and subsequent release of cytochrome c from the mitochondrial intermembrane space [51, 52]. When cytochrome c gets into the cytoplasm, it binds Apaf1 and together with Caspase-9 they form an apoptosome [53, 54]. That, in turn, starts a caspase signaling cascade and leads to apoptosis (reviewed by [42, 45]).

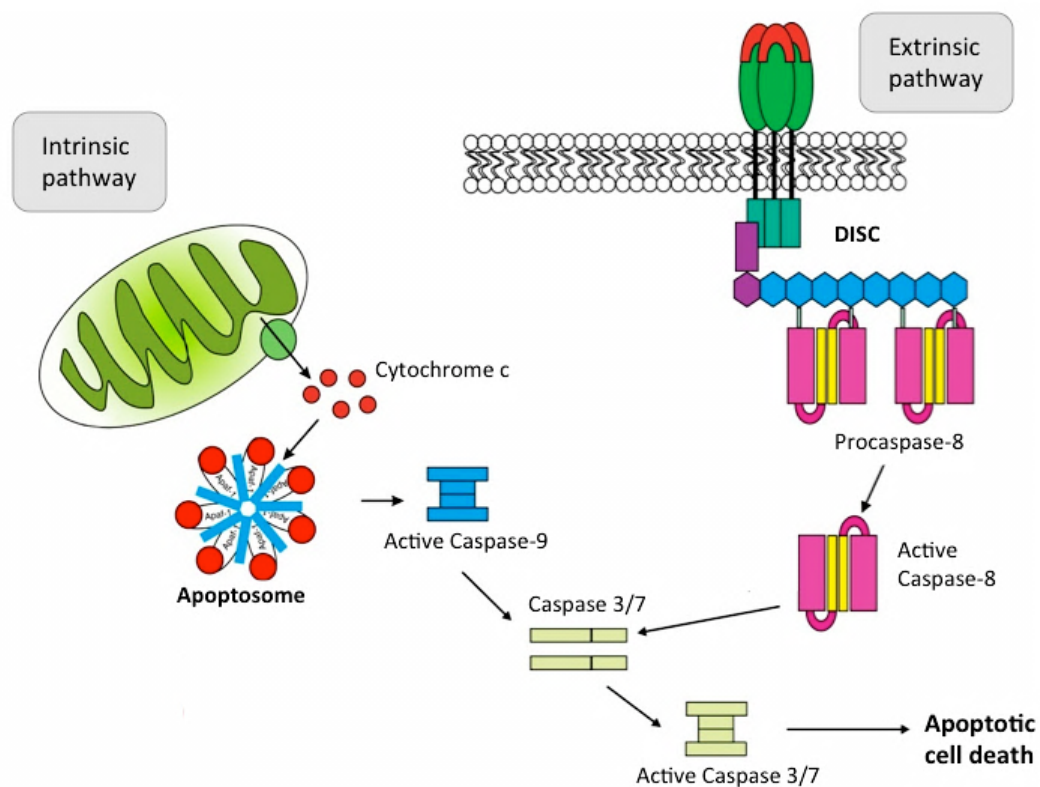


**Figure 1.2: p53-dependent apoptosis: the intrinsic and the extrinsic pathway**

The intrinsic apoptosis pathway is associated with the depolarization of the mitochondrial membrane and subsequent release of cytochrome c. Formation of an apoptosome activates Caspase-9 and starts the caspase signaling cascade resulting in apoptotic cell death. In the extrinsic apoptosis pathway, a ligand binds to so-called ‘death receptors’ which in turn bind to FAAD. The recruitment of Procaspase-8 leads to DISC formation. Similar to the intrinsic pathway, activation of Caspase-8 initiates apoptosis by further caspase activation. (Modified after [60]).

Homologs of p53 have been found throughout the animal kingdom as well as in unicellular choanoflagellates [55-57]. *Trichoplax adhaerens* harbors homologs of p53 and Mdm2, possessing all domains which are necessary for functional protein interactions [58, 59]. Further research on the p53 signaling network at the base of the metazoan ToL is needed to understand the evolution p53's functions.

### **The Myc/Max transcription factor network**

Transcription factor networks have evolved in order to control, coordinate and separate the functions of regulatory genes spatially and temporally. The proto-oncogene *c-myc*, which encodes the Myc protein, is the key player in the Myc transcription factor network. It is estimated to directly regulate at least 15 % of all human genes and is mainly involved in cell proliferation, differentiation, cell cycle control and apoptosis (cf. [61-63]). The function of Myc is modulated by alterations in its cellular distribution. The expression of Myc is repressed in differentiating cells and its inactive form can be found in the cytoplasm [64, 65]. In the nucleus of proliferating cells, however, transcriptionally active Myc endorses ribosome biogenesis and regulates the cell cycle as well as nucleotide and amino acid biosynthesis [66].

Like p53, the Myc gene family was discovered in a phase of extensive research on oncogenic retroviruses in the 1970s. First, *v-myc* was identified as an oncogene, causing myelocytomatosis in chicken [67-69]. Shortly after that, *c-myc* was found in the host cell genome as a proto-oncogenic version of the co-opted *v-myc* [70]. Other members of the Myc gene family are *L-myc* and *N-myc* (reviewed by [71]). Later on, a Myc associated factor X (Max) was discovered to play an important role in the transcriptional control of Myc target genes [72].

Myc and Max belong to a family of basic-helix-loop-helix leucine-zip (bHLHZ) proteins which form heterodimers in order to bind specific DNA enhancer boxes (E-box) [73]. Their dimerization leads to the transcriptional activation or repression of target genes, respectively [62, 72]. The bHLHZ motif is located at the C-terminus of the Myc protein and builds a scissor-like structure after dimerization to bind DNA [74]. The N-terminus harbors four Myc boxes (MB I-IV), which are associated with further protein interaction and Myc degradation [75-77]. Max contains a bHLHZ domain that directly interacts with Myc (Fig. 1.3) [74]. However, Max does not exclusively bind to

Myc but can also antagonize its function indirectly by formation of homodimers or dimerization with other members of the Myc transcription factor network, e.g. Mxd or Mnt [78, 79]. Even though Max plays an essential role in Myc's functions, Max-independent activities have been reported but little is known from those activities in vertebrates (reviewed by [80]).

The Myc transcription factor network is not restricted to bilaterians and functional proteins have also been found in diploblastic cnidarians [81, 82] as well as in the unicellular relatives *Monosiga brevicollis* and *Capsaspora owczarzaki* [56, 66, 83]. A recent study shows, that homologs of Myc and Max play an important role in apoptosis and differentiation in placozoans [84]. However, a biochemical characterization of both proteins is still pending; this could be critical to close the gap between unicellular and multicellular organisms.

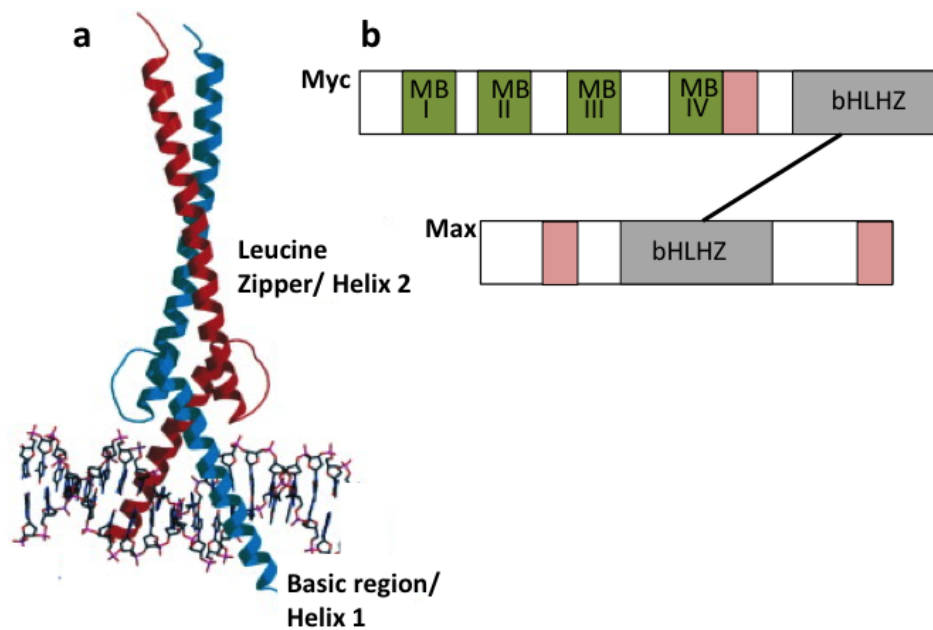


**Figure 1.3: Structures of Myc/Max dimerization**

(a) Crystal structure of the bHLHZ domain of a Myc:Max heterodimer bound to DNA (modified after [74]). (b) Myc contains four conserved Myc boxes (MB I-IV) (green) at the N-terminus, a nuclear localization signal (red) and a C-terminal bHLHZ motif (grey). Max consists of a central bHLHZ domain (grey) which is crucial for the formation of heterodimers with Myc and two nuclear localization signals (red) (modified after [63]).

### Aims of this thesis

Cancer is one of the most common death-related diseases in modern societies. It is caused by malfunction of a few genes, which regulate a variety of fundamental cellular processes. Despite extensive efforts and large investments into applied cancer research, the complex regulatory pathways that underlie tumor development are still not well understood. Research in less complex organisms allow to study significantly simplified interaction networks which in turn, may provide valuable impulses for human research.

In this thesis, I aim to contribute to a better understanding of regulatory processes controlled by the tumor suppressor p53, by exploring the most primitive metazoan, *Trichoplax adhaerens*. In detail, alterations on the cellular protein concentration levels of tap53 will be investigated. Functional genetic studies and transcriptomic approaches will help to elucidate tap53 activities at a molecular level and identify interaction partners. I further aspire to characterize the full-length proteins taMyc and taMax. Biochemical approaches to elucidate their structure and interaction *in vitro*, will help to understand the evolution of this transcription factor network. Finally, I aim to demonstrate the accessibility and importance of placozoans as model systems in applied evolutionary research

### References

1. Schulze, F.E., *Über Trichoplax adhaerens*. In Abhandlungen der Königlichen Preuss. Akademie der Wissenschaften zu Berlin. (Berlin: Verlag der königlichen Akademie der Wissenschaften), 1882: p. pp. 1-23.
2. Schulze, F.E., *Trichoplax adhaerens, nov. gen., nov. spec.* Zool Anz, 1883. 6: p. 92-97.
3. Krumbach, T., *Trichoplax, die umgewandelte Planula einer Hydromedusae*. Zool Anz, 1907. Zool Anz: p. Zool Anz.
4. Grell, K.G., *Embryonalentwicklung bei Trichoplax adhaerens F. E. Schulze*. Naturwiss, 1971. 58: p. 570.
5. Bütschli, O., *Bemerkungen zur Gastraea-Theorie*. Morph Jahrb, 1884. 9: p. 415-427.
6. Grell, K.G., *Trichoplax adhaerens F.E. Schulze und die Entstehung der Metazoan*. Naturw. Rdsch., 1971(24): p. 160-161.
7. Syed, T.a.S., B., *Trichoplax adhaerens: discovering a missing link, forgotten as a hydrozoan, re-discovered as a key to metazoan evolution*. Vie Milieu, 2002. 52: p. 177-187.
8. Ender, A. and B. Schierwater, *Placozoa are not derived cnidarians: evidence from molecular morphology*. Mol Biol Evol, 2003. 20(1): p. 130-4.

9. Voigt, O., et al., *Placozoa -- no longer a phylum of one*. *Curr Biol*, 2004. 14(22): p. R944-5.
10. Eitel, M. and B. Schierwater, *The phylogeography of the Placozoa suggests a taxon-rich phylum in tropical and subtropical waters*. *Mol Ecol*, 2010. 19(11): p. 2315-27.
11. Dellaporta, S.L., et al., *Mitochondrial genome of Trichoplax adhaerens supports placozoa as the basal lower metazoan phylum*. *Proc Natl Acad Sci U S A*, 2006. 103(23): p. 8751-6.
12. Schierwater, B., et al., *Concatenated analysis sheds light on early metazoan evolution and fuels a modern "urmetazoon" hypothesis*. *PLoS Biol*, 2009. 7(1): p. e20.
13. Feuda, R., et al., *Improved Modeling of Compositional Heterogeneity Supports Sponges as Sister to All Other Animals*. *Curr Biol*, 2017. 27(24): p. 3864-3870 e4.
14. Nosenko, T., et al., *Deep metazoan phylogeny: when different genes tell different stories*. *Mol Phylogenet Evol*, 2013. 67(1): p. 223-33.
15. Varoqueaux, F., et al., *High Cell Diversity and Complex Peptidergic Signaling Underlie Placozoan Behavior*. *Curr Biol*, 2018. 28(21): p. 3495-3501 e2.
16. Sebe-Pedros, A., et al., *Early metazoan cell type diversity and the evolution of multicellular gene regulation*. *Nat Ecol Evol*, 2018. 2(7): p. 1176-1188.
17. Guidi, L., et al., *Ultrastructural analyses support different morphological lineages in the phylum Placozoa Grell, 1971*. *J Morphol*, 2011. 272(3): p. 371-8.
18. Smith, C.L., et al., *Novel cell types, neurosecretory cells, and body plan of the early-diverging metazoan Trichoplax adhaerens*. *Curr Biol*, 2014. 24(14): p. 1565-1572.
19. Srivastava, M., et al., *The Trichoplax genome and the nature of placozoans*. *Nature*, 2008. 454(7207): p. 955-60.
20. Hynes, R.O., *The evolution of metazoan extracellular matrix*. *J Cell Biol*, 2012. 196(6): p. 671-9.
21. Schierwater, B. and R. DeSalle, *Placozoa*. *Curr Biol*, 2018. 28(3): p. R97-R98.
22. Mayorova, T.D., et al., *Cells containing aragonite crystals mediate responses to gravity in Trichoplax adhaerens (Placozoa), an animal lacking neurons and synapses*. *PLoS One*, 2018. 13(1): p. e0190905.
23. Thiemann, M., and Ruthmann, A., *Trichoplax adhaerens Schulze, F. E. (Placozoa) - The formation of swarmers*. *Z. Naturforsch.*, 1988. 43(3): p. 955-957.
24. Thiemann, M., and Ruthmann, A., *Alternative modes of sexual reproduction in Trichoplax adhaerens (Placozoa)*. *Zoomorphology*, 1991(110): p. 165-174.
25. Signorovitch, A.Y., S.L. Dellaporta, and L.W. Buss, *Molecular signatures for sex in the Placozoa*. *Proc Natl Acad Sci U S A*, 2005. 102(43): p. 15518-22.
26. Eitel, M., et al., *New insights into placozoan sexual reproduction and development*. *PLoS One*, 2011. 6(5): p. e19639.
27. DuBuc, T.Q., J.F. Ryan, and M.Q. Martindale, *"Dorsal-Ventral" Genes Are Part of an Ancient Axial Patterning System: Evidence from Trichoplax adhaerens (Placozoa)*. *Mol Biol Evol*, 2019. 36(5): p. 966-973.
28. Eitel, M., et al., *Comparative genomics and the nature of placozoan species*. *PLoS Biol*, 2018. 16(7): p. e2005359.
29. Eitel, M., et al., *Global diversity of the Placozoa*. *PLoS One*, 2013. 8(4): p. e57131.

30. Signorovitch, A.Y., S.L. Dellaporta, and L.W. Buss, *Caribbean placozoan phylogeography*. Biol Bull, 2006. 211(2): p. 149-56.
31. Osigus, H.J., et al., *Polyplacotoma mediterranea is a new ramified placozoan species*. Curr Biol, 2019. 29(5): p. R148-R149.
32. Kamm, K., et al., *Trichoplax genomes reveal profound admixture and suggest stable wild populations without bisexual reproduction*. Sci Rep, 2018. 8(1): p. 11168.
33. Kamm, K., B. Schierwater, and R. DeSalle, *Innate immunity in the simplest animals - placozoans*. BMC Genomics, 2019. 20(1): p. 5.
34. DeLeo, A.B., et al., *Detection of a transformation-related antigen in chemically induced sarcomas and other transformed cells of the mouse*. Proc Natl Acad Sci U S A, 1979. 76(5): p. 2420-4.
35. Linzer, D.I. and A.J. Levine, *Characterization of a 54K dalton cellular SV40 tumor antigen present in SV40-transformed cells and uninfected embryonal carcinoma cells*. Cell, 1979. 17(1): p. 43-52.
36. Lane, D.P. and L.V. Crawford, *T antigen is bound to a host protein in SV40-transformed cells*. Nature, 1979. 278(5701): p. 261-3.
37. Finlay, C.A., P.W. Hinds, and A.J. Levine, *The p53 proto-oncogene can act as a suppressor of transformation*. Cell, 1989. 57(7): p. 1083-93.
38. Kasthuber, E.R. and S.W. Lowe, *Putting p53 in Context*. Cell, 2017. 170(6): p. 1062-1078.
39. Lane, D.P., *Cancer. p53, guardian of the genome*. Nature, 1992. 358(6381): p. 15-6.
40. Vogelstein, B., D. Lane, and A.J. Levine, *Surfing the p53 network*. Nature, 2000. 408(6810): p. 307-10.
41. Momand, J., et al., *The mdm-2 oncogene product forms a complex with the p53 protein and inhibits p53-mediated transactivation*. Cell, 1992. 69(7): p. 1237-45.
42. Haupt, S., et al., *Apoptosis - the p53 network*. J Cell Sci, 2003. 116(Pt 20): p. 4077-85.
43. Nishida, K., O. Yamaguchi, and K. Otsu, *Crosstalk between autophagy and apoptosis in heart disease*. Circ Res, 2008. 103(4): p. 343-51.
44. Cohen, G.M., et al., *Formation of large molecular weight fragments of DNA is a key committed step of apoptosis in thymocytes*. J Immunol, 1994. 153(2): p. 507-16.
45. Elmore, S., *Apoptosis: a review of programmed cell death*. Toxicol Pathol, 2007. 35(4): p. 495-516.
46. Locksley, R.M., N. Killeen, and M.J. Lenardo, *The TNF and TNF receptor superfamilies: integrating mammalian biology*. Cell, 2001. 104(4): p. 487-501.
47. Xiao, C., et al., *Tumor necrosis factor-related apoptosis-inducing ligand-induced death-inducing signaling complex and its modulation by c-FLIP and PED/PEA-15 in glioma cells*. J Biol Chem, 2002. 277(28): p. 25020-5.
48. Kischkel, F.C., et al., *Cytotoxicity-dependent APO-1 (Fas/CD95)-associated proteins form a death-inducing signaling complex (DISC) with the receptor*. EMBO J, 1995. 14(22): p. 5579-88.
49. Kim, J.W., E.J. Choi, and C.O. Joe, *Activation of death-inducing signaling complex (DISC) by pro-apoptotic C-terminal fragment of RIP*. Oncogene, 2000. 19(39): p. 4491-9.

50. Cory, S. and J.M. Adams, *The Bcl2 family: regulators of the cellular life-or-death switch*. Nat Rev Cancer, 2002. 2(9): p. 647-56.
51. Cai, J., J. Yang, and D.P. Jones, *Mitochondrial control of apoptosis: the role of cytochrome c*. Biochim Biophys Acta, 1998. 1366(1-2): p. 139-49.
52. Liu, K., et al., *The role of cytochrome c on apoptosis induced by Anagrapha falcifera multiple nuclear polyhedrosis virus in insect Spodoptera litura cells*. PLoS One, 2012. 7(8): p. e40877.
53. Cain, K., S.B. Bratton, and G.M. Cohen, *The Apaf-1 apoptosome: a large caspase-activating complex*. Biochimie, 2002. 84(2-3): p. 203-14.
54. Wu, C.C., et al., *The Apaf-1 apoptosome induces formation of caspase-9 homo- and heterodimers with distinct activities*. Nat Commun, 2016. 7: p. 13565.
55. Belyi, V.A., et al., *The origins and evolution of the p53 family of genes*. Cold Spring Harb Perspect Biol, 2010. 2(6): p. a001198.
56. King, N., et al., *The genome of the choanoflagellate Monosiga brevicollis and the origin of metazoans*. Nature, 2008. 451(7180): p. 783-8.
57. Rutkowski, R., K. Hofmann, and A. Gartner, *Phylogeny and function of the invertebrate p53 superfamily*. Cold Spring Harb Perspect Biol, 2010. 2(7): p. a001131.
58. Lane, D.P., et al., *Mdm2 and p53 are highly conserved from placozoans to man*. Cell Cycle, 2010. 9(3): p. 540-7.
59. Siau, J.W., et al., *Functional characterization of p53 pathway components in the ancient metazoan Trichoplax adhaerens*. Sci Rep, 2016. 6: p. 33972.
60. Fox, J.L. and M. MacFarlane, *Targeting cell death signalling in cancer: minimising 'Collateral damage'*. Br J Cancer, 2016. 115(1): p. 5-11.
61. Luscher, B. and J. Vervoorts, *Regulation of gene transcription by the oncoprotein MYC*. Gene, 2012. 494(2): p. 145-60.
62. Muller, J. and M. Eilers, *Ubiquitination of Myc: proteasomal degradation and beyond*. Ernst Schering Found Symp Proc, 2008(1): p. 99-113.
63. Carroll, P.A., et al., *The MYC transcription factor network: balancing metabolism, proliferation and oncogenesis*. Front Med, 2018. 12(4): p. 412-425.
64. Craig, R.W., et al., *Altered cytoplasmic/nuclear distribution of the c-myc protein in differentiating ML-1 human myeloid leukemia cells*. Cell Growth Differ, 1993. 4(5): p. 349-57.
65. Conacci-Sorrell, M., C. Ngouenet, and R.N. Eisenman, *Myc-nick: a cytoplasmic cleavage product of Myc that promotes alpha-tubulin acetylation and cell differentiation*. Cell, 2010. 142(3): p. 480-93.
66. Young, S.L., et al., *Premetazoan ancestry of the Myc-Max network*. Mol Biol Evol, 2011. 28(10): p. 2961-71.
67. Duesberg, P.H., K. Bister, and C. Moscovici, *Avian acute leukemia virus MC29: conserved and variable RNA sequences and recombination with helper virus*. Virology, 1979. 99(1): p. 121-34.
68. Hu, S.S., et al., *Avian oncovirus MH2: preferential growth in macrophages and exact size of the genome*. Virology, 1979. 96(1): p. 302-6.
69. Sheiness, D. and J.M. Bishop, *DNA and RNA from uninfected vertebrate cells contain nucleotide sequences related to the putative transforming gene of avian myelocytomatosis virus*. J Virol, 1979. 31(2): p. 514-21.



70. Vennstrom, B., et al., *Isolation and characterization of c-myc, a cellular homolog of the oncogene (v-myc) of avian myelocytomatosis virus strain 29*. J Virol, 1982. 42(3): p. 773-9.
71. Dang, C.V., *MYC on the path to cancer*. Cell, 2012. 149(1): p. 22-35.
72. Blackwood, E.M. and R.N. Eisenman, *Max: a helix-loop-helix zipper protein that forms a sequence-specific DNA-binding complex with Myc*. Science, 1991. 251(4998): p. 1211-7.
73. Luscher, B. and L.G. Larsson, *The basic region/helix-loop-helix/leucine zipper domain of Myc proto-oncoproteins: function and regulation*. Oncogene, 1999. 18(19): p. 2955-66.
74. Nair, S.K. and S.K. Burley, *X-ray structures of Myc-Max and Mad-Max recognizing DNA. Molecular bases of regulation by proto-oncogenic transcription factors*. Cell, 2003. 112(2): p. 193-205.
75. Henriksson, M. and B. Luscher, *Proteins of the Myc network: essential regulators of cell growth and differentiation*. Adv Cancer Res, 1996. 68: p. 109-82.
76. Oster, S.K., et al., *Functional analysis of the N-terminal domain of the Myc oncoprotein*. Oncogene, 2003. 22(13): p. 1998-2010.
77. Schwinkendorf, D. and P. Gallant, *The conserved Myc box 2 and Myc box 3 regions are important, but not essential, for Myc function in vivo*. Gene, 2009. 436(1-2): p. 90-100.
78. Ayer, D.E. and R.N. Eisenman, *A switch from Myc:Max to Mad:Max heterocomplexes accompanies monocyte/macrophage differentiation*. Genes Dev, 1993. 7(11): p. 2110-9.
79. Grandori, C., et al., *The Myc/Max/Mad network and the transcriptional control of cell behavior*. Annu Rev Cell Dev Biol, 2000. 16: p. 653-99.
80. Conacci-Sorrell, M., L. McFerrin, and R.N. Eisenman, *An overview of MYC and its interactome*. Cold Spring Harb Perspect Med, 2014. 4(1): p. a014357.
81. Hartl, M., et al., *Hydra myc2, a unique pre-bilaterian member of the myc gene family, is activated in cell proliferation and gametogenesis*. Biol Open, 2014. 3(5): p. 397-407.
82. Hartl, M., et al., *Stem cell-specific activation of an ancestral myc protooncogene with conserved basic functions in the early metazoan Hydra*. Proc Natl Acad Sci U S A, 2010. 107(9): p. 4051-6.
83. Suga, H., et al., *The Capsaspora genome reveals a complex unicellular prehistory of animals*. Nat Commun, 2013. 4: p. 2325.
84. v.d.Chevallerie, K., *Experimental studies on the tumor suppressor p53, the myc proto-oncogene and tissue compatibility in the basal metazoan phylum Placozoa*. Dissertation (2013), Leibniz Universität Hannover

### Thesis outline and authors contributions

This thesis comprises four experimental studies, chapter I – IV. Chapters I and II have already been published in peer-reviewed scientific journals, the manuscripts in chapters III and IV are in preparation for submission to peer-reviewed scientific journals. The authors' contributions to the respective chapters are as follows:

#### Chapter I

von der Chevallerie, K., **Rolfes, S.**, Schierwater, B., Inhibitors of the p53-Mdm2 interaction increase programmed cell death and produce abnormal phenotypes in the placozoan *Trichoplax adhaerens* (F.E. Schulze), *Dev Genes Evol* (2014) 224:79-85.

Conceived and designed the experiments: KvdC BS

Performed the experiments: SR KvdC

Analyzed the data: SR KvdC BS

Funding acquisition: BS

Resources: BS

Supervision: BS

Visualization: KvdC

Writing – original draft: KvdC

Writing – review & editing: SR KvdC BS

#### Chapter II

Osigus, H.J., **Rolfes, S.**, Herzog, R., Kamm, K., Schierwater, B., *Polyplacotoma mediterranea* is a new ramified placozoan species, *Curr Biol* 29(5) (2019) R148-R149.

Conceptualization: HJO BS

Data curation: HJO KK BS

Formal analysis: HJO KK BS

Investigation: HJO SR RH KK BS

Field work: SR RH BS

Resources: BS

Funding acquisition: BS

Writing: HJO SR KK BS

Visualization: HJO KK BS  
Supervision: BS  
Project administration: BS

### Chapter III

**Rolfes, S.**, Kamm, K., Richardson, J., Berglund, A., Schierwater, B., The role of p53 in the regulation of apoptosis in the placozoan *Trichoplax adhaerens*. Unpublished.

Conceived and designed the experiments: SR AB BS  
Performed the experiments: SR JR  
Analyzed the data: SR KK BS  
Funding acquisition: BS  
Resources: AB BS  
Supervision: BS  
Visualization: SR KK  
Writing – original draft: SR  
Writing – review & editing: SR BS

### Chapter IV

**Rolfes, S.**, von der Chevallerie K., Curth, U., Tsiavaliaris, G., Schierwater, B., New insights into the protein biochemistry of Myc and Max in the placozoan *Trichoplax adhaerens*. Unpublished.

Conceived and designed the experiments: SR KvdC GT BS  
Performed the experiments: SR KvdC UC  
Analyzed the data: SR UC GT  
Funding acquisition: BS  
Resources: GT BS  
Supervision: BS  
Visualization: SR UC  
Writing – original draft: SR  
Writing – review & editing: SR BS

## ***2. Experimental Studies***

---

## Chapter I

### **Inhibitors of the p53-Mdm2 interaction increase programmed cell death and produce abnormal phenotypes in the placozoon *Trichoplax adhaerens* (F.E. Schulze).**

v.d.Chevallerie, K., Rolfes, S., Schierwater., B.

Dev Genes Evol (2014) 224:79-85

<https://link.springer.com/article/10.1007%2Fs00427-014-0465-0>

doi: 10.1007/s00427-014-0465-0

#### **Abstract**

Recent identification of genes homologous to human p53 and Mdm2 in the basal phylum Placozoa raised the question whether the network undertakes the same functions in the most primitive metazoan organism as it does in more derived animals. Here, we describe inhibition experiments on p53/Mdm2 interaction in *Trichoplax adhaerens* by applying the inhibitors nutlin-3 and roscovitine. Both inhibitors had a strong impact on the animals' survival by significantly increasing programmed cell death (cf. apoptosis, measured via terminal deoxynucleotidyl transferase-mediated deoxyuridine triphosphate nick end labeling assay). Treatment with roscovitine decreased cell proliferation (visualized by means of bromodeoxyuridine incorporation), which is likely reducible to its function as cyclin-dependent kinase inhibitor. Obvious phenotypic abnormalities have been observed during long-term application of both inhibitors, and either treatment is highly lethal in *T. adhaerens*. The findings of this study suggest a conserved role of the p53/Mdm2 network for programmed cell death since the origin of the Metazoa and advocate the deployment of Placozoa as a model for p53, apoptosis, and possibly cancer research.

## Chapter II

### ***Polyplacotoma mediterranea* is a new ramified placozoan species.**

Osigus, H.J., Rolfes, S., Herzog, R., Kamm, K., Schierwater, B.

Curr Biol 29(5) (2019) R148- R149.

[https://www.cell.com/current-biology/fulltext/S0960-9822\(19\)30097-1](https://www.cell.com/current-biology/fulltext/S0960-9822(19)30097-1)

doi: 10.1016/j.cub.2019.01.068

### **Abstract**

The enigmatic phylum Placozoa is harboring an unknown number of cryptic species and has become a challenge for modern systematics. Only recently, a second species has been described [1], while the presence of more than a hundred additional species has been suggested [2]. The original placozoan species *Trichoplax adhaerens* [3], the second species *Hoilungia hongkongensis* [1] and all yet undescribed species are morphologically indistinguishable (i.e. no species diagnostic characters are available [4]). Here, we report on a new placozoan species, *Polyplacotoma mediterranea* gen. nov., spec. nov., which differs from other placozoans in its completely different morphological habitus, including long polytomous body branches and a maximum body length of more than 10 mm. *Polyplacotoma mediterranea* also necessitates a different view of placozoan mitochondrial genetics. *P. mediterranea* harbors a highly compact mitochondrial genome with overlapping mitochondrial tRNA and protein coding genes. Furthermore, the new species lacks typical placozoan features, including the *cox1* micro exon and *cox1* barcode intron. As phylogenetic analyses suggest a sister group relationship of *P. mediterranea* to all other placozoans, this new species may also be relevant for studies addressing the relationships at the base of the metazoan tree of life.

## Chapter III

### **The role of p53 in the regulation of apoptosis in the placozoan *Trichoplax adhaerens*.**

Rolfes, S.<sup>1</sup>, Kamm, K.<sup>1</sup>, Richardson, J.<sup>2</sup>., Berglund, J. A.<sup>2</sup>, Schierwater, B.<sup>1</sup>

<sup>1</sup> Institute of Animal Ecology, University of Veterinary Medicine Hannover, Foundation,  
Bünteweg 17d, 30559 Hannover, Germany

<sup>2</sup> Center for Neurogenetics, University of Florida, Gainesville, FL 3261, USA

This manuscript is an authors' version in preparation for submission to *PLOS ONE*

### **Abstract**

p53 is a key regulator in apoptosis signaling pathways and therefore tightly regulated in metazoans. Recent studies have shown that the most primitive animal, *Trichoplax adhaerens*, possesses a functional p53 homolog, tap53. However, little is known about its ancestral functions and regulatory mechanisms. Here, we describe the effects of silencing tap53 via RNAi in *Trichoplax*. tap53 knockdowns were highly lethal for the animals and led to a surprising increase of apoptosis. Transcriptomic analyses uncovered an unusual set of differentially expressed genes after silencing tap53. Such genes belong to *Trichoplax*' unique repertoire of Apaf1 proteins, and to immunity response genes. These findings support the idea of an alternative p53-independent apoptosis pathway and add a new layer to the already complex interactome of p53 at the base of the metazoan Tree of life.

### **Introduction**

Cancer and cancer-like growths have been found in almost all vertebrates and many invertebrate species [1]. Though an organisms' integrity is orchestrated by a variety of genes and signaling pathways, the *p53* gene has come to ambivalent fame over the last four decades. Normal p53 protein acts as a tumor-suppressor and is widely known as the 'guardian of the genome' [2], by regulating the cell's fate during stress or DNA damage. As such, p53 initiates the apoptotic cascade when up-regulated but also regulates many other cellular processes such as cell cycle control, autophagy and metabolism to name just a few (reviewed by [3]). p53 expression is tightly regulated and protein concentrations are kept low by various regulators [4-6]. However, mutant p53 can be found in more than 50 % of all human malignancies and its activity is alternated in many other cancer cases [7-9]. p53's association with severe cancer phenotypes is mainly due to a lack of apoptosis and cell cycle arrest in damaged cells [10, 11].

Two converging apoptotic signaling pathways are initiated by p53, both resulting in the activation of caspases. The extrinsic pathway works via the so-called 'death receptors', which belong to the family of tumor necrosis factor receptors (TNF-R), and leads to the formation of a death-induced-signaling-complex (DISC) [12]. The intrinsic pathway involves a depolarization of the mitochondrial membrane, including the



release of cytochrome c into the cytoplasm and formation of the apoptosome [13]. The activation of caspases through both pathways ignites programmed cell death.

After the discovery of a *p53* homolog (*tap53*) in the simplest metazoan, *Trichoplax adhaerens* [14], experimental studies have shown that *tap53* initiates apoptosis and is regulated by the ubiquitin ligase *taMdm2* [15, 16]. To further shed light onto the regulatory mechanisms, we silenced *tap53* by means of RNAi. *tap53* knockdown (KD) was highly lethal for *Trichoplax* and significantly increased apoptosis. RNA sequencing (RNASeq) revealed differentially expressed genes, which are activated in the p53-dependent mitochondrial apoptosis pathway, as well as immunity response genes. These results strongly suggest an alternative apoptosis pathway in *Trichoplax*, in absence of *tap53*. They further underline the complexity of *tap53*'s regulatory network in the morphological simplest animal.

### Material and Methods

#### *Animal material*

In all experiments, *Trichoplax adhaerens* (haplotype 1, "Grell" clone) was used and cultured under standard conditions and fed on the chlorophyta *Pyrenomonas helgolandii* (obtained from SAG Göttingen, Germany) [17, 18]. In order to counteract potential biases by morphological indistinguishable developmental stages, animals of all sizes were randomly distributed among the experiments. Knockdowns by means of RNAi were performed under standard culturing conditions.

#### *Total RNA isolation and cDNA synthesis*

For total RNA isolation, 100 animals were rinsed in artificial seawater (ASW) and starved for 24 h. Afterwards they were homogenized in 500 µl HomI buffer (0.1 M Tris HCl pH 8, 0.01 M ethylenediaminetetraacetic acid (EDTA) pH 8, 0.1 M NaCl, 0.025 M dithiothreitol (DTT) and 0.5 % sodium dodecyl sulfate (SDS) in ddH<sub>2</sub>O) with 25 µl Proteinase K (10 mg/ml, Carl Roth, Germany) for 30 min at 55 °C. RNA was subsequently isolated with Phenol/Chlorophorm/Isoamyl alcohol (Roti® Aqua-Phenol/C/I, Carl Roth, Germany) and precipitated using isopropanol. The pellet was dissolved in diethylpyrocarbonate-treated (DEPC, Carl Roth) water and remaining DNA was digested with DNaseI (Fermentas) according to manufacturer's instructions. RNA

## 2. Experimental studies

---

quality was measured by gel electrophoresis and 100 ng RNA was used for full-length cDNA synthesis with BioScript™ Reverse Transcriptase (Bioline), following the manufacturer's protocol.

### *Molecular cloning and probe synthesis*

A 442 bp fragment of the *tap53* N-terminus and a 794 bp fragment of the dragonfly *Trithemis stictica* internal transcribed spacer region (ITS) were amplified via PCR (sequences are shown in Tab. A1.2). The fragments were recovered from agarose gel electrophoresis and subsequently cloned into the pGEM-T® vector (Promega) for sequencing.

Probes for *tap53* and ITS were amplified by PCR from the respective fragments, cloned into a pGEM-T vector. The DNA was precipitated, using 3 vol. 98 % ethanol (Carl Roth) and 0.1 vol. 3 M sodium acetate (pH 5.2; Carl Roth). The samples were incubated for 30 min at room temperature, followed by centrifugation for 30 min at 15,700 rcf and 4 °C. The DNA was rinsed with 500 µl 70 % ethanol (v/v) and the samples were centrifuged again for 15 min at 15,700 rcf and 4 °C. Subsequently, the DNA pellet was dried in a centrifugal evaporator at room temperature and resuspended in 10 µl ddH<sub>2</sub>O. The RNA was synthesized with both, T7-RNA polymerase and Sp6-RNA polymerase, respectively (both from Promega). The reaction volume of 10 µl contained 2 µl DEPC-H<sub>2</sub>O, 2 µl RNA polymerase buffer, 1 µl RNase out, 1 µl Fluorescein RNA Labeling Mix (Roche), 1 µl of the particular RNA polymerase and 3 µl DNA. The transcription reaction was incubated overnight at 37 °C. To purify the ssRNA, the remaining DNA was digested with DNase I for 30 min at 37 °C. The DNase I was subsequently inactivated for 15 min at 65 °C. To precipitate the nucleic acids, 2 µl lithium chloride and 50 µl 70 % ethanol (v/v, in DEPC-H<sub>2</sub>O) were added and incubated for 30 min at 80 °C. Proceeding this, samples were centrifuged at 4 °C for 30 min at 15,700 rcf, followed by removal of the supernatant. The ssRNA was rinsed with 500 µl 70 % ethanol (v/v) (in DEPC-H<sub>2</sub>O) and incubated for at least 1 h to get rid of excessive fluorescein. Again, the samples were centrifuged at 15,700 rcf for 30 min at room temperature. The supernatant was discarded and the ssRNA was dried in a centrifugal evaporator and then resolved in 20 µl DEPC-H<sub>2</sub>O. To hybridize complementary RNA strands, 20 µl of both ssRNA samples (T7 and Sp6) were added to the reaction mix with

## 2. Experimental studies

---

a total volume of 200 µl, containing 750 mM sodium chloride (Carl Roth) and 75 mM sodium citrate (Carl Roth). The reaction was then incubated for 30 min at 65 °C. Afterwards, 10 µl lithium chloride (4 M) and 300 µl 98 % ethanol (v/v) was added to precipitate the dsRNA at -80 °C for 24 h. To clean the probes, they were centrifuged at 4 °C for 30 min at 15,700 rcf and the supernatant was discarded. The RNA pellet was rinsed with 100 µl 70 % ethanol (v/v) and centrifuged for 5 min at 15,700 rcf and 4 °C. The supernatant was discarded. The dsRNA probes were dried in a centrifugal evaporator, resolved in 30 µl ddH<sub>2</sub>O and stored at -80 °C.

### *tap53 knockdown by RNAi*

For gene knockdowns by means of RNAi, 40 animals were transferred into 4-well chamber slides (Lab-Tek®, ThermoFisher). The animals were transfected with 207 nM tap53 or *T. stictica* ITS dsRNA, respectively, using INTERFERin® (Polyplus-transfection® SA, France) (IF), following the manufacturer's protocol. Controls were set up to exclude effects of transfection medium (same treatment, no dsRNA) and culture conditions (ASW control). Animals were observed under a light microscope (Zeiss Axiovert 200M) twice a day to document possible morphological changes. ASW was changed every other day and the animals were fed with *Pyrenomonas helgolandii ad libitum*. For the following RNA sequencing, total RNA of 20 animals was isolated using TRIzol® Reagent (ambion) according to manufacturer's instructions. Quality and quantity of RNA were measured using a Nanodrop (Nanodrop Technologies) and Bioanalyzer (Agilent Technologies). Successful gene inhibition was verified via semi-quantitative PCR.

### *Detection of apoptotic cell death via TUNEL assay and DAPI staining*

Apoptotic cells were detected by means of enzymatic dUTP nick end labeling. For each experiment, 40 animals were collected and either transfected with tap53 RNA or IF (see above) for 21 h. The animals were fixated with Lavdowsky fixative (ethanol/TBS/Acetic Acid/Formaldehyde: 11/11/1/2) for 20 minutes and permeabilized with 1x TBS (0.5 % Tween-20 and TritonX; Carl Roth) at 4 °C overnight. Afterwards, staining was performed using ApopTag® Red *In Situ* Apoptosis Detection Kit (Millipore), as per manufacturer's recommendations. After staining apoptotic cells, the nuclei were counterstained with DAPI. 700 µl DAPI (1.0 %) in 1x TBS were administered to the

## 2. Experimental studies

---

samples and incubated for 15 min at room temperature. Afterwards, the animals were washed three times with 1x TBS and kept in a wet chamber at 4 °C overnight. Subsequently, the samples were placed on microscope slides, covered with Vectashield® mounting medium for fluorescence (with DAPI) (Vector Laboratories, Inc.).

### *Microscopy*

A Zeiss Axiovert 200M that was connected to a digital camera (Zeiss, Axio Cam MRn) was used for taking microscopic images. For fluorescence pictures, Zeiss filter sets (02 for DAPI, 25 for Alexa Fluor 546) were used. Animal sizes and amount of apoptotic cells were analyzed with ImageJ v2.0.0. Signals of apoptotic cells (TUNEL) were calculated in relation to DAPI signals.

### *Statistical testing*

The examination of the effects of the tap53 knockdown in *Trichoplax* was conducted using two-sided t-tests in Microsoft® Excel® for Mac 2011 (v14.1.0). tap53 KD samples were compared to each control to analyze the population and animal body sizes. The amount of apoptotic cells was compared to the control group (IF).

### *RNASeq library preparation and Illumina sequencing*

Extracted RNA of tap53 KD, ITS and IF controls with RIN (RNA Integrity Number) values > 7 were used for cDNA library construction. Each sample was split into two technical replicates and rRNA was removed using NEBNext rRNA Depletion Kit (New England Biolabs #E6310). Sequencing was performed on an Illumina NextSeq 500 (Illumina, Inc.) (2 × 75 nt) at the Center for NeuroGenetics, UF Gainesville, USA.

### *De novo assembly and annotation*

Paired-end reads were examined for quality by FastQC [19] and adapter sequences and low quality reads were removed with Trimmomatic [20] prior to assembly. The *de novo* assembly was conducted using Trinity v2.8.3 [21, 22] with default settings, except for strand specification (RF) and read normalization. Quality of the assembly was

evaluated by Trinity's Nx and Ex90N50 statistics and transcript count and redundant sequences were filtered using CD-Hit (95 % nucleotide similarity) [23].

Open reading frames (ORFs) were identified via TransDecoder v.5.5.0 [22], followed by a local BLAST search [24] against the Swiss-Prot database (downloaded June 2019). HMM (hidden Markov model) searches against the Pfam-A protein domain database (downloaded June 2019) [25] were subsequently performed using HMMER v. 3.1.2 [26].

### *Identification of differentially expressed genes*

Transcript abundance was estimated for each sample using the alignment-based RSEM tool [27]. Therefore, the transcripts were mapped back separately to the previously assembled reference transcriptome by Bowtie [28], followed by subsequent transcript-level estimation and normalized measure of transcript expression with RSEM's default parameters.

Differentially expressed (DE) genes were identified using R version 3.5.0 with the packages limma and voom (downloaded from the Bioconductor webpage). The voom method was used to identify DE features according to the *run\_DE\_analysis.pl* script provided by Trinity, as well as with an R in house script. The criteria for DE genes were set with a *p*-value cut off for FDR to < 0.001 and log<sub>2</sub>-fold changes to < -2 and > 2.

The amino acid sequences of the DE genes were extracted from the TransDecoder annotations (see above). Proteins belonging to *Trichoplax adhaerens* were verified by a BLASTp search on the BLAST® webserver (<https://blast.ncbi.nlm.nih.gov/Blast.cgi>) using the NCBI non-redundant sequences database. The domain structures of the proteins were analyzed with the HMMScan web-tool (<https://ebi.ac.uk/Tools/hmmer/search/hmmscan>).

## **Results and Discussion**

### *tap53 knockdown affects Trichoplax' viability*

The animals were inspected visually 21 hours post transfection (hpt) via microscopy, RNAi was verified by semi-quantitative PCR (Fig. A1.1 & A1.2, as described in Jakob et al. [29]). Changes in population size were followed and pictures were taken to document the animals' morphology. Importantly, the fitness of the control groups remained

## 2. Experimental studies

---

stable over the course of the experiment. tap53 KD was lethal within 72 hpt while the number of animals increased in the three control groups (Fig. 2.1a). After 21 h, the effect of tap53 silencing was detectable and the animals died at a faster rate (Fig. 2.1a, black line). In the untreated group, cultured in artificial ASW only, animal numbers increased constantly, doubling after 40 h. They reached a plateau phase of approximately 100 animals (Fig. 2.1a, dotted line). The stalling of further reproduction likely is a result of limited space in the culture dish. Animals treated with transfection reagent (IF) and the internal transcribed spacer (ITS) from *Trithemis stictica*, performed almost equally well, showing a slow but steady reproduction rate within the monitored 72 hours (Fig. 2.1a, dashed lines). The slightly slower growth rates in the IF and ITS control groups compared to ASW control may be caused by the transfection medium.

Animals belonging to the tap53 group showed a significant reduction in body size after 48 h ( $p < 0.005$ ), while no prominent changes were detected in the control groups. Signs of degeneration were visible 21 hpt which further exacerbated 48 hpt (round body shapes and only loosely connected upper and lower epithelium). No differences in shape were seen in the control groups (Fig. 2.1b).

The quick death of animals with silenced tap53 was unexpected and no tumor-like growth was observed in *Trichoplax* specimen after tap53 KD (Fig. 2.2). In comparison with vertebrates, p53  $-/-$  mice have been shown to live four to six months before succumbing to lymphomas. Except for tumor growth in early life stages, the mice displayed a normal development [30-32]. This is consistent with studies by van Boxtel and colleagues [33], who showed that p53 knockout rats developed mostly sarcomas with an onset of four months. Eventually, tumors and accompanying health conditions irreversibly terminated the viability of p53 knockout mutants. p53-deficient invertebrate models like *C. elegans* or *Drosophila*, however, do not display increased tumor-like phenotypes. They also lack aspects of p53 response, e.g. developmental impairment, under physiological conditions [34-36].

## 2. Experimental studies

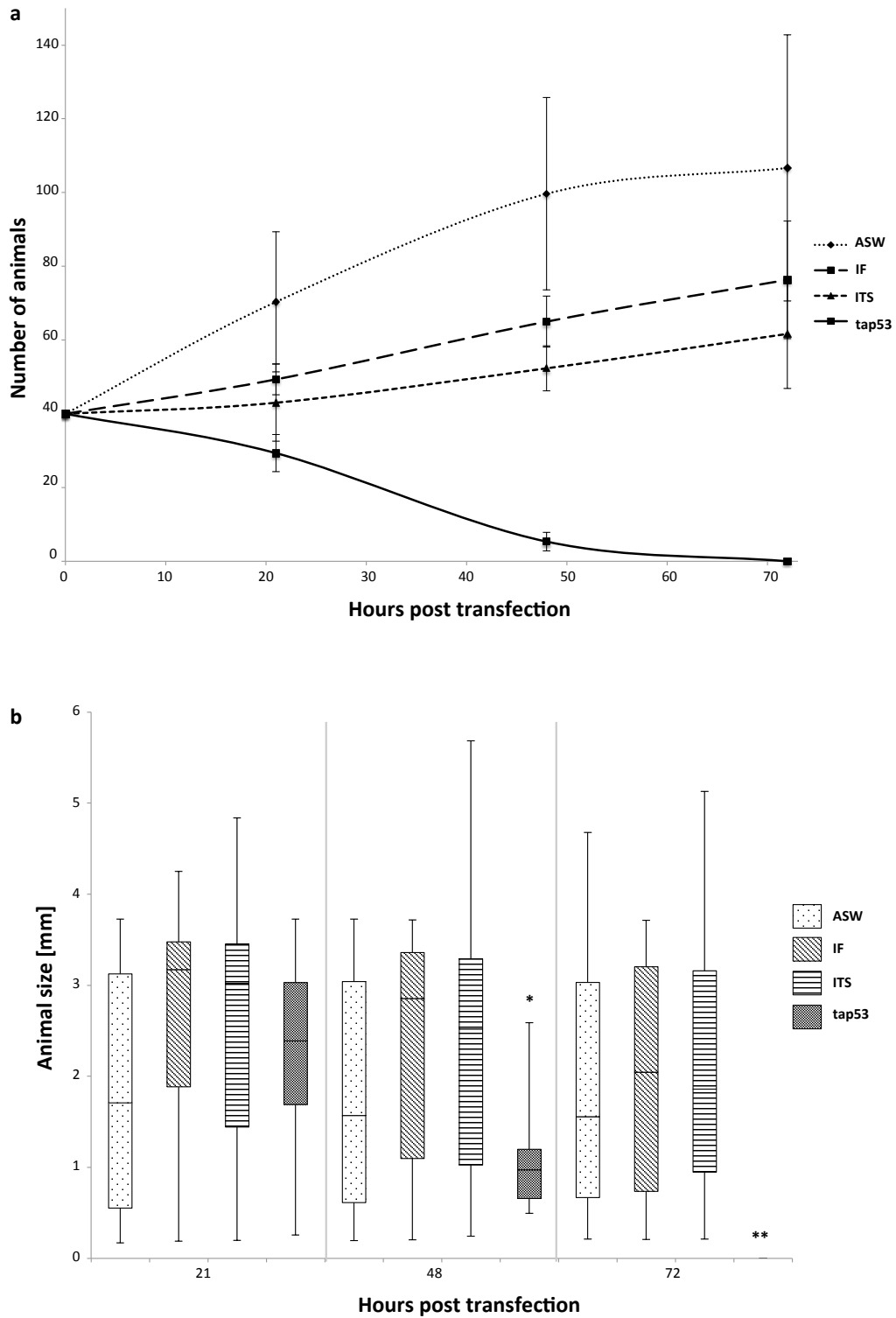


**Figure 2.1: Time course of population and body size after tap53 knockdown.**

tap53 knockdown was lethal within 72 hours. (a) The number of animals decreased significantly within 40 hours and no animal was left 72 hours post transfection with tap53 RNAi probe. The control groups ASW, Interferin (IF) and *T. stictica* ITS show steady growth. (b) A significant decrease in body size was observed after 48 hours of tap53 knockdown ( $p < 0.05$ ). The variation in body sizes increases within the control groups. Asterisks mark significances ( $*p < 0.05$ ,  $**p < 0.005$ ). Whiskers mark minimum and maximum body sizes, boxes mark upper and lower quartile, median is indicated by a horizontal line.

## 2. Experimental studies

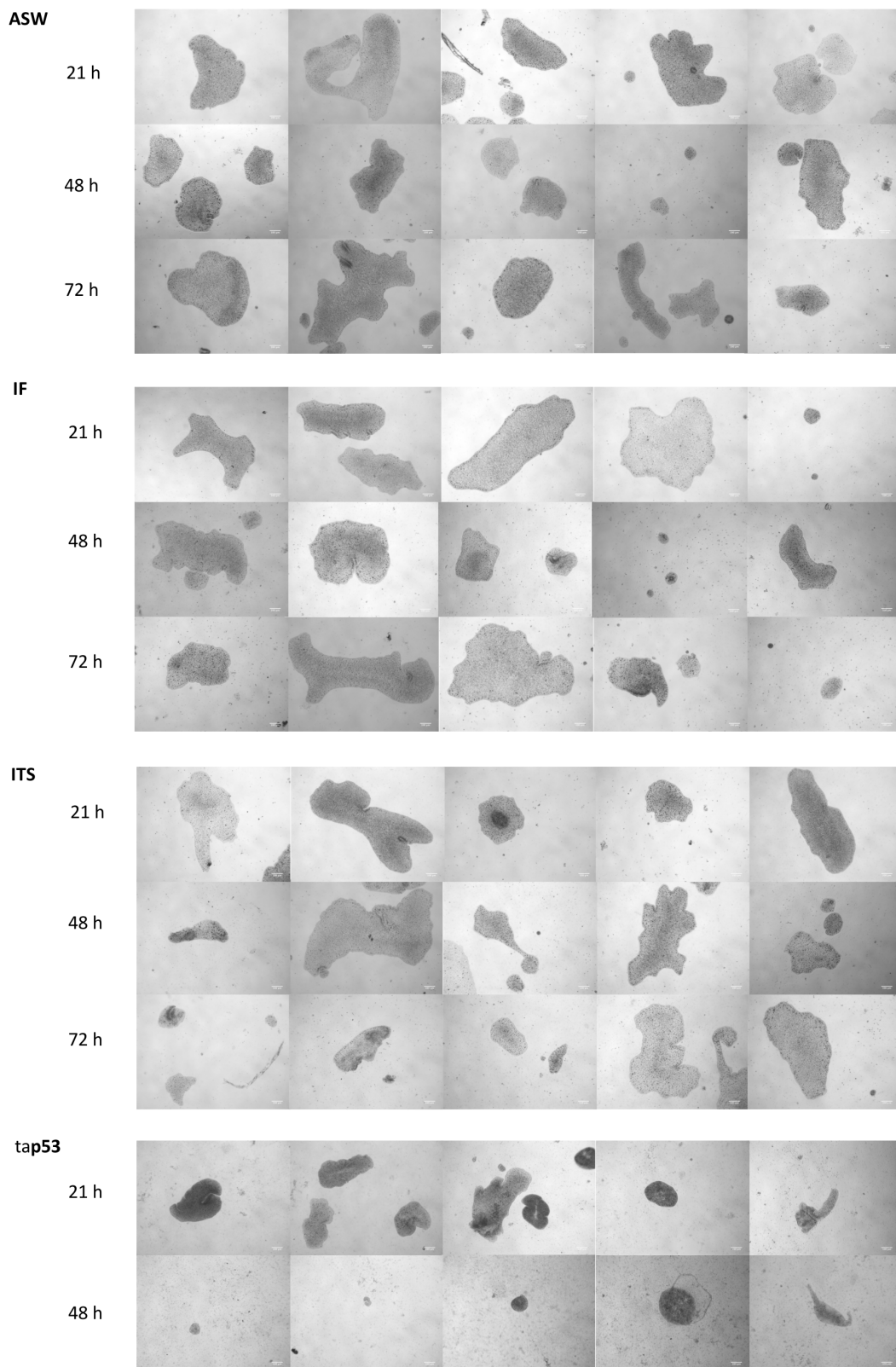


**Figure 2.2: Phenotypic variability in *Trichoplax* specimen after tap53 knockdown.**

Light microscopy of animals treated with tap53 and *T. stictica* ITS RNAi probes, respectively, Interferin (IF) and ASW. Images were taken 21 h, 48 h and 72 h after the initial knockdown. tap53 KD animals showed a significant reduction in body size ( $p < 0.05$ ) 21 hours post transfection (hpt). All tap53 KD animals were dead 72 hpt. The control groups ASW, IF, ITS vary in sizes and shapes. Size bars mark 100  $\mu\text{m}$ .



### *Apoptosis increases after tap53 knockdown*

While tap53 accumulation by inhibition of tap53-taMdm2 interaction is lethal in *Trichoplax* and initiates an apoptotic pathway [15], its down-regulation has likewise severe consequences on the animal's health status. To examine whether apoptosis was affected, tap53 KD mutants were TUNEL stained 21 hpt. tap53 KD was compared to animals treated with IF as a control (Fig. 2.3a). Surprisingly, a significant increase ( $p < 0.005$ ) of apoptotic cells was detected after tap53 silencing (Fig. 2.3a).

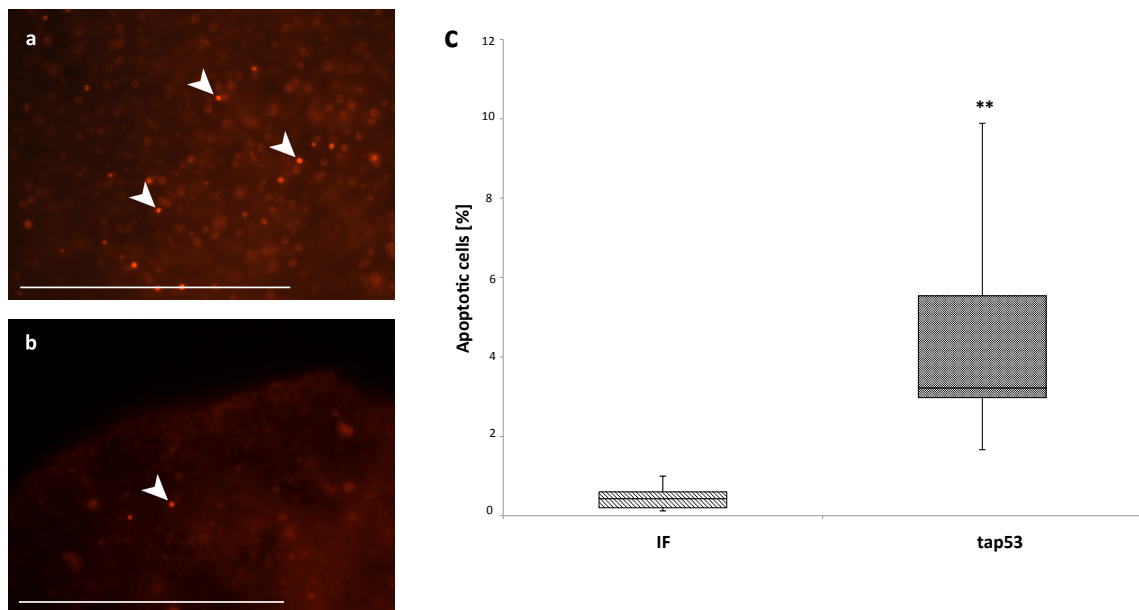


**Figure 2.3: TUNEL staining 21 h after tap53 knockdown.**

TUNEL staining of apoptotic cells 21 h after tap53 knockdown (a) and Interferin (IF) control (b). Apoptosis significantly increased in tap53 knockdown animals compared to a IF treated group ( $p < 0.005$ ) (c). Asterisks mark significant aberrations from the IF control. The size bars mark 20  $\mu\text{m}$ . For raw data and statistics see table A1.1.

The increase of apoptosis after tap53 KD suggests the presence of an alternative, tap53-independent apoptosis pathway in *Trichoplax*. So far, p53-independent apoptosis has been found in various cancer types, which are not able to initiate apoptosis via normal p53-dependent pathways [37-39]. The p53-independent apoptosis signaling in mammalian cancer cells appropriates the mitochondrial pathway. It initiates cell death by interacting with genes which belong to the Bcl-2 family [40]. These genes provoke the release of cytochrome c into the cell cytoplasm, which in turn leads to the formation of an apoptosome and subsequent caspase activation [41, 42]. Therefore, therapeutic research (in humans) focuses on members of the Bcl-2 family, as well as on their interaction partners, as promising targets in

cancer cells [43, 44]. This process was also observed in p53-deficient *Drosophila* when exposed to ionizing radiation (IR) [45], yet little is known about the underlying mechanisms. Some authors, however, suggest that there is not one single dominant mechanism but rather a complex collaboration of differently involved responses (e.g. [46]).

There are no published studies about p53-independent apoptosis in other diploblastic animals so far. That makes the initiation of an alternative apoptosis pathway in *Trichoplax* after tap53 KD without additional activators (e.g. UV radiation or drug treatment) even more remarkable. The tap53-independent apoptosis (and specifically the perception of low tap53 levels) in *Trichoplax*, likely is an ancestral function which dates back to the origin of metazoan animals.

### *tap53 down-regulation affects a variety of genes*

To gain a broader perspective of the tap53 regulatory network in *Trichoplax*, RNASeq was performed 21 h after tap53 KD. The total amount of 328,009,556 trimmed, paired-end reads was employed for *de novo* transcriptome assembly with a Trinity pipeline [21, 22]. This approach was chosen to capture the majority of transcripts and to avoid loss of information due to an incomplete reference genome. The resulting new transcriptome assembly was used as a reference, containing 160,183 contigs (Tab. 2.1). It displays a N50 value of 2,170 bp (based on the longest isoform per gene) (Tab. 2.1) and an Ex90N50 of 938 bp (Tab. 2.1) after transcript abundance estimation [27].

**Table 2.1: Assembly and reference transcriptome statistics.**

<b>Total No. of Trimmed Reads</b>	328,009,556
<b>Total No. of Contigs following Trinity Assembly</b>	160,183
<b>Reference Transcriptome Statistics</b>	
Median Contig Length	337 bp
Average Contig Length	832.83 bp
No. of Annotated Contigs	46,241
N50 Contig Length	2,170 bp
Ex90N50 Length	938 bp

## 2. Experimental studies

To detect differentially expressed genes (DEGs), the tap53 KD transcriptome was compared to both controls (ITS, IF) independently. In sum, 1,122 DEGs were identified (Tab. 2.2), of which 919 genes were assigned to prokaryotes and non-metazoan eukaryotes by BLASTp search against a non-redundant database [24] (Tab. 2.2). The high amounts of genes that do not belong to *Trichoplax* were a result of insufficient filtering at the beginning of transcriptome analysis. However, rigorous filtering methods come at the cost of losing lowly expressed genes [47]. Although this background noise might have hampered the correct classification of DEGs to some extent, 203 genes belonged to *Trichoplax* (Tab. 2.2). 51 genes were up-regulated in tap53 KD, 24 genes were down-regulated (Tab. 2.2, Fig. 2.4a). Numbers represent overlapping results of tap53 KD vs IF and tap53 KD vs ITS, respectively.

**Table 2.2: Comparison of differentially expressed genes**

<b>DEGs with TransDecoder Hit</b>	<b>1,122</b>		
<b>Total Number of DEGs from <i>Trichoplax</i></b>	203		
<b>Total Number of DEGs from other Organisms</b>	919		
<b>Compared Conditions:</b>			
	<b>tap53 vs ITS</b>	<b>ta53 vs IF</b>	<b>Overlap</b>
<b>Up-Regulated Total</b>	498	456	
<b>Up-Regulated <i>Trichoplax</i></b>	68	77	51
<b>Up-Regulated Other</b>	430	379	
<b>Down-Regulated Total</b>	74	94	
<b>Down-Regulated <i>Trichoplax</i></b>	34	24	24
<b>Down-Regulated Other</b>	40	70	

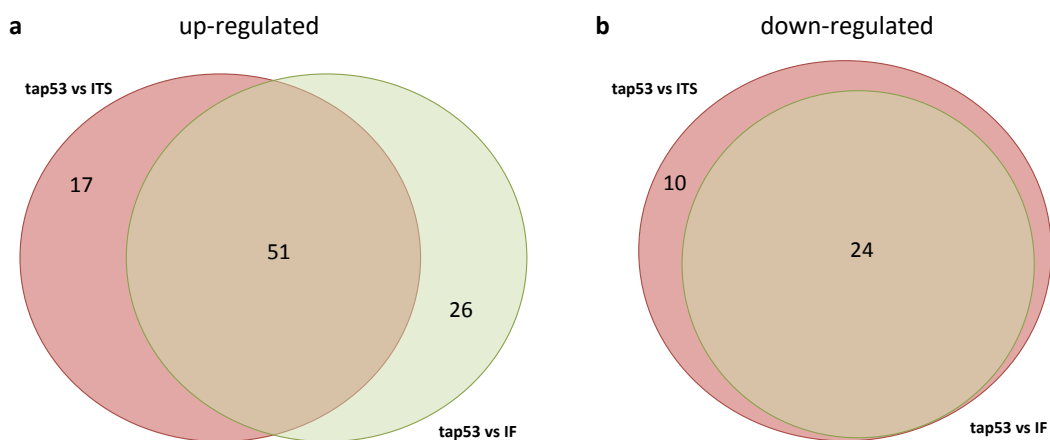


**Figure 2.4: Comparison of differentially expressed genes.**

The differentially expressed genes (DEGs) in tap53 knockdown (KD) transcriptomes are compared with each control transcriptome (Interferin (IF), *T. stictica* ITS). (a) 68 genes are up-regulated in a tap53 vs

ITS comparison, 77 genes are up-regulated in tap53 compared to IF. 51 genes are found to be identical in both sample comparisons. (b) 34 genes are down-regulated in tap53 vs ITS, all 24 down-regulated genes in tap53 vs IF overlap with tap53 vs ITS. For further data comparison see table 2.2.

### *Differential expression of pro-apoptotic genes*

The rapid death of *Trichoplax* specimen after tap53 KD was unexpected, since p53 down-regulation was expected to inhibit apoptosis [48, 49]. An even bigger surprise was the significant increase of apoptotic cells as a result of tap53 KD (as discussed above). Domain identification via HMMScan of all *Trichoplax*' DEGs revealed unexpected up-regulation of proteins belonging to the p53-dependent intrinsic apoptosis pathway (Tab. 2.3). Two proteins were extracted that belong to the recently described NOD-like receptor repertoire of placozoans [50]. One of these proteins contains an NB-ARC domain and an Apaf-1 helical domain, and was identified as Apoptotic protease-activation factor 1 (Apaf1). The other protein was described as a hypothetical protein that harbors a CARD domain (Tab. 2.3).

Genes belonging to the NOD-like receptor family show complex expression patterns. In the placozoan *Trichoplax*, some members were up-regulated after tap53 KD and some were down-regulated. Two of them were assigned to hypothetical proteins, each containing a NACHT domain (Tab. 2.3). The third protein harbored the NB-ARC and Apaf1-helical domains and was identified as Apaf1 (Tab. 2.3). Although belonging to the same gene family, the respective up- and down-regulated genes differ in their domain composition [50]. These findings suggest a complex interplay of genes of the same family in *Trichoplax*, leading to programmed cell death. However, Apaf1 usually plays a key role in the intrinsic apoptosis pathway. Its activation leads to the formation of an apoptosome and the recruitment of downstream caspases [51, 52]. p53 thereby promotes cytochrome c release from the mitochondria into the cell's cytoplasm through the activation of pro-apoptotic genes, which belong to the Bcl-2 family. The apoptosome is built through oligomerization of cytochrome c, Apaf1 and Caspase-9 and passes the death signal by association of both proteins' CARDS [7, 53]. Homologous proteins of Apaf1 were up-regulated in *Trichoplax* when tap53 was silenced (Tab. 2.3). This leads to the assumption of an alternative mechanism regulating apoptosis and highlights the importance of tap53 for the animal's integrity. It is possible that this primitive animal has checkpoints that recognize the absence of tap53.

### *Up-regulation of immunity and stress response genes*

tap53 KD by RNAi not only increased apoptosis in *Trichoplax*, but cells also reacted with activation of cellular defense mechanisms. Interleukin-1 receptor-associated kinase-like 2 (IRAK-like) was up-regulated after tap53 KD, as well as a protein with ankyrin-repeats (ANK) (Tab. 2.3). IRAKs are part of the Toll-like receptor signaling cascade that serves as downstream effectors guiding the activation of the transcription factors NF- $\kappa$ B, AP-1 and Interferon regulatory factor (IRF). Both, NF- $\kappa$ B and AP-1, lead to the expression of inflammatory cytokines and other immune response genes in vertebrates ([54] and references therein). The signaling pathway leading to NF- $\kappa$ B activation seems to be incomplete in placozoans, as they lack the essential NF-kappa-B inhibitor alpha ( $\text{I}\kappa\text{B}\alpha$ ) [50]. However, ANKs are the only conserved domains in  $\text{I}\kappa\text{B}\alpha$  and related proteins. 200 ANK-containing proteins are present in *Trichoplax*, and some possibly fulfill a similar role [50]. Albeit it remains speculative at this time if the up-regulated protein with ANKs functions as  $\text{I}\kappa\text{B}\alpha$ , the up-regulation of immunity-related proteins after tap53 KD is nevertheless worth mentioning.

Furthermore, the up-regulation of heat shock protein 70 (Hsp70) and a BAG-domain containing protein (Tab. 2.3) after silencing tap53 underlines the complexity of apoptosis and cell survival regulation in *Trichoplax*. Generally, Hsp70 is up-regulated in severely stressed cells, promoting the refolding or degradation of mislead proteins [55, 56]. BAG-domain proteins can bind Hsp70 and thereby modulate and support their chaperone activity [57]. Hsp70 interferes with the apoptotic pathway, through inhibition of pro-apoptotic proteins. For instance, it blocks the oligomerization of Apaf1 and Caspase-9, preventing the cell from the formation of an apoptosome and apoptosis, respectively [58, 59].

## 2. Experimental studies

**Table 2.3: Proteins belonging to the apoptosis pathway, innate immunity system and stress response were found differentially expressed after tap53 knockdown.**

Organism	Name	Trinity ID	NCBI Acc. No.	Domain
<b>up-regulated genes:</b>				
Trichoplax sp. H2	BAG domain-containing protein Samui	DN10746	RDD40779	BAG domain
Trichoplax adhaerens	hypothetical protein	DN2041	XP_002109144	Caspase recruitment domain (CARD)
Trichoplax sp. H2	Interleukin-1 receptor-associated kinase-like 2 (IRAK-like)	DN2637	RDD46737	Protein tyrosine kinase
Trichoplax sp. H2	Apoptotic protease-activating factor 1 (APAF-1)	DN3347	RDD41288	NB-ARC domain, APAF-1 helical domain
Trichoplax adhaerens	hypothetical protein	DN3829	XP_002114285	Hsp70
<b>down-regulated genes:</b>				
Trichoplax sp. H2	hypothetical protein Trisph2_010969	DN148	RDD37032	NACHT domain
Trichoplax sp. H2	Apoptotic protease-activating factor 1 (APAF-1)	DN2135	RDD41632	NB-ARC domain , APAF-1 helical domain
Trichoplax adhaerens	predicted protein	DN329	XP_002115553	NACHT domain

The up-regulation of proteins, which are associated with cell survival rather than cell death, seems contrary to the observed death of animals through apoptosis. This observation might hint to a cellular discrepancy whether to sacrifice cells or rescue them. The tap53 KD in this study apparently exceeded a threshold that led to programmed cell death. It is interesting that proteins of both, cell survival and cell death, were up-regulated together when apoptosis had already increased. Possibly, the RNA extraction and subsequent sequencing 21 hpt, might have been conducted right after a cellular switch from cell survival mechanisms to apoptosis had occurred, which would come along with progressing tap53 silencing.

The identified DEGs exhibit very incomplete signaling pathways and leave space for speculations on the regulatory mechanisms taking place in *Trichoplax* after tap53 knockdown. This study revealed some fascinating and exciting first insights into the regulation of apoptosis in the simplest living animal, underlining the complex interactions of different apoptotic signaling pathways in *Trichoplax*.

### **Conclusions**

tap53 is a master control gene and crucial for homeostasis of *Trichoplax adhaerens*. The increase of apoptosis and up-regulation of apoptotic genes after tap53 knockdown strongly suggests the presence of an alternative, tap53-independent apoptosis pathway. Absence of tap53 lead to programmed cell death in *Trichoplax* but also to an immune response. This calls for further studies (including single-animal sequencing) to identify further tap53 interaction partners and shed light onto its complex interactome in the most primitive metazoan.

### **Acknowledgements**

SR was funded by an 'Otto Bütschli' scholarship from the University of Veterinary Medicine Hannover, Foundation and a PhD Completion Grant and a Scholarship for a Research Stay Abroad from the Leibniz University Hannover. We acknowledge support from the German Science Foundation (DFG Schi-277/26, Schi-277/27, Schi-277/29).

### **Supplementary data**

Further data can be found in the appendix and digital appendix.

### References

1. Aktipis, C.A., et al., *Cancer across the tree of life: cooperation and cheating in multicellularity*. *Philos Trans R Soc Lond B Biol Sci*, 2015. 370(1673).
2. Lane, D.P., *Cancer. p53, guardian of the genome*. *Nature*, 1992. 358(6381): p. 15-6.
3. Kasthuber, E.R. and S.W. Lowe, *Putting p53 in Context*. *Cell*, 2017. 170(6): p. 1062-1078.
4. Haupt, Y., et al., *Mdm2 promotes the rapid degradation of p53*. *Nature*, 1997. 387(6630): p. 296-9.
5. Honda, R., H. Tanaka, and H. Yasuda, *Oncoprotein MDM2 is a ubiquitin ligase E3 for tumor suppressor p53*. *FEBS Lett*, 1997. 420(1): p. 25-7.
6. Kubbutat, M.H., S.N. Jones, and K.H. Vousden, *Regulation of p53 stability by Mdm2*. *Nature*, 1997. 387(6630): p. 299-303.
7. Haupt, S., et al., *Apoptosis - the p53 network*. *J Cell Sci*, 2003. 116(Pt 20): p. 4077-85.
8. Haupt, S., I. Louriya-Hayon, and Y. Haupt, *P53 licensed to kill? Operating the assassin*. *J Cell Biochem*, 2003. 88(1): p. 76-82.
9. Vogelstein, B., D. Lane, and A.J. Levine, *Surfing the p53 network*. *Nature*, 2000. 408(6810): p. 307-10.
10. Muller, P.A., et al., *Mutant p53 regulates Dicer through p63-dependent and -independent mechanisms to promote an invasive phenotype*. *J Biol Chem*, 2014. 289(1): p. 122-32.
11. Petitjean, A., et al., *Impact of mutant p53 functional properties on TP53 mutation patterns and tumor phenotype: lessons from recent developments in the IARC TP53 database*. *Hum Mutat*, 2007. 28(6): p. 622-9.
12. Ashkenazi, A. and V.M. Dixit, *Death receptors: signaling and modulation*. *Science*, 1998. 281(5381): p. 1305-8.
13. Fulda, S. and K.M. Debatin, *Extrinsic versus intrinsic apoptosis pathways in anticancer chemotherapy*. *Oncogene*, 2006. 25(34): p. 4798-811.
14. Srivastava, M., et al., *The Trichoplax genome and the nature of placozoans*. *Nature*, 2008. 454(7207): p. 955-60.
15. von der Chevallerie, K., S. Rolfes, and B. Schierwater, *Inhibitors of the p53-Mdm2 interaction increase programmed cell death and produce abnormal phenotypes in the placozoon Trichoplax adhaerens (F.E. Schulze)*. *Dev Genes Evol*, 2014. 224(2): p. 79-85.
16. Siau, J.W., et al., *Functional characterization of p53 pathway components in the ancient metazoan Trichoplax adhaerens*. *Sci Rep*, 2016. 6: p. 33972.
17. Schierwater, B. and K. Kuhn, *Homology of Hox genes and the zootype concept in early metazoan evolution*. *Mol Phylogenet Evol*, 1998. 9(3): p. 375-81.
18. Schierwater, B., *My favorite animal, Trichoplax adhaerens*. *Bioessays*, 2005. 27(12): p. 1294-302.
19. Andrews, S., *FastQC: A quality control tool for high throughput sequence data*. Reference Source, 2010.
20. Bolger, A.M., M. Lohse, and B. Usadel, *Trimmomatic: a flexible trimmer for Illumina sequence data*. *Bioinformatics*, 2014. 30(15): p. 2114-20.
21. Grabherr, M.G., et al., *Full-length transcriptome assembly from RNA-Seq data without a reference genome*. *Nat Biotechnol*, 2011. 29(7): p. 644-52.



22. Haas, B.J., et al., *De novo transcript sequence reconstruction from RNA-seq using the Trinity platform for reference generation and analysis*. Nat Protoc, 2013. 8(8): p. 1494-512.
23. Huang, Y., et al., *CD-HIT Suite: a web server for clustering and comparing biological sequences*. Bioinformatics, 2010. 26(5): p. 680-2.
24. Altschul, S.F., et al., *Basic local alignment search tool*. J Mol Biol, 1990. 215(3): p. 403-10.
25. Finn, R.D., et al., *The Pfam protein families database: towards a more sustainable future*. Nucleic Acids Res, 2016. 44(D1): p. D279-85.
26. Wheeler, T.J. and S.R. Eddy, *nhmmer: DNA homology search with profile HMMs*. Bioinformatics, 2013. 29(19): p. 2487-9.
27. Li, B. and C.N. Dewey, *RSEM: accurate transcript quantification from RNA-Seq data with or without a reference genome*. BMC Bioinformatics, 2011. 12: p. 323.
28. Langmead, B. and S.L. Salzberg, *Fast gapped-read alignment with Bowtie 2*. Nat Methods, 2012. 9(4): p. 357-9.
29. Jakob, W., et al., *The Trox-2 Hox/ParaHox gene of Trichoplax (Placozoa) marks an epithelial boundary*. Dev Genes Evol, 2004. 214(4): p. 170-5.
30. Gottlieb, E., et al., *Transgenic mouse model for studying the transcriptional activity of the p53 protein: age- and tissue-dependent changes in radiation-induced activation during embryogenesis*. EMBO J, 1997. 16(6): p. 1381-90.
31. Venkatachalam, S., et al., *Is p53 haploinsufficient for tumor suppression? Implications for the p53+/- mouse model in carcinogenicity testing*. Toxicol Pathol, 2001. 29 Suppl: p. 147-54.
32. Colombel, M., et al., *Androgen suppressed apoptosis is modified in p53 deficient mice*. Oncogene, 1995. 10(7): p. 1269-74.
33. van Boxtel, R., et al., *Homozygous and heterozygous p53 knockout rats develop metastasizing sarcomas with high frequency*. Am J Pathol, 2011. 179(4): p. 1616-22.
34. Derry, W.B., A.P. Putzke, and J.H. Rothman, *Caenorhabditis elegans p53: role in apoptosis, meiosis, and stress resistance*. Science, 2001. 294(5542): p. 591-5.
35. Ollmann, M., et al., *Drosophila p53 is a structural and functional homolog of the tumor suppressor p53*. Cell, 2000. 101(1): p. 91-101.
36. Jin, S., et al., *Identification and characterization of a p53 homologue in Drosophila melanogaster*. Proc Natl Acad Sci U S A, 2000. 97(13): p. 7301-6.
37. Merlo, G.R., et al., *p53-dependent and p53-independent activation of apoptosis in mammary epithelial cells reveals a survival function of EGF and insulin*. J Cell Biol, 1995. 128(6): p. 1185-96.
38. Gjoerup, O., D. Zaveri, and T.M. Roberts, *Induction of p53-independent apoptosis by simian virus 40 small t antigen*. J Virol, 2001. 75(19): p. 9142-55.
39. Lian, F., et al., *p53-independent apoptosis induced by genistein in lung cancer cells*. Nutr Cancer, 1999. 33(2): p. 125-31.
40. Qiu, W., et al., *Growth factors protect intestinal stem cells from radiation-induced apoptosis by suppressing PUMA through the PI3K/AKT/p53 axis*. Oncogene, 2010. 29(11): p. 1622-32.
41. Gross, A., J.M. McDonnell, and S.J. Korsmeyer, *BCL-2 family members and the mitochondria in apoptosis*. Genes Dev, 1999. 13(15): p. 1899-911.

## 2. Experimental studies

---

42. Ashkenazi, A., et al., *From basic apoptosis discoveries to advanced selective BCL-2 family inhibitors*. Nat Rev Drug Discov, 2017. 16(4): p. 273-284.
43. Perini, G.F., et al., *BCL-2 as therapeutic target for hematological malignancies*. J Hematol Oncol, 2018. 11(1): p. 65.
44. Kang, M.H. and C.P. Reynolds, *Bcl-2 inhibitors: targeting mitochondrial apoptotic pathways in cancer therapy*. Clin Cancer Res, 2009. 15(4): p. 1126-32.
45. Wichmann, A., B. Jaklevic, and T.T. Su, *Ionizing radiation induces caspase-dependent but Chk2- and p53-independent cell death in Drosophila melanogaster*. Proc Natl Acad Sci U S A, 2006. 103(26): p. 9952-7.
46. van Bergeijk, P., et al., *Genome-wide expression analysis identifies a modulator of ionizing radiation-induced p53-independent apoptosis in Drosophila melanogaster*. PLoS One, 2012. 7(5): p. e36539.
47. Paulson, J.N., et al., *Tissue-aware RNA-Seq processing and normalization for heterogeneous and sparse data*. BMC Bioinformatics, 2017. 18(1): p. 437.
48. Schuler, M., et al., *p53 induces apoptosis by caspase activation through mitochondrial cytochrome c release*. J Biol Chem, 2000. 275(10): p. 7337-42.
49. Aubrey, B.J., et al., *How does p53 induce apoptosis and how does this relate to p53-mediated tumour suppression?* Cell Death Differ, 2018. 25(1): p. 104-113.
50. Kamm, K., B. Schierwater, and R. DeSalle, *Innate immunity in the simplest animals - placozoans*. BMC Genomics, 2019. 20(1): p. 5.
51. Li, Y., et al., *Mechanistic insights into caspase-9 activation by the structure of the apoptosome holoenzyme*. Proc Natl Acad Sci U S A, 2017. 114(7): p. 1542-1547.
52. Wu, C.C. and S.B. Bratton, *Caspase-9 swings both ways in the apoptosome*. Mol Cell Oncol, 2017. 4(2): p. e1281865.
53. Reubold, T.F., S. Wohlgemuth, and S. Eschenburg, *Crystal structure of full-length Apaf-1: how the death signal is relayed in the mitochondrial pathway of apoptosis*. Structure, 2011. 19(8): p. 1074-83.
54. Jain, A., S. Kaczanowska, and E. Davila, *IL-1 Receptor-Associated Kinase Signaling and Its Role in Inflammation, Cancer Progression, and Therapy Resistance*. Front Immunol, 2014. 5: p. 553.
55. Park, S.L., et al., *HSP70-1 is required for interleukin-5-induced angiogenic responses through eNOS pathway*. Sci Rep, 2017. 7: p. 44687.
56. Park, Y.H., et al., *Hsp70 acetylation prevents caspase-dependent/independent apoptosis and autophagic cell death in cancer cells*. Int J Oncol, 2017. 51(2): p. 573-578.
57. Doong, H., A. Vrailas, and E.C. Kohn, *What's in the 'BAG'?--A functional domain analysis of the BAG-family proteins*. Cancer Lett, 2002. 188(1-2): p. 25-32.
58. Saleh, A., et al., *Negative regulation of the Apaf-1 apoptosome by Hsp70*. Nat Cell Biol, 2000. 2(8): p. 476-83.
59. Ravagnan, L., et al., *Heat-shock protein 70 antagonizes apoptosis-inducing factor*. Nat Cell Biol, 2001. 3(9): p. 839-43.

## Chapter IV

### **New insights into the protein biochemistry of Myc and Max in the placozoan *Trichoplax adhaerens*.**

Rolfes, S.<sup>1</sup>, von der Chevallerie, K.<sup>1</sup>, Curth, U.<sup>2</sup>, Tsiavaliaris, G.<sup>2</sup>, Schierwater, B.<sup>1</sup>

<sup>1</sup> Institute of Animal Ecology, University of Veterinary Medicine Hannover, Foundation, Bünteweg 17d, 30559 Hannover, Germany

<sup>2</sup> Institute for Biophysical Chemistry, OE435, Hannover Medical School, 30623 Hannover, Germany

This manuscript is an authors' version in preparation for submission to *Archives of Biochemistry and Biophysics*

### Abstract

The proto-oncogene *c-myc* encodes the transcription factor Myc that belongs to a family of basic helix-loop-helix leucine-zip (bHLHLZ) proteins. Together with its interaction partner Max, it forms heterodimers in order to bind to specific DNA sequences, thereby regulating a plethora of cellular processes. A malfunction of Myc has been shown to be associated with multiple forms of cancer in humans. Homologs have been found in all metazoan lineages and in unicellular choanoflagellates. Myc and Max homologs are conserved in one of the most primitive metazoan, the placozoan *Trichoplax adhaerens*, enabling the functional and structural characterization of the full-length proteins. This study revealed the first data of the biochemical composition of the taMyc protein and its interaction with taMax in a metazoan animal. Recombinant taMyc and taMax form heterodimers, which are crucial for DNA binding and thus their functional activity as transcription factors. Here, we show that monomeric taMyc exhibits a state with a high intrinsic disorder propensity but also displays significant  $\alpha$ -helical structures. Our results suggest a conserved function of taMyc and taMax proteins from placozoans to vertebrates.

### Introduction

The *myc* oncogene was discovered in 1979 as a retroviral allele (*v-myc*), causing bird myelocytomatosis [1]. Human homologs were later identified and described as a gene family, including *c-myc*, *N-myc* and *L-myc*, with proto-oncogenic potential [2, 3]. Since its discovery, the Myc family has been studied intensively. Its members are linked with human tumors, with 30 % of those tumors showing Myc deregulation. Myc is a transcription factor and mainly involved in cell cycle control. It is estimated to directly regulate up to 15 % of all vertebrate genes [4, 5].

Myc is a basic helix-loop-helix leucine-zip protein (bHLHLZ) which forms heterodimers with other proteins from this family binding the specific DNA enhancer box (E-box) CACGTG [6, 7]. The most prominent binding partner of Myc is the small Myc-associated-factor X (Max) [8, 9]. Dimerization of Myc and Max activates target genes, yet Myc is also associated with transcriptional repression [5]. The bHLHLZ regions of dimeric Myc:Max can further oligomerize forming tetramers. However,

the physiological significance of this higher-order form has not yet been demonstrated [10-12]. Myc proteins consist of a distinctive structure, that contains the C-terminal bHLHLZ motif, but also an N-terminus with four Myc boxes I-IV (MBI-IV) [13]. The best characterized Myc boxes are MBI and MBII. MBI comprises several phosphorylation sites and is involved in ubiquitylation and proteasomal degradation of Myc protein [14]. MBII binds to various key interactors, such as components of histone acetyltransferase complexes, and it is also involved in the Myc protein turnover. The remaining MBIII and MBIV are associated with Myc's cellular-transforming activity, transcription and apoptosis ([15]).

Besides the well-studied vertebrate Myc and Max proteins, homologs have been identified in invertebrates and even in the unicellular choanoflagellate *Monosiga brevicollis* [16]. Myc and Max were also found in the genome of *Trichoplax adhaerens* in 2008 [17], but their mode of interaction has been unclear.

This study presents the first isolation of full-length taMyc and taMax proteins from the placozoan *Trichoplax adhaerens*, and the biochemical and structural characteristics of their interactions. Protein alignments of taMyc and taMax, with respective homologs, revealed highly conserved motifs throughout the metazoan animals. The secondary structure of taMyc and disorder modeling also support this observation. Interaction of recombinantly expressed and purified taMyc and taMax was analyzed by means of microscale thermophoresis and analytical ultracentrifugation. taMyc and taMax form heterodimers, which is the necessary first step before binding to DNA and to be able to partake in transcriptional regulation. This study also highlights the potential of *Trichoplax* as a model organism for evolutionary research on cellular regulatory networks.

### **Material and Methods**

#### *Animal material*

Clonal lineages of *Trichoplax adhaerens* (Grell, H1) were used in this study and cultured under standard conditions as previously described [18, 19]. Animals were fed *ad libitum* with *Pyrenomonas helgolandii*.

### *RNA isolation and cDNA synthesis*

For total RNA isolation, 100 animals were rinsed in artificial seawater (ASW) and starved for 24 hours prior to the experiment. Animals were homogenized in 500  $\mu$ l HOMI buffer (0.1 M Tris HCl pH 8, 0.01 M ethylenediaminetetraacetic acid (EDTA), 0.1 M sodium chloride, 0.025 M dithiothreitol (DTT) and 0.5 % sodium dodecyl sulfate (SDS) in ddH<sub>2</sub>O) with 25  $\mu$ l Proteinase K (10 mg/ml, Carl Roth) for 30 min at 55 °C. RNA was isolated with Phenol/Chlorophorm/Isoamyl alcohol (Roti® Aqua-Phenol/C/I, Carl Roth) and precipitated using isopropanol. The pellet was dissolved in diethylpyrocarbonate-treated (DEPC, Carl Roth, Germany) water and the remaining DNA was digested with DNase I (Fermentas) according to the manufacturer's instructions. The RNA quality was measured through gel electrophoresis and 100 ng RNA was used for a full-length cDNA synthesis with BioScript™ Reverse Transcriptase (Bioline), following the manufacturer's protocol.

### *Amplification of full-length tamyc and tamax genes and plasmid construction*

The full-length genes *tamyc* and *tamax* were amplified from full-length cDNA using the Phusion® High-Fidelity DNA polymerase (NEB) for subsequent cloning into protein expression vectors (see below). The primers used for amplification are listed in table A2.1. The following PCR parameters were used to amplify target sequences: 3 min - 98°C, 35 cycles of (10 sec - 98 °C, 30 sec - 60 °C, 1 min - 72 °C) and 5 min - 72 °C. The PCR products were precipitated and cloned into pGEM®-T vector system (Promega) for sequencing. Appropriate clones were identified and both genes were cut out of the vector using HindIII and NotI (both Fermentas) for *tamax*, and BamHI and XhoI (both Fermentas) for *tamyc*. After the insertion of *tamyc* into pET23a-YFP-mcs (provided by G. Tsiavaliaris) and *tamax* into pETDuet-1™ (Novagen), the plasmids were transformed into *Escherichia coli* (One Shot® TOP10F' Chemically Competent *E. coli*, Invitrogen). Colonies were selected by means of chloramphenicol and ampicillin resistance and plasmids were verified via PCR, using gene specific primer sets as mentioned previously (Tab. A2.1).

### *Expression and purification of taMyc and taMax proteins*

Constructs of pET23a-YFP/*tamyc* and pETDuet-1/*tamax* were each transformed into

## 2. Experimental studies

---

Rosetta (BL21), F-opmT hsdSB (rB- mB-) gal dcm pRARE (*Cam<sup>R</sup>*). Bacteria were grown overnight in 300 ml LB broth medium (with 35 ng/ml chloramphenicol and 75 ng/ml ampicillin) at 37 °C with orbital agitation. The pre-cultures were inoculated into six liters of LB broth medium each and grown with agitation to an optical density of 0.4 – 0.8, measured at 600 nm. Protein over-expression was induced using isopropyl- $\beta$ -D-thiogalactoside (IPTG, 0.4 mM for taMyc, 0.1 mM for taMax) and the preparatory bacteria cultures were cultivated at 20 °C for 16 h with agitation. Cells were harvested and resuspended in lysis buffer (50 mM 4-(2-hydroxyethyl)-1-piperazineethanesulfonic acid (HEPES), pH 7.4, 3 mM benzamidine and 3 mM 2-Mercaptoethanol), with protease inhibitor cocktail tablets (cOmplete Tablets EDTA-free, EASYpack, Roche) and 5 mg/100 ml lysozyme (Carl Roth). Samples were incubated for 30 min on ice and were sonicated for 3 min in total (Branson Sonifier 250, Heinemann Ultraschall und Labortechnik). Lysates were subsequently incubated with Benzoase (5000 units, Sigma) for 30 min on ice and cleared by centrifugation at  $39,191 \times g$  (Avanti™ J30I, JA-30.50 Ti, Beckmann Coulter) for 60 min at 4 °C. Supernatants were collected, filtered and loaded on a nickel NTA column (Ni-NTA Superflow, Qiagen) and affinity chromatography was performed at 4 °C in an ÄKTA purifier (FPLC system ÄKTA purifier 10, GE Healthcare). After column equilibration with buffer A (50 mM HEPES, pH 7.4, 100 mM sodium chloride, 3 mM 2-Mercaptoethanol, flow rate 3 ml/min, 6 column volume), proteins were injected (0.5 ml/min) and washed with buffer A (flow rate 3 ml/min, 5 column volume). Then the columns were washed with buffer B (50 mM HEPES, pH 7.4, 500 mM sodium chloride, 3 mM 2-Mercaptoethanol, flow rate 3 ml/min, column volume), followed by washing with buffer A (flow rate 3 ml/min, 5 column volume). Before elution, the columns were washed with 10 % elution buffer (50 mM HEPES, pH 7.4, 100 mM sodium chloride, 1 M imidazole, 3 mM 2-Mercaptoethanol, flow rate 3 ml/min, 5 column volume). Elution was carried out in a gradient-like fashion until elution buffer reached 100 % (flow rate 1 ml/min). The protein elution was fractionated (Frac-900, GE Healthcare) and checked on a 12 % SDS polyacrylamide gel. The proteins were further purified by gel permeation chromatography (ÄKTA system, mentioned above) on a HiLoad 26/60 Superdex 200 PG (GE Healthcare) and equilibrated in storage buffer (50 mM Tris-HCl, pH 7.5, 100 mM sodium chloride,

1 mM DTT, 3 mM benzamidine). Fractions were checked on an SDS polyacrylamide gel and purified proteins were concentrated using VIVASPIN 20 Centrifugal Concentrators (Sartorius Stedim Biotech).

### *Sequence analyses*

The sequences of taMyc and taMax were obtained from the full-length gene amplification (as described above). The DNA sequences were translated into amino acid sequences and collated with protein predictions from the National Center for Biotechnology Information, Bethesda, Maryland (NCBI). After downloading the protein sequences of c-Myc from *Homo sapiens* (human) (GenBank accession no. NP\_002458.2), *Gallus gallus* (chicken) (GenBank accession no. NP\_001026123.1) and *Hydra vulgaris* Myc1 (GenBank accession no. GQ856263.1), as well as respective sequences of Max (GenBank accession nos.: human NP\_002373.3, chicken P52162.1, *Hydra* ACX32069.1), alignments and sequence analyses with taMyc (XP\_002113957) and taMax (XP\_002107861) were performed using Geneious v.8.1.7 and the therein implemented ClustalW software [20]. The manual modifications were carried out according to Hartl et al. [21].

### *Protein disorder prediction and Circular Dichroism Spectroscopy*

Predictions of natively disordered regions of taMyc and taMax were performed with the respective amino acid sequences using the Protein DisOrder prediction System (PrDOS) online server [22].

For circular dichroism spectroscopy (CD), the taMyc storage buffer was replaced with a CD buffer (100 mM sodium chloride, 25 mM NaH<sub>2</sub>PO<sub>4</sub> and 0.1 mM TCEP, pH 7.6) overnight at 4 °C. Because aggregations have been observed, samples were centrifuged at 13.000 rpm at 4 °C. The supernatant was used for further experiments. 150 µl samples were prepared for measurement with 2.5 µM taMyc in CD buffer. The samples were stored at room temperature for 30 min prior to measurement, to ensure proper protein folding and functionality. The CD data was collected on an Applied Photophysics PiStar-180 Circular Dichroism spectrometer in a 3 mm path-length quartz glass cell at 20 °C and spectra were measured in the wavelength region between 260 and 190 nm at 0.2 increments, for 1.5 seconds. The



resulting spectrum is the average of three scans with CD buffer as the control spectrum (measured three times) subtracted. The protein's secondary structure content was calculated with the CDSSTR algorithm [23, 24] and reference data set 4 [25], which is available on the DichroWeb server [26, 27].

### *Microscale thermophoresis*

Prior to microscale thermophoresis (MST), respective protein storage buffers were exchanged by dialysis (50 mM Tris-HCl, pH 7.5, 100 mM sodium chloride, 1 mM DTT, 3 mM benzamidine), to remove any remaining glycerol. Differently coated capillaries were tested using 500 nM taMyc in a Monolith NT.115 microscale thermophoresis spectrometer (NanoTemper, Munich, Germany). The hydrophilic capillaries performed best and were used in further experiments. taMax was titrated to 500 nM taMyc, in following concentrations (nM): 10, 20, 50, 100, 200, 500, 1000, 5000 and measurements were carried out in triplets with a laser power of 40 %. The data was analyzed using Origin v.2018b and fitted by both quadratic and Hill functions.

### *Analytical ultracentrifugation*

The storage buffers of taMyc and taMax, respectively were substituted by CD buffer to minimize signal artifacts. Analytical ultracentrifugation (AUC) experiments were performed in a ProteomeLab™ XL-1 centrifuge with an An50Ti rotor (both Beckman Coulter). For the determination of sedimentation coefficients, 400 µl protein solutions (3 µM and 12 µM taMyc each and 33 µM and 112 µM taMax, respectively) were applied to the sample sector and 400 µl CD buffer was placed in the reference sector. The system was cooled down to 4 °C and the rotor was accelerated to 50,000 rpm. Data were collected at 280 nm using the installed absorbance detection. For co-sedimentation experiments, 12 µM taMyc and 6 µM, 12 µM and 24 µM taMax, were centrifuged in the same sample vector according to settings described above, respectively. The absorption of the sample was obtained as a function of the radial position and the centrifuge was programmed with the ProteomeLab™ (Beckman Coulter). The SEDFIT program [28] uses a model for diffusion-corrected differential sedimentation coefficient distributions ( $c(s)$  distributions), which was also used to evaluate the measured data. In  $c(s)$  distributions, the absorbance of a

specific protein complex species is exhibited by areas under the separate peaks and therefore can be used to determine binding isotherms [29].

### Results and Discussion

#### *Conservation of the taMyc and taMax proteins*

Sequencing of full-length *tamyc* and *tamax* genes revealed coding sequences (CDS) with a size of 966 bp (*tamyc*) and 501 bp (*tamax*), respectively, which corroborates with former predictions [17]. The 5' untranslated region (UTR) of *tamyc* encompasses 135 bp, contains a 4125 bp intron and an alternative start methionine 33 bp prior to the predicted start. In contrast, *tamax* has a 5' UTR with a size of 150 bp and a 437 bp intron [51]. The alternative start methionine in the 5' UTR of *tamyc* indicates different protein isoforms that were also found in the *Trichoplax* transcriptome and may indicate an additional type of control gene expression [30]. By comparing the taMyc amino acid sequence to human and chicken c-Myc and *Hydra* Myc1, a conserved bHLHLZ motif was identified, as well as all four N-terminal Myc-boxes (MBI-IV) (Fig. 2.5A). The overall genetic distance between taMyc and human c-Myc, based on the amino acid sequence identity, amounts to 26.06 %, 27.73 % chicken and 18.36 % *Hydra* proteins. The highest sequence identity was found between taMyc and the human protein in MBIIIa and MBIIIb (66.67 % and 87.50 %). Comparison between taMyc and the diploblastic *Hydra* Myc1 shows sequence identities lower than 30 % in all conserved regions except for MBIIIb (37.50 %) (Tab. A2.3). Sequence analyses revealed a conserved exon-intron structure of Myc proteins, with taMyc and *Hydra* Myc1 containing an additional intron [21]. Compared to known homologs, the bHLHZ motif in taMyc possesses a glutamic acid residue at position 302, and seven leucine residues instead of the crucial octameric leucines. These substitutions may lead to differences in its dimerization ability with taMax. Yet, two important arginine residues were found at the C-terminus of taMyc (Arg<sub>305-306</sub>) that are known to mediate binding specificity in human Myc (Arg<sub>423-424</sub>) and Max proteins [10] That might compensate for the amino acid substitution in the bHLHLZ domain. The taMax protein is less than half the size of taMyc and more conserved throughout the analyzed species (Fig. 2.5B). The overall sequence identities of taMax, human, chicken and *Hydra* sequences, amounts to 43.53 %, 43.53 %, 43.53 % and 43.53 %, respectively.

## 2. Experimental studies

44.71 % and 43.18 % respectively. The bHLHLZ motif comprises the biggest part of the protein. A sequence identity of 47.48 % was detected between taMax and human Max (Tab. A2.3). These findings propose similar functions for taMyc and taMax, like dimerization and binding to enhancer boxes in order to activate or suppress target genes known from higher animals [31]. To test these hypotheses experimental data are needed and we suggest to use *Trichoplax adhaerens* as a suitable model organism for such studies.

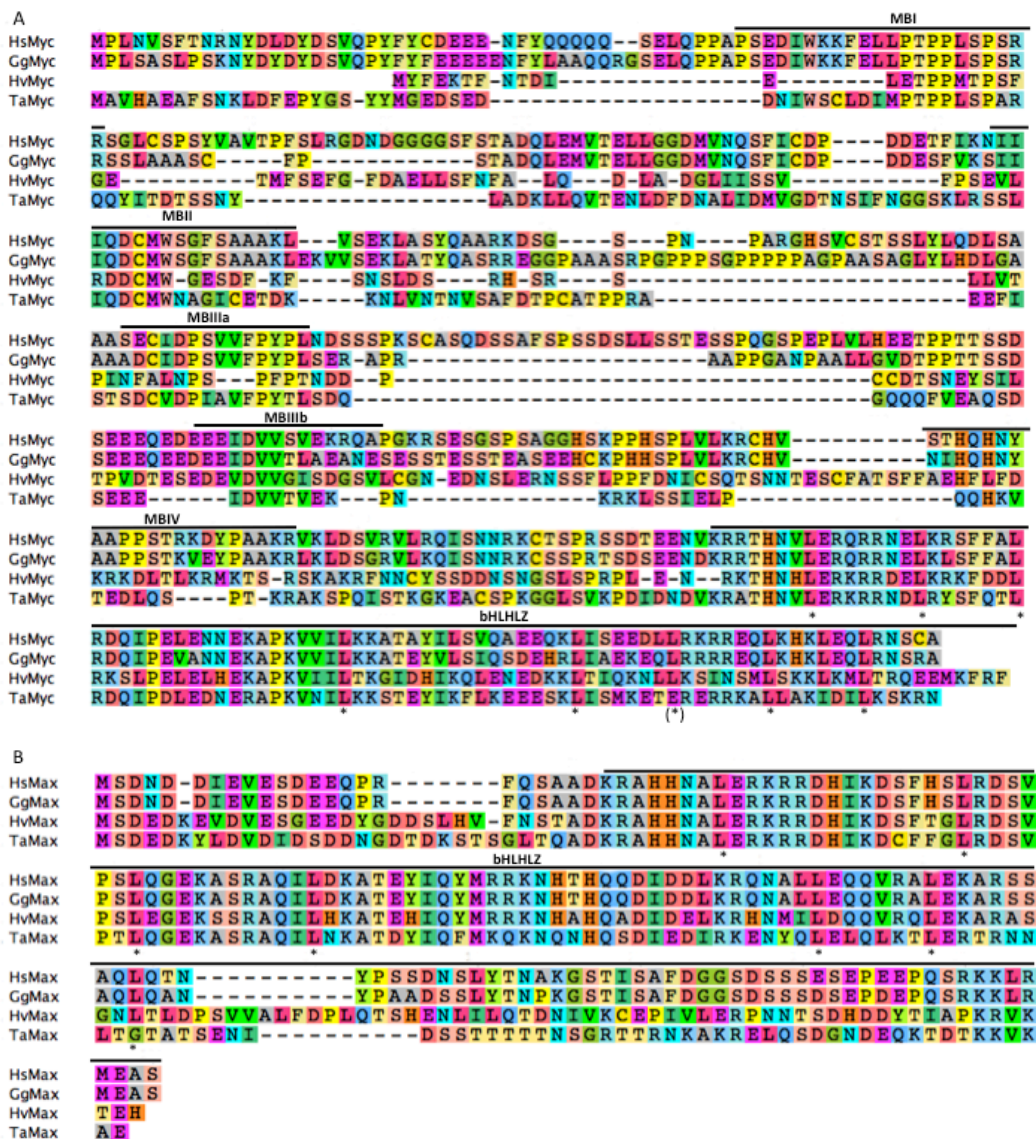


**Figure 2.5: Alignment of amino acid sequences of *Trichoplax* taMyc and taMax proteins with their homologs from human, chicken and *Hydra*.**

(A) Myc protein alignment, GenBank accession nos.: Hs c-Myc: NP\_002458.2, Gg Myc: NP\_001026123.1, Hv Myc1: GQ856263.1, Ta taMyc: XP\_002113957 (B) Max protein alignment, GenBank accession nos.: Hs Max: NP\_002373.3, Gg Max: P52162.1, Hv Max: ACX32069.1, Ta taMax: XP\_002107861. Alignments were generated with ClustalW algorithm implemented in Geneious v8.1.7 and adjusted manually. Gaps are indicated by dashes, the Myc boxes (MB) I-IV and the bHLHL-zip motifs are highlighted. Conserved

## 2. Experimental studies

leucine residues in the bHLH motif are marked by asterisks.

### *Expression and purification of full-length recombinant taMyc and taMax*

For the first time, the recombinant full-length proteins taMyc, containing both 6His and YFP tags, and 6His-tagged taMax, have been successfully expressed with inducible T7 expression vectors in *E. coli* BL21(DE3)pLysS (Fig. 2.6). 6His-taMax was more successful with regards to expression than 6His-YFP-taMyc, which showed low solubility. Soluble 6His-YFP-taMyc displayed degradation and was truncated at its C-terminus (data not shown). Both proteins were purified using nickel-affinity chromatography and gel permeation chromatography, yet they contained 10-20 % bacterial protein contamination. In order to improve purification results, protein preparation with a different tag should be considered to enhance the solubility [32]. The theoretical molecular weight of 6His-YFP-taMyc is 65.4 kDa and 20.5 kDa for 6His-taMax. However, both purified proteins show higher molecular weights (Fig. 2.6). The high amount of degraded 6His-YFP-taMyc protein is consistent with former studies [33-35]. Even purifications of the full-length proteins, under denaturing conditions from inclusion bodies, have led to considerable quantities of degraded c-Myc protein. This was most likely caused by hampered translation processes [36]. Reasons for partially degraded human c-Myc proteins were the high overall proline content (8 %) and an arginine-enriched C-terminus. Both are known to cause a strong bias in codon usage between human cells and bacteria, in which the proteins were recombinantly expressed [36]. Albeit the proline content of the *Trichoplax* Myc protein (6 %) is slightly lower than in humans, it holds a similar level of almost 14 % arginine residues (Fig. 2.5A) [36], making it also prone to codon bias and shortage of specific tRNAs during translation.

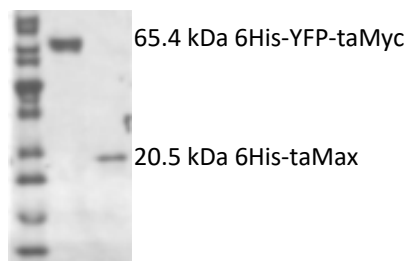


**Figure 2.6: Expression of taMyc and taMax proteins.**

SDS-PAGE of the recombinantly expressed and purified 6His-YFP-taMyc (65.4 kDa) and 6His-taMax (20.5 kDa) proteins.

### *Structural characterization of taMyc and taMax*

Since human c-Myc and Max proteins are known to have a high tendency for being unordered and lacking conformations [37, 38], *Trichoplax* taMyc and taMax amino acid sequences were analyzed in terms of their intrinsic structure. Prior to experimental structural characterization, the theoretical protein disorder probabilities were calculated for both proteins using the PrDOS algorithm [22]. Calculations were performed for 6His-YFP-taMyc, 6His-taMax, taMyc and taMax (Fig. 2.7). More than 50 % of both taMax and 6His-taMax amino acid sequences display high disorder probabilities which have almost 20 % more disordered regions than taMyc and 6His-YFP-taMyc (Tab. A2.4-A2.7). The disorder probability of taMyc is 9 % higher than 6His-YFP-taMyc (39.56 % vs 30.86 %), which is most likely due to its YFP tag. The low propensity of conformation in the *Trichoplax* proteins are in line with Myc and Max characteristics throughout the animal kingdom [39]. Predictions of disorder probabilities of single amino acid residues within the proteins have shown lower scores in the conserved motifs (MBI-IV and bHLHLZ) [39], which also coincide with PrDOS modeling of both *Trichoplax* proteins. Interestingly, the intrinsically disordered N-terminus of human c-Myc is prone to mutations, leading to cancer-related amino acid substitutions [40-42]. These mutations likely decrease conformation within the protein, causing malfunctions ([39] and references therein). This disordered N-terminus already emerged at the base of Metazoa or even in unicellular relatives as homologs were found in *Monosiga brevicollis* and *Capsaspora owczarzaki* [16].

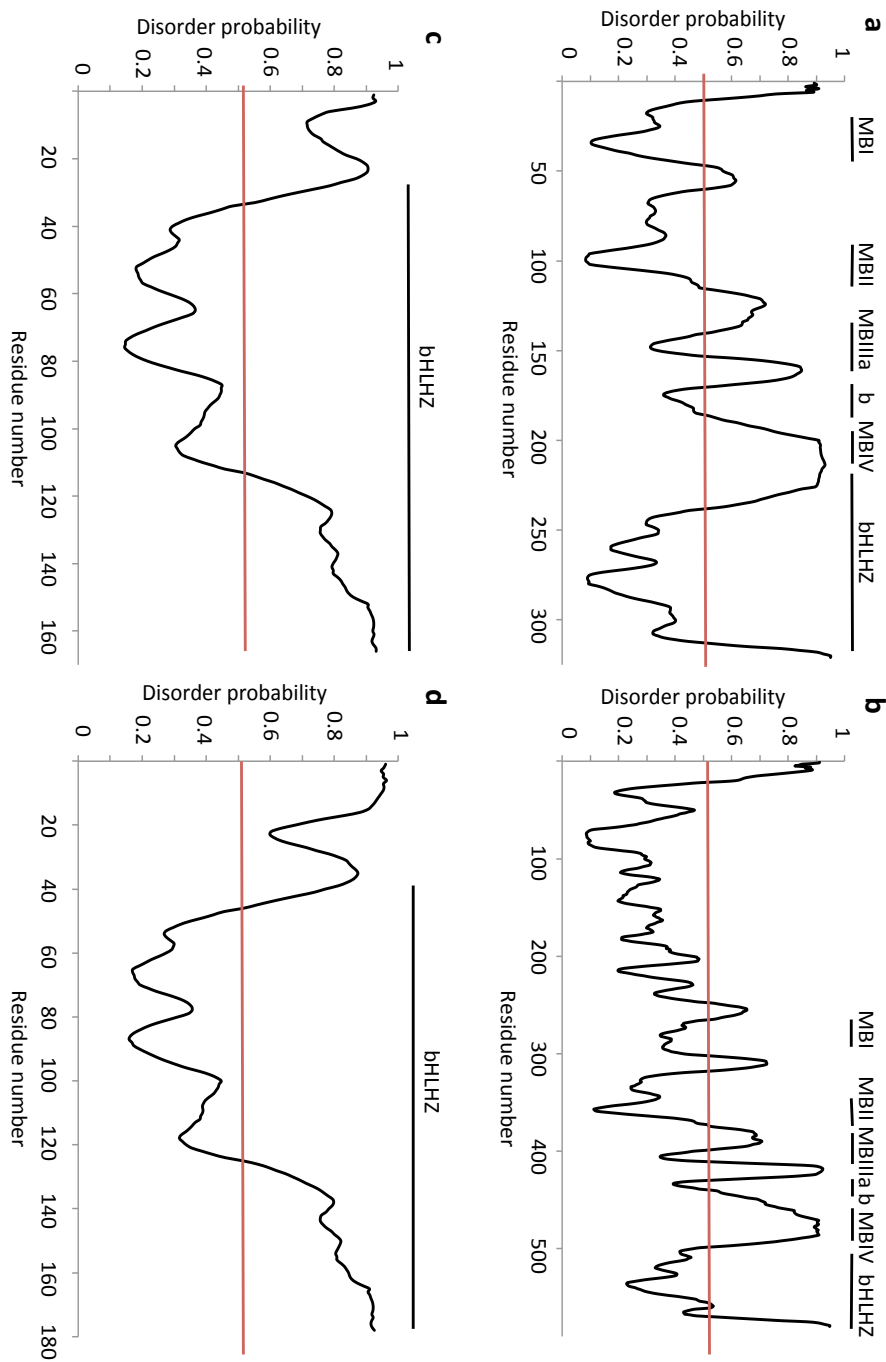


**Figure 2.7: Disorder probabilities of taMyc and taMax.**

Disorder probabilities of taMyc (a), 6His-YFP-taMyc (b), taMax (c) and 6His-taMax (d) have been modeled with the PrDOS software. The disorder probability is plotted against the amino acid sequence and the red line marks the threshold. Every amino acid above 0.5 (50 %) is anticipated to be unordered whereas everything below is supposed to be structured. (a) The N-terminus of taMyc, containing the Myc boxes (MBI-MBIV), shows a higher amount of unordered amino acids than the C-terminal; (b) the ordered region at 6His-YFP-taMyc's N-terminus contains the YFP-tag. (c, d) The overall amount of disordered amino acids in taMax and 6His-taMax is higher than in taMyc and ordered regions are only detected in the middle of the protein and start of the bHLHZ motif.

Structural information for human c-Myc is only available for some specific motifs within the protein, although the function of human c-Myc and its interaction with other proteins depends on its structure. So far, crystallization attempts of the full-length protein monomer failed due to its intrinsic disorder [39]. It is important to understand the structural characteristics of the Myc protein in basal metazoans with respect to the evolution of bHLHLZ transcription factors, if we seek better understanding of key regulators in the cell cycle and homeostasis [4, 5]. Therefore, the different proportions of secondary structures within 6His-YFP-taMyc full-length protein were measured via CD spectrometry and calculated by DirchoWeb's CDSSTR algorithm [23, 24, 26, 27] with reference data set 4 [25] (Fig. 2.8; Tab. 2.4). 6His-YFP-taMyc consists of 14 %  $\alpha$ -helices, 30 %  $\beta$ -strands and 24 % turns. 32 % of the protein's amino acids do not belong to any ordered secondary structure. The measured data differ only 1 % from the predicted disorder probability (Tab. A2.5). These results are in contrast to the significant propensity of disordered protein regions (as described earlier [39]), but can be explained when compared to the human c-Myc:Max heterodimer (containing the C-terminal bHLHLZ domain). The truncated heterodimers consist of 70 %  $\alpha$ -helices in structured coiled-coil formations. This number increases to up to 84 % when binding to DNA [43, 44]. However, studies from Lavigne et al. [45] already indicated a strong buffer bias for both human c-Myc bHLHLZ motif and for the c-Myc:Max heterodimer. Especially c-Myc's association with tumor formation pleads for new therapeutic strategies and amino acid residues in the highly disordered N-terminus seem to be suitable candidates for small-molecule inhibitors [44, 46]. Although computationally generated structure information is easily available, it cannot imitate physiological conditions. Experimental characterization is therefore necessary. The data from basal metazoans will further help to understand the evolution of these proteins and might give new impulses for applied research.

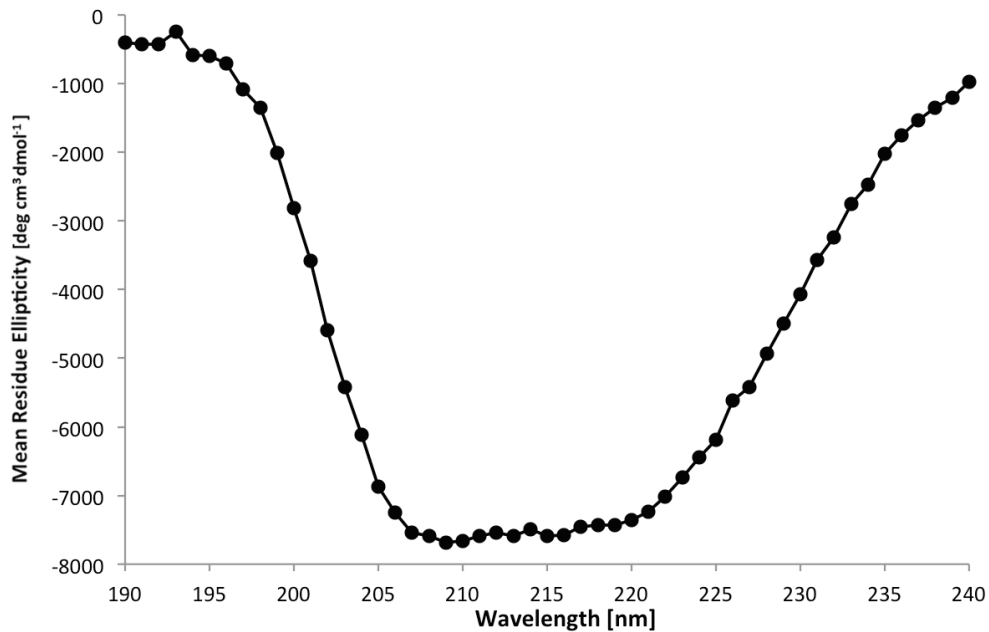


**Figure 2.8 Far-ultraviolet circular dichroism of 6His-YFP-taMyc.**

Mean residue ellipticity at 20 °C is plotted as a function of wavelength with a total concentration of 2.5  $\mu$ M 6-His-YFP-taMyc. Secondary structures have been calculated with the CDSSTR algorithm at the DichroWeb server. 6His-YFP-taMyc contains 14 %  $\alpha$ -helices, 30 %  $\beta$ -strands, 24 % turns and 32 % unordered regions.

**Table 2.4: Ratio of secondary structures within the 6His-YFP-taMyc protein.**

The ratio of secondary structures within the tagged *Trichoplax* 6His-YFP-taMyc protein was measured by CD-spectrometry at 20 °C and calculated with the CDSSTR algorithm at the DichroWeb server.

$\alpha$ -helices	$\beta$ -strands	Turns	Unordered
14 %	30 %	24 %	32 %

### *Binding affinities of taMyc and taMax*

Myc and Max proteins belong to the family of bHLHLZ transcription factors, which form homo- (Max:Max) and heterodimers (c-Myc:Max) in order to bind to DNA [5, 7, 8]. Little data is available from early branching metazoans, except for *Hydra* Myc and Max proteins [21, 47]. Information on dimer formation of the full-length proteins from *Trichoplax* will further help to shed light on their evolution.

The recombinant expressed and purified full-length proteins 6His-YFP-taMyc and 6His-taMax formed heterodimers during sedimentation experiments in an analytical ultracentrifugation experiment at 4 °C (Fig. 2.9). Monomeric 6His-YFP-taMyc has a sedimentation coefficient of 2 S (Fig. 2.9). Unfortunately, no data is available for 6His-taMax protein thus far.



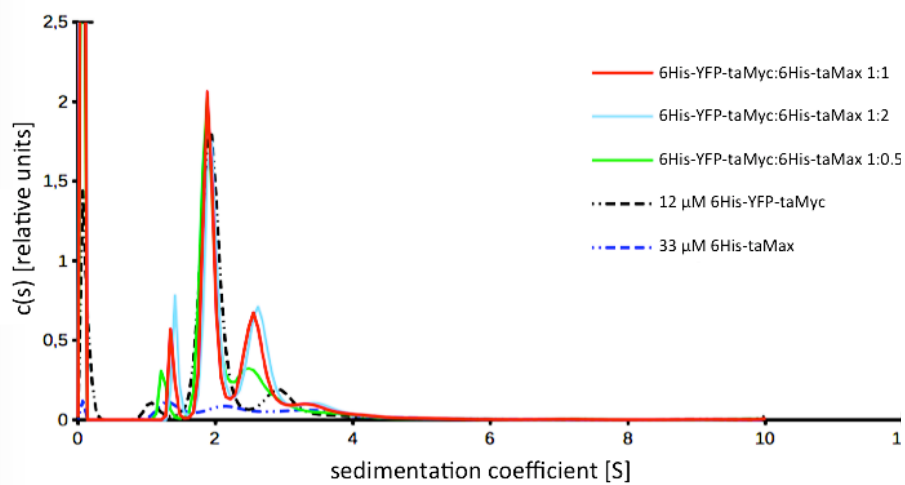


**Figure 2.9: Sedimentation of 6His-YFP-taMyc:6His-taMax heterodimers and 6His-YFP-taMyc and 6His-taMax monomers by analytical ultracentrifugation.**

The sedimentation velocity ( $c(s)$ ) is plotted against the sedimentation coefficient to determine the interaction level of 6His-YFP-taMyc:6His-taMax. 6His-YFP-taMyc is constantly held at  $12\ \mu\text{M}$  whereas 6His-taMax was added in different concentrations. The appearance of new peaks at 1.5 S and 2.5 S after adding 6His-taMax to 6His-YFP-taMyc, indicate heterodimerization. Monomeric 6His-YFP-taMyc (black dashed line) exhibits a sedimentation coefficient of 2 S but no value can be assigned for monomeric 6His-taMax (blue dashed line) with the used concentration of  $33\ \mu\text{M}$ .

The protein-protein binding between 6His-YFP-taMyc and 6His-taMax was further investigated at room temperature by means of MST. 6His-YFP-Myc concentration was set to  $500\ \text{nM}$  and titrated with increasing concentrations of 6His-taMax. Figure 2.10 shows the fitted binding curves of 6His-YFP-taMyc:6His-taMax heterodimers. The titration of unlabeled 6His-taMax results in a gradual shift in thermophoresis, which is plotted as normalized fluorescence. The dissociation constant ( $K_d$ ) of the recombinant 6His-YFP-taMyc:6His-taMax complex was calculated by both the Hill and quadratic functions [48] and amounts to  $100 \pm 10\ \text{nM}$ . The high variability within the  $K_d$  values of known Myc fragments (mostly human) makes a classification of the measured *Trichoplax* Myc:Max  $K_d$  value challenging. Former studies that targeted the kinetics of homo- and heterodimer formation of human Myc and Max proteins concentrated on the bHLHLZ motif [44, 49, 50]. Even within these studies, the dissociation constants differed immensely from  $K_d = 6\ \text{nM}$  [44] to  $K_d = 460\ \mu\text{M}$  [50]. Interestingly, slightly different constructs as well as different buffer conditions and

analytical methods seem to lead to a high variability in data. Albeit the  $K_d$  value of the full-length 6His-YFP-taMyc:6His-taMax heterodimer gives a better idea of the interaction of these proteins, more data is needed. Future studies should focus on increasing the understanding of the co-evolution of Myc and Max proteins, for instance, by studying taMyc without a probably interfering YFP-tag.

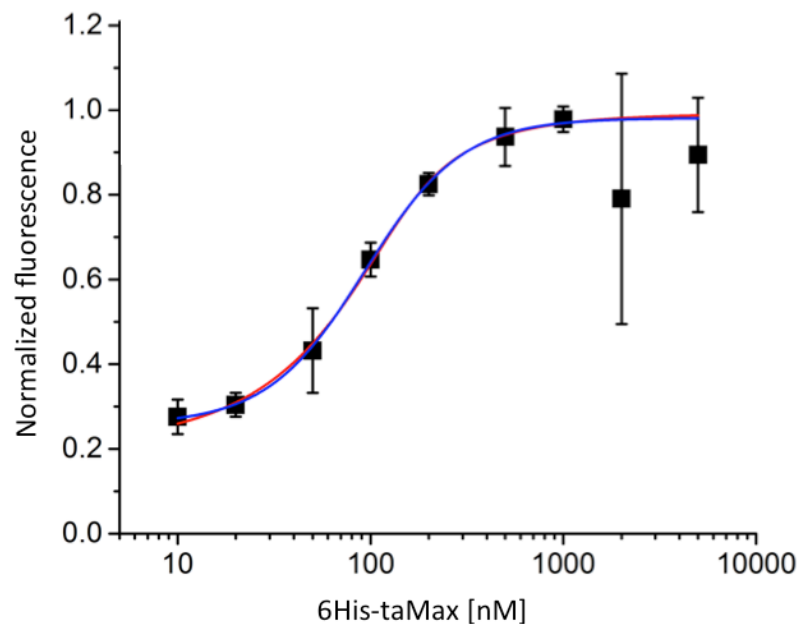


**Figure 2.10: 6His-YFP-taMyc:6His-taMax interaction measured by microscale thermophoresis.**

To determine the affinity of the binding reaction, a titration series (10 nM to 5000 nM) of 6His-taMax was performed while 6His-YFP-taMyc was kept at a constant concentration of 500 nM. The change in the thermophoretic signal leads to a  $K_d = 100 \pm 10$  nM. The blue line exhibits the Hill function fit, the red line shows the quadratic fit.

### Conclusion

taMyc and taMax proteins in placozoans contain important conserved areas for protein interaction and DNA-binding, suggesting similar roles in cell cycle control and homeostasis as known from morphological more complex animals. First kinetic and structural insights of the purified full-length proteins *in vitro*, confirm their mutual interaction but the poor stability of the taMyc protein hampers experimental studies. Future studies on these proteins from *Trichoplax* should focus on their DNA-binding ability to stabilize the taMyc:taMax heterodimers, in order to get a better understanding of the evolution of these essential transcription factors.

### Acknowledgements

SR was funded by an 'Otto Bütschli' scholarship from the University of Veterinary Medicine Hannover, Foundation and a PhD Completion Grant from the Leibniz University Hannover. We acknowledge support from the German Science Foundation (DFG Schi-277/26, Schi-277/27, Schi-277/29).

### Supplementary data

Further information related to this chapter can be found in the appendix and digital appendix of this thesis.

### References

1. Sheiness, D. and J.M. Bishop, *DNA and RNA from uninfected vertebrate cells contain nucleotide sequences related to the putative transforming gene of avian myelocytomatosis virus*. J Virol, 1979. 31(2): p. 514-21.
2. Dalla-Favera, R., et al., *Human c-myc onc gene is located on the region of chromosome 8 that is translocated in Burkitt lymphoma cells*. Proc Natl Acad Sci U S A, 1982. 79(24): p. 7824-7.
3. Nesbit, C.E., J.M. Tersak, and E.V. Prochownik, *MYC oncogenes and human neoplastic disease*. Oncogene, 1999. 18(19): p. 3004-16.
4. Luscher, B. and J. Vervoorts, *Regulation of gene transcription by the oncoprotein MYC*. Gene, 2012. 494(2): p. 145-60.
5. Eilers, M. and R.N. Eisenman, *Myc's broad reach*. Genes Dev, 2008. 22(20): p. 2755-66.
6. Luscher, B. and L.G. Larsson, *The basic region/helix-loop-helix/leucine zipper domain of Myc proto-oncoproteins: function and regulation*. Oncogene, 1999. 18(19): p. 2955-66.
7. Grandori, C., et al., *The Myc/Max/Mad network and the transcriptional control of cell behavior*. Annu Rev Cell Dev Biol, 2000. 16: p. 653-99.
8. Blackwood, E.M. and R.N. Eisenman, *Max: a helix-loop-helix zipper protein that forms a sequence-specific DNA-binding complex with Myc*. Science, 1991. 251(4998): p. 1211-7.
9. Blackwood, E.M., et al., *The Myc:Max protein complex and cell growth regulation*. Cold Spring Harb Symp Quant Biol, 1991. 56: p. 109-17.
10. Nair, S.K. and S.K. Burley, *X-ray structures of Myc-Max and Mad-Max recognizing DNA. Molecular bases of regulation by proto-oncogenic transcription factors*. Cell, 2003. 112(2): p. 193-205.
11. Walhout, A.J., et al., *c-Myc/Max heterodimers bind cooperatively to the E-box sequences located in the first intron of the rat ornithine decarboxylase (ODC) gene*. Nucleic Acids Res, 1997. 25(8): p. 1493-501.
12. Lebel, R., et al., *Direct visualization of the binding of c-Myc/Max heterodimeric b-HLH-LZ to E-box sequences on the hTERT promoter*. Biochemistry, 2007. 46(36): p. 10279-86.

13. Henriksson, M. and B. Luscher, *Proteins of the Myc network: essential regulators of cell growth and differentiation*. Adv Cancer Res, 1996. 68: p. 109-82.
14. Oster, S.K., et al., *Functional analysis of the N-terminal domain of the Myc oncoprotein*. Oncogene, 2003. 22(13): p. 1998-2010.
15. Conacci-Sorrell, M., L. McFerrin, and R.N. Eisenman, *An overview of MYC and its interactome*. Cold Spring Harb Perspect Med, 2014. 4(1): p. a014357.
16. Young, S.L., et al., *Premetazoan ancestry of the Myc-Max network*. Mol Biol Evol, 2011. 28(10): p. 2961-71.
17. Srivastava, M., et al., *The Trichoplax genome and the nature of placozoans*. Nature, 2008. 454(7207): p. 955-60.
18. Schierwater, B. and K. Kuhn, *Homology of Hox genes and the zootype concept in early metazoan evolution*. Mol Phylogenet Evol, 1998. 9(3): p. 375-81.
19. Schierwater, B., *My favorite animal, Trichoplax adhaerens*. Bioessays, 2005. 27(12): p. 1294-302.
20. Thompson, J.D., D.G. Higgins, and T.J. Gibson, *CLUSTAL W: improving the sensitivity of progressive multiple sequence alignment through sequence weighting, position-specific gap penalties and weight matrix choice*. Nucleic Acids Res, 1994. 22(22): p. 4673-80.
21. Hartl, M., et al., *Stem cell-specific activation of an ancestral myc protooncogene with conserved basic functions in the early metazoan Hydra*. Proc Natl Acad Sci U S A, 2010. 107(9): p. 4051-6.
22. Ishida, T. and K. Kinoshita, *PrDOS: prediction of disordered protein regions from amino acid sequence*. Nucleic Acids Res, 2007. 35(Web Server issue): p. W460-4.
23. Compton, L.A. and W.C. Johnson, Jr., *Analysis of protein circular dichroism spectra for secondary structure using a simple matrix multiplication*. Anal Biochem, 1986. 155(1): p. 155-67.
24. Manavalan, P. and W.C. Johnson, Jr., *Variable selection method improves the prediction of protein secondary structure from circular dichroism spectra*. Anal Biochem, 1987. 167(1): p. 76-85.
25. Sreerama, N. and R.W. Woody, *Estimation of protein secondary structure from circular dichroism spectra: comparison of CONTIN, SELCON, and CDSSTR methods with an expanded reference set*. Anal Biochem, 2000. 287(2): p. 252-60.
26. Whitmore, L. and B.A. Wallace, *DICHROWEB, an online server for protein secondary structure analyses from circular dichroism spectroscopic data*. Nucleic Acids Res, 2004. 32(Web Server issue): p. W668-73.
27. Whitmore, L. and B.A. Wallace, *Protein secondary structure analyses from circular dichroism spectroscopy: methods and reference databases*. Biopolymers, 2008. 89(5): p. 392-400.
28. Schuck, P., *Size-distribution analysis of macromolecules by sedimentation velocity ultracentrifugation and lamm equation modeling*. Biophys J, 2000. 78(3): p. 1606-19.
29. Witte, G., R. Fedorov, and U. Curth, *Biophysical analysis of Thermus aquaticus single-stranded DNA binding protein*. Biophys J, 2008. 94(6): p. 2269-79.

30. Cenik, C., et al., *Genome-wide functional analysis of human 5' untranslated region introns*. *Genome Biol*, 2010. 11(3): p. R29.
31. Blackwell, T.K., et al., *Sequence-specific DNA binding by the c-Myc protein*. *Science*, 1990. 250(4984): p. 1149-51.
32. Hengen, P., *Purification of His-Tag fusion proteins from Escherichia coli*. *Trends Biochem Sci*, 1995. 20(7): p. 285-6.
33. Watt, R.A., A.R. Shatzman, and M. Rosenberg, *Expression and characterization of the human c-myc DNA-binding protein*. *Mol Cell Biol*, 1985. 5(3): p. 448-56.
34. Kato, G.J., et al., *Max: functional domains and interaction with c-Myc*. *Genes Dev*, 1992. 6(1): p. 81-92.
35. Reddy, C.D., et al., *Mutational analysis of Max: role of basic, helix-loop-helix/leucine zipper domains in DNA binding, dimerization and regulation of Myc-mediated transcriptional activation*. *Oncogene*, 1992. 7(10): p. 2085-92.
36. Farina, A., F. Faiola, and E. Martinez, *Reconstitution of an E box-binding Myc:Max complex with recombinant full-length proteins expressed in Escherichia coli*. *Protein Expr Purif*, 2004. 34(2): p. 215-22.
37. Liu, J., et al., *Intrinsic disorder in transcription factors*. *Biochemistry*, 2006. 45(22): p. 6873-88.
38. Xue, B., et al., *Protein intrinsic disorder and induced pluripotent stem cells*. *Mol Biosyst*, 2012. 8(1): p. 134-50.
39. Mahani, A., J. Henriksson, and A.P. Wright, *Origins of Myc proteins--using intrinsic protein disorder to trace distant relatives*. *PLoS One*, 2013. 8(9): p. e75057.
40. McEwan, I.J., et al., *Functional interaction of the c-Myc transactivation domain with the TATA binding protein: evidence for an induced fit model of transactivation domain folding*. *Biochemistry*, 1996. 35(29): p. 9584-93.
41. Andresen, C., et al., *Transient structure and dynamics in the disordered c-Myc transactivation domain affect Bin1 binding*. *Nucleic Acids Res*, 2012. 40(13): p. 6353-66.
42. Chang, D.W., et al., *The c-Myc transactivation domain is a direct modulator of apoptotic versus proliferative signals*. *Mol Cell Biol*, 2000. 20(12): p. 4309-19.
43. Saraogi, I., et al., *Synthetic alpha-helix mimetics as agonists and antagonists of islet amyloid polypeptide aggregation*. *Angew Chem Int Ed Engl*, 2010. 49(4): p. 736-9.
44. Macek, P., et al., *Myc phosphorylation in its basic helix-loop-helix region destabilizes transient alpha-helical structures, disrupting Max and DNA binding*. *J Biol Chem*, 2018. 293(24): p. 9301-9310.
45. Lavigne, P., et al., *Preferential heterodimeric parallel coiled-coil formation by synthetic Max and c-Myc leucine zippers: a description of putative electrostatic interactions responsible for the specificity of heterodimerization*. *J Mol Biol*, 1995. 254(3): p. 505-20.
46. Jung, K.Y., et al., *Perturbation of the c-Myc-Max protein-protein interaction via synthetic alpha-helix mimetics*. *J Med Chem*, 2015. 58(7): p. 3002-24.
47. Hartl, M., et al., *Hydra myc2, a unique pre-bilaterian member of the myc gene family, is activated in cell proliferation and gametogenesis*. *Biol Open*, 2014. 3(5): p. 397-407.

## 2. Experimental studies

---

48. Wienken, C.J., et al., *Protein-binding assays in biological liquids using microscale thermophoresis*. Nat Commun, 2010. 1: p. 100.
49. Hu, J., A. Banerjee, and D.J. Goss, *Assembly of b/HLH/z proteins c-Myc, Max, and Mad1 with cognate DNA: importance of protein-protein and protein-DNA interactions*. Biochemistry, 2005. 44(35): p. 11855-63.
50. Jouaux, E.M., et al., *Targeting the c-Myc coiled coil with interfering peptides*. J Pept Sci, 2008. 14(9): p. 1022-31.
51. v.d.Chevallier, K., *Experimental studies on the tumor suppressor p53, the myc proto-oncogene and tissue compatibility in the basal metazoan phylum Placozoa*. Dissertation (2013), Leibniz Universität Hannover

## ***3. Discussion***

---

Mechanisms which ensure cellular integrity have to be highly regulated in all living beings. Morphological complexity and the number of regulatory genes have risen during course of evolution, but several key components are conserved from simple organisms to humans. Among those are cell cycle control and regulation of programmed cell death, which are crucial for a successful development of multicellularity. Little is known about functions and interactions of related signaling pathways in animal phyla close to the root of metazoan Tree of Life. This thesis illuminates some basic regulatory mechanisms by exemplarily analyses of p53, Myc and Max homologs in the placozoan *Trichoplax adhaerens*.

#### **tap53 and the regulation of apoptosis in *Trichoplax***

When the first placozoan genome was sequenced in 2008, it revealed a remarkable variety of genes, including many homologs of cell signaling pathways known from vertebrates [1]. This was somewhat surprising, considering the extreme primitive or simple bauplan of *Trichoplax*. Five new placozoan genomes have recently been published (H2, *Hoilungia hongkongensis* (H13), H4, H6 and H11) [2-4] which has given further insights into the complex genome structure and genetic repertoire of the phylum Placozoa. Although the phylogenetic position of placozoans remains controversial [5-7], their simple morphology and several genetic features suggest that placozoans resemble the best living surrogate for a bilaterian ancestor or even the urmetazoan [5, 8, 9]. This implicates a primordial gene set [10, 11] and opens up the possibility to study the ancestral function of complex cell signaling pathways.

tap53, the *Trichoplax* homolog of the human tumor suppressor p53, initiated apoptosis after chemical interruption of the tap53/taMdm2 interaction *in vivo*. This leads to the assumption of a conserved function of tap53 and taMdm2 in apoptosis among metazoans. The formation of phenotypic abnormalities (impaired ratio of central-marginal tissue) after inhibitor treatment further suggested a wider spectrum of regulatory functions of tap53 (Chapter I).

Surprisingly, tap53 knockdown was lethal within 72 hours and led to an increase of apoptotic cells, with the latter already observed after tap53 accumulation (Chapter III). This differs remarkably from previous studies, e.g. in which knockdown of a p53 homolog in the sea anemone *Nematostella vectensis* was shown to decrease apoptotic



events after UV radiation [12]. Furthermore, p53  $-/-$  mice survived up to six months, before the knockout animals succumbed to developing tumors, enhanced by a lack of apoptotic response [13, 14]. This raises the possibility of an alternative apoptosis pathway in *Trichoplax*, in absence of tap53. p53-independent apoptosis is known to eliminate cancer cells, which lack p53-dependent apoptosis due to mutant proteins [15]. It initiates programmed cell death through recruitment of pro-apoptotic members of the Bcl-2 gene family, and thus starts an apoptosis signaling cascade via the mitochondrial apoptosis pathway [16, 17]. The RNASeq data generated here support the idea of p53-independent apoptosis in *Trichoplax*. Proteins belonging to the placozoan Apaf1/NOD-like receptor family were up-regulated. Together with Caspase-9, Apaf1 forms the apoptosome – a crucial construct in the mitochondrial apoptosis pathway, to pass the death signal to the downstream Caspase cascade [18-20]. Thus far, the here described p53-independent apoptosis has neither been observed in unicellular choanoflagellates nor in other diploblastic animals. Further research on placozoans is needed to shed light on the mechanisms of apoptosis regulation in early metazoan evolution in general and on tap53 interaction partners in detail.

#### **tap53's broader reach**

Although p53 is best known for its role in the regulation of apoptosis, it harbors the most complex interactome and is crucial for cellular integrity in multicellular organisms (reviewed by [15]). Experimental evidence confirmed the association of tap53 with apoptosis in *Trichoplax* (Chapter I & III), but studies which characterize other functions were missing until today. RNASeq performed after tap53 knockdown, and subsequent identification of differentially expressed genes uncovered proteins, which are linked to immunity and stress response (Chapter III). The up-regulation of an IRAK-like protein, Hsp70 and a protein that belongs to the Bcl-2 family, suggests a functional role of tap53 in cellular defense mechanisms, like innate immunity and stress responses [21-23]. As the absence of tap53 is highly lethal for *Trichoplax*, placozoans may have developed tap53 protein-concentration-dependent checkpoints. Factors which cause tap53 deregulation have been shown to be harmful for the organism, and the cells may react with defense and cell survival response or apoptosis, respectively, to eliminate the affected cell. Though the described pathways are incomplete and require

additional experimental verification, they are nevertheless the first experimental proof that tap53 is a master control gene in *Trichoplax*. Furthermore, it leaves space for discussions about the ancestral functions of p53, as the complexity of its regulatory network might not have increased proportional to morphological specialization.

#### **Proto-oncogenes in *Trichoplax* – lessons from taMyc and taMax protein structures**

Another key regulator which controls fundamental cellular processes like growth, proliferation, differentiation and apoptosis, is the proto-oncogene *c-myc* [24, 25]. Homologs have been found throughout metazoans, as well as in unicellular choanoflagellates [26, 27]. *Trichoplax* harbors homologs of both Myc and its interaction partner Max (taMyc and taMax), which form heterodimers in order to bind to DNA and regulate transcription of target genes [28, 29]. Although Myc and Max are well studied, structural characterization of the full-length proteins are missing. Recombinant expression and purification of full-length taMyc and taMax proteins performed in the course of this thesis showed high instability of taMyc, experimentally requiring a stabilizing YFP-tag (Chapter IV). Purified taMyc and taMax proteins have been shown to be functional and to be able to form heterodimers. The dissociation constant of the heterodimeric proteins in the absence of DNA was  $100 \pm 10$  nM, which is most likely to be higher in the presence of DNA. The secondary structure of taMyc revealed an unexpected high amount of  $\beta$ -sheets and turns, but only 32 % of the protein have been found unordered (Chapter IV) – probably due to the YFP-tag. Further studies on the full-length proteins are needed, as the N-terminal part of taMyc harbors Myc boxes, which are supposed to be important for the interaction with other proteins [30, 31]. In sum, *Trichoplax* has already been shown to be an important model system to further understand primordial processes underlying the interaction of Myc with other proteins. Future studies should focus on the binding affinities of taMyc and taMax in the presence of DNA and to specifically stabilize taMyc. Although those experiments cannot represent physiological conditions in a cellular environment, it will give important information about the N-terminal Myc boxes and their interaction with other proteins.

#### **Why is it important to find new placozoan species?**

The classification of new species in the phylum Placozoa is challenging for several reasons, which include a highly uniform morphology (with one exception, see below), very few morphological characters, little information about habitat preferences and the general ecology, and a broad lack of knowledge on sexual reproduction and possible reproductive barriers [3]. Nevertheless, the description of the new placozoan species, *Polyplacotoma mediterranea* (Chapter II) is a major step to overcoming some of these barriers. *Polyplacotoma* shows remarkable differences compared to all other placozoans known. It exhibits a long body with polytomous branches, a compact mitochondrial genome and grows very slowly under laboratory conditions (Chapter II). This might hint to nuclear genomic differences, which could further affect cellular regulatory mechanisms. Future functional genetic and comparative physiological studies on *Polyplacotoma* will clearly help to deepen our knowledge of the enigmatic phylum Placozoa. Furthermore, the characterization of a previously unknown placozoan genus highlights the importance of extensive taxon sampling and comprehensive field work.

#### **Conclusions**

In multicellular organisms, the regulation of key cellular processes is controlled by complex molecular interaction networks. Functional genetic studies, comparative analyses at the transcriptome level and biochemical approaches revealed new and important insights into the regulation of apoptosis and cell cycle control in the early-branching metazoan phylum Placozoa. The results underline the importance of simple model organisms predating the Bilateria to study multi-component signaling pathways, in a less complex environment. This also opens new perspectives for applied research.

#### **References**

1. Srivastava, M., et al., *The Trichoplax genome and the nature of placozoans*. Nature, 2008. 454(7207): p. 955-60.
2. Kamm, K., et al., *Trichoplax genomes reveal profound admixture and suggest stable wild populations without bisexual reproduction*. Sci Rep, 2018. 8(1): p. 11168.
3. Eitel, M., et al., *Comparative genomics and the nature of placozoan species*. PLoS Biol, 2018. 16(7): p. e2005359.

4. Laumer, C.E., et al., *Support for a clade of Placozoa and Cnidaria in genes with minimal compositional bias*. *Elife*, 2018. 7.
5. Schierwater, B., et al., *Concatenated analysis sheds light on early metazoan evolution and fuels a modern "urmetazoan" hypothesis*. *PLoS Biol*, 2009. 7(1): p. e20.
6. Philippe, H., et al., *Resolving difficult phylogenetic questions: why more sequences are not enough*. *PLoS Biol*, 2011. 9(3): p. e1000602.
7. Nosenko, T., et al., *Deep metazoan phylogeny: when different genes tell different stories*. *Mol Phylogenet Evol*, 2013. 67(1): p. 223-33.
8. Dellaporta, S.L., et al., *Mitochondrial genome of *Trichoplax adhaerens* supports placozoa as the basal lower metazoan phylum*. *Proc Natl Acad Sci U S A*, 2006. 103(23): p. 8751-6.
9. Schierwater, B. and R. Desalle, *Can we ever identify the Urmetazoan?* *Integr Comp Biol*, 2007. 47(5): p. 670-6.
10. Schierwater, B., D. de Jong, and R. Desalle, *Placozoa and the evolution of Metazoa and intrasomatic cell differentiation*. *Int J Biochem Cell Biol*, 2009. 41(2): p. 370-9.
11. de Jong, D., et al., *Multiple dicer genes in the early-diverging metazoa*. *Mol Biol Evol*, 2009. 26(6): p. 1333-40.
12. Pankow, S. and C. Bamberger, *The p53 tumor suppressor-like protein nvp63 mediates selective germ cell death in the sea anemone *Nematostella vectensis**. *PLoS One*, 2007. 2(9): p. e782.
13. Gottlieb, E., et al., *Transgenic mouse model for studying the transcriptional activity of the p53 protein: age- and tissue-dependent changes in radiation-induced activation during embryogenesis*. *EMBO J*, 1997. 16(6): p. 1381-90.
14. Colombel, M., et al., *Androgen suppressed apoptosis is modified in p53 deficient mice*. *Oncogene*, 1995. 10(7): p. 1269-74.
15. Kasthuber, E.R. and S.W. Lowe, *Putting p53 in Context*. *Cell*, 2017. 170(6): p. 1062-1078.
16. Alphonse, G., et al., *p53-independent early and late apoptosis is mediated by ceramide after exposure of tumor cells to photon or carbon ion irradiation*. *BMC Cancer*, 2013. 13: p. 151.
17. Kang, M.H. and C.P. Reynolds, *Bcl-2 inhibitors: targeting mitochondrial apoptotic pathways in cancer therapy*. *Clin Cancer Res*, 2009. 15(4): p. 1126-32.
18. Gross, A., J.M. McDonnell, and S.J. Korsmeyer, *BCL-2 family members and the mitochondria in apoptosis*. *Genes Dev*, 1999. 13(15): p. 1899-911.
19. Li, Y., et al., *Mechanistic insights into caspase-9 activation by the structure of the apoptosome holoenzyme*. *Proc Natl Acad Sci U S A*, 2017. 114(7): p. 1542-1547.
20. McNamee, L.M. and M.H. Brodsky, *p53-independent apoptosis limits DNA damage-induced aneuploidy*. *Genetics*, 2009. 182(2): p. 423-35.
21. Kamm, K., B. Schierwater, and R. DeSalle, *Innate immunity in the simplest animals - placozoans*. *BMC Genomics*, 2019. 20(1): p. 5.
22. Park, S.L., et al., *HSP70-1 is required for interleukin-5-induced angiogenic responses through eNOS pathway*. *Sci Rep*, 2017. 7: p. 44687.
23. Park, Y.H., et al., *Hsp70 acetylation prevents caspase-dependent/independent apoptosis and autophagic cell death in cancer cells*. *Int J Oncol*, 2017. 51(2): p. 573-578.

### 3. Discussion

---

24. Conacci-Sorrell, M., L. McFerrin, and R.N. Eisenman, *An overview of MYC and its interactome*. Cold Spring Harb Perspect Med, 2014. 4(1): p. a014357.
25. Conacci-Sorrell, M., et al., *Stress-induced cleavage of Myc promotes cancer cell survival*. Genes Dev, 2014. 28(7): p. 689-707.
26. King, N., et al., *The genome of the choanoflagellate Monosiga brevicollis and the origin of metazoans*. Nature, 2008. 451(7180): p. 783-8.
27. Young, S.L., et al., *Premetazoan ancestry of the Myc-Max network*. Mol Biol Evol, 2011. 28(10): p. 2961-71.
28. Luscher, B. and L.G. Larsson, *The basic region/helix-loop-helix/leucine zipper domain of Myc proto-oncoproteins: function and regulation*. Oncogene, 1999. 18(19): p. 2955-66.
29. Grandori, C., et al., *The Myc/Max/Mad network and the transcriptional control of cell behavior*. Annu Rev Cell Dev Biol, 2000. 16: p. 653-99.
30. Schwinkendorf, D. and P. Gallant, *The conserved Myc box 2 and Myc box 3 regions are important, but not essential, for Myc function in vivo*. Gene, 2009. 436(1-2): p. 90-100.
31. Oster, S.K., et al., *Functional analysis of the N-terminal domain of the Myc oncoprotein*. Oncogene, 2003. 22(13): p. 1998-2010.

# ***A. Appendix***

---

## A.1 The role of p53 in the regulation of apoptosis in the placozoan *Trichoplax adhaerens*. (Chapter III)

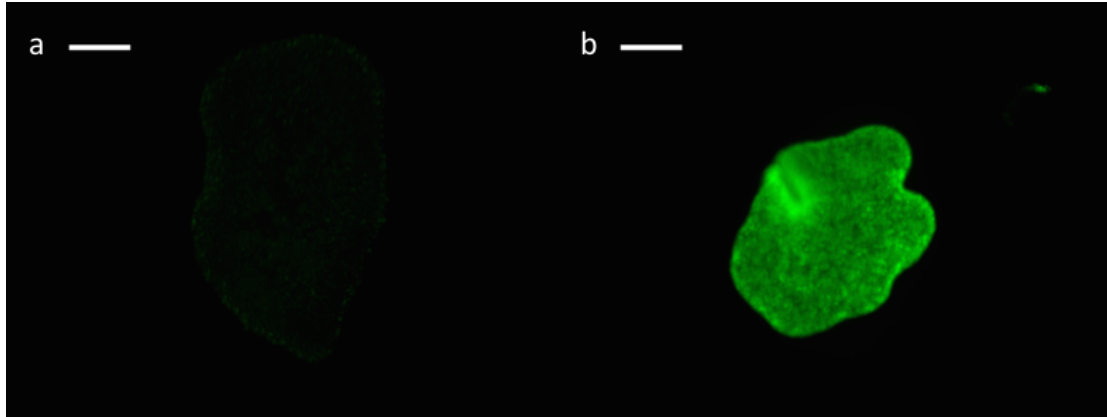


**Figure A1.1: Live image of transfected animals.**

Images of *Trichoplax adhaerens* were taken 21 h after transfection with fluorescent dsRNA probes of (a) Interferin (IF) and (b) tap53. Signal is equally distributed in the tap53 KD animal. The IF control does not show any signal but a low amount of autofluorescence. The bars mark 100  $\mu\text{m}$ .

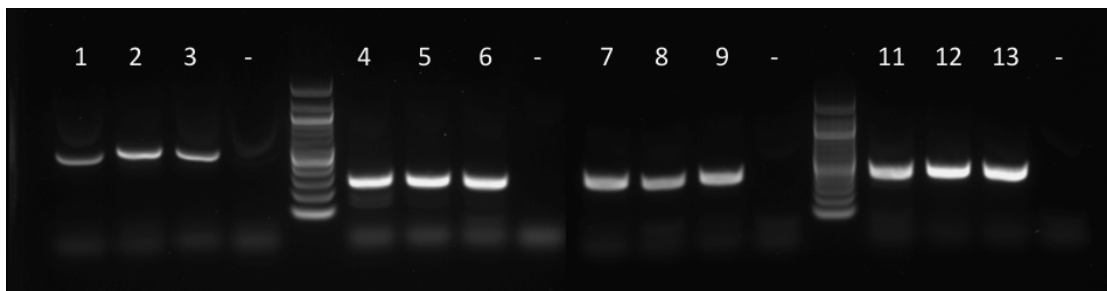


**Figure A1.2: Semi-quantitative PCR after tap53 knockdown.**

21 h after tap53 KD, a semi-quantitative PCR was conducted to quantify the down-regulation of tap53. tap53 KD samples are shown on lane 1, 4, 7, 11. Control groups were ITS (2, 5, 8, 11) and Interferin (3, 6, 9, 12). Primer sets for the following genes were used for amplification in each treatment. tap53 amplification: 1-3, taMdm2 amplification: 4-6, taMBL amplification: 7-9, taQuaking amplification: 10-12. Respective dsRNA probes and primer sets are listed in the Appendix.

**Table A1.1: Sequences of primer sets used in Chapter III.**  
Forward and reverse primers that were used for dsRNA probe synthesis are highlighted in black and purple, respectively.

Primer	Sequence
ITS-Odo_fw	5' <b>CGTAGGTGAACCTGCAGAAG</b> 3'
ITS-Odo_rv	5' <b>CGACCTCAGAGCAGGTGAG</b> 3'
Ta_p53_fw	5' <b>TCTATCTCAGTTATCGTTCTCG</b> 3'
Ta_p53_rv	5' <b>CGACATCGCTATTGATCAGAA</b> 3'
TaMBL_fw	5' TGGCTTCGTAACCTGCCTG 3'
TaMBL_rv	5' GGTCAACTTTAGCAGGCTTC 3'
TaQuaking_fw	5' CACATTCCTTCACTGCGAAC 3'
TaQuaking_rv	5' CCCTGGTTGGTGTATCTTCC 3'

**Table A1.2: Sequences of RNAi probes.**

RNAi probes were generated for a ITS sequence from *Trithemis stictica* and tap53 from *Trichoplax adhaerens*. Forward and reverse primers are highlighted in black and purple, respectively.

***Trithemis stictica* ITS:**

**CGTAGGTGAACCTGCAGAAG**GATCATTACCGTTTGTGTTTTGCGATTAATTCGCTGAAACGA  
GAGAAGAGAGAGAAAAGACAGTGAAAATGAGACAAAGAGGCAACGAGAGGGATGTCCCG  
TCCTGGAACGATGGAGGGCACCTGTGTGTGGTTTTAAAAGTCTCACGCCCTTCGGRCGGAA  
GATGGAAAGAARATCCCCGTTACATGACCAACTCGTGGTGAGAGCGAGTATTGATGCATTT  
TGTATGGTCTCTCGCATTTCGTGAGAGAGAGAAAAAAATTTGAAAACGTATCCTAAACGGT  
GGATCACTCGGCTCGTGGATCGATGAAGGACGCAGCAAACCTGCGCGTCAATTGTGAACT  
GCAGGACACATGAACATCGACGCTTCGAACGCACATTGCAGCCCACGGATTCTGTTCCCGG  
GCTACGCCTGGCTGAGGGCCGGCTAAAAAGTTTGACGGACCGCTCGTCTTCGGACGGGCG  
AGTTCCACGTCACGGTGGGGGACGCCCTCTACGAGTGCGAGCGTGCCCCGGATCGC  
CTAGACGGCGGGCGCCGGTGCCTGGAGGAGACCGCGAGTTCCTGCGGGACGGTGC  
GGAGTCGAATCCTCGAGGACGCGGGTCTGCGAACGCCTTCATGCTTCATGCGGCGTTC  
TCCCAGGCCCGTCTCGAGTCGGCCCGCTCCCTCTCGGGCGAGAGCGCACCTCCTCGCC  
GCCGAGCGAACGATGCGTCCGCGTGTATATTCAATTTGC**CGACCTCAGAGCAGGTGAG**

***Trichoplax adhaerens* tap53:**

**TCTATCTCAGTTATCGTTCTCG**CAAGAAGTGTGCTTTCATGGCAATTGATGATCGATGAAAT  
TACTCAAGGAAAGTTCAACACTAACGAAGACGAGGGTACAGCTATTTATTCGTAACCGAG  
CAAAATCCTGATGATCGCTATTTAATGAGGCCAAACGAGCCTCAATACATTAGCGCTGGTTA  
TCCAGATGGGCAGGTAGGGCAACTTCTCGGAATTTGCCGTTAATCAAATCCGTCCCCAA  
GAACATTTAGTGACAACGTTTCCAGTTCTGCTGATAAAGCTCGCGAAGCGTATTACGGCCAA  
GCCGTTAACGGTGTGCTGCTGAAACGTCACCACCGCTAAAGAGGGATCCGTCTCTGCCTTC  
AAATGCTGAATATATTGGCAATTTGGCTT**CGACATCGCTATTGATCAGAA**



## A. Appendix

---

**Table A1.3: Raw data of animals' population sizes after tap53 knockdown.**

Given are numbers of animals over the duration of 72 h after initial knockdown in three independent experiments (KD1, KD2, KD3). Averages and standard deviations were used for graphical visualization. Statistical analyses have been performed with a two-sided t-test.

Treatment	0 h	21 h	48 h	72 h	two-sided t-test			
					tap53 vs ASW	tap53 vs ITS	tap53 vs IF	
<b>KD1</b>					21 hpt	0.0225	0.1106	0.0060
ASW	40	51	70	65	48 hpt	0.0033	0.0002	0.0001
IF	40	46	61	72	72 hpt	0.0068	0.0019	0.0011
ITS	40	48	47	49				
tap53	40	24	5	0				
<b>KD2</b>								
ASW	40	89	119	127				
IF	40	54	61	94				
ITS	40	31	51	58				
tap53	40	30	3	0				
<b>KD3</b>								
ASW	40	71	110	128				
IF	40	48	73	63				
ITS	40	50	59	78				
tap53	40	34	8	0				

## A. Appendix

Raw data on the animals' body sizes after tap53 knockdown is provided in the digital appendix.

**Table A1.4: Statistics of animals' body sizes after tap53 knockdown.**

Sizes of *Trichoplax* specimen were measured daily after knockdown in three independent experiments. Averages and standard deviations were used for graphical visualization. Statistical analyses have been performed with a two-sided t-test.

	ASW 21h	IF 21h	ITS 21h	p53 21h	ASW 48h	IF 48h	ITS 48h	p53 48h	ASW 72h	IF 72h	ITS 72h	p53 72h
Min	0.17	0.19	0.2	0.26	0.2	0.2	0.24	0.5	0.21	0.21	0.21	0
Q1	0.55	1.88	1.44	1.69	0.61	1.1	1.03	0.66	0.67	0.74	0.95	0
Median	1.71	3.17	3.02	2.39	1.57	2.85	2.52	0.97	1.56	2.05	1.86	0
Q3	3.12	3.48	3.45	3.03	3.04	3.36	3.29	1.2	3.03	3.2	3.16	0
Max	3.73	4.25	4.84	3.73	3.73	3.72	5.68	2.59	4.68	3.71	5.13	0
Min	0.17	0.19	0.2	0.26	0.2	0.2	0.24	0.5	0.21	0.21	0.21	0
Q1-Min	0.38	1.69	1.25	1.43	0.42	0.89	0.78	0.16	0.46	0.53	0.74	0
Median-Q1	1.16	1.29	1.58	0.7	0.96	1.76	1.49	0.31	0.89	1.31	0.91	0
Q3-Median	1.42	0.3	0.43	0.64	1.47	0.5	0.77	0.23	1.47	1.16	1.3	0
Max-Q3	0.6	0.77	1.38	0.7	0.69	0.36	2.4	1.39	1.65	0.51	1.97	0

Two-sided t-test			
	tap53 vs ASW	tap53 vs ITS	tap53 vs IF
<b>21 hpt</b>	0.0031	0.1113	0.0109
<b>48 hpt</b>	0.0156	0.0003	4.86E-05

A. Appendix

**Table A1.5: Raw data obtained from TUNEL staining after tap53 knockdown.**

21 h after tap53 knockdown the amount of apoptotic cells in *Trichoplax adhaerens* was monitored, IF served as a control. Statistical analyses have been performed with a two-sided t-test.

Animal	Nuclei	Apoptotic cells	Quotient	Percentage	IF	tap53
<b>IF (21h)</b>						
1.a	632	3	0.0047	0.47	Min	0.12 1.66
1.b	612	1	0.0016	0.16	Q1	0.1975 2975
1.c	343	2	0.0058	0.58	Median	0.43 3.22
2.a	301	3	0.0099	0.99	Q3	0.595 5.54
2.b	482	2	0.0041	0.41	Max	0.99 9.89
2.c	662	1	0.0015	0.15	Q1-Min	0.08 1315
3.a	668	5	0.0075	0.75	Median-Q1	0.23 0.245
3.b	459	6	0.0131	0.13	Q3-Median	0.17 2.32
3.c	663	4	0.0060	0.6	Max-Q3	0.4 4.35
4.a	444	2	0.0045	0.45		
4.b	843	1	0.0012	0.12		
5.a	559	5	0.0089	0.89		
5.b	633	2	0.0031	0.31		
5.c	287	1	0.0035	0.35		
<b>Two-sided t-test</b>						
						0.0039
<b>tap53 KD (21h)</b>						
1.a	283	20	0.0707	7.07		
1.b	374	37	0.0989	9.89		
1.c	432	8	0.0185	1.85		
2.a	484	15	0.0309	3.09		
2.b	364	11	0.0302	3.02		
2.c	539	16	0.0297	2.97		
3.a	259	20	0.0772	7.72		
3.b	421	7	0.0166	1.66		
3.c	369	11	0.0298	2.98		
4.a	352	13	0.0369	3.69		
4.b	491	9	0.0182	1.82		
4.c	142	9	0.0634	6.34		
5.a	466	15	0.0322	3.22		
5.b	422	20	0.0474	4.74		
5.c	408	18	0.0441	4.41		

## A. Appendix

**Table A1.6: Statistics on all differentially expressed genes after tap53 knockdown in a tap53 vs IF comparison.**

Differential gene expression was performed on RSEM transcript quantifications with limma-voom in R. Transcripts were identified as differentially expressed by 4-fold changes and  $p < 0.001$ .

Trinity ID	logFC	logCPM	p-value	FDR	Trinity ID	logFC	logCPM	p-value	FDR
<b>tap53 vs IF up-regulated:</b>					<b>tap53 vs IF up-regulated:</b>				
DN1028_c0_g2	-2.3724	2.321	0.0000	0.0003	DN4837_c0_g1	-2.0863	0.9271	0.0001	0.0009
DN1028_c0_g1	-1.3006	0.5282	0.0510	0.0861	DN5052_c0_g1	-2.3659	2.2814	0.0001	0.0010
DN10746_c0_g1	-4.1728	0.6394	0.0000	0.0003	DN5052_c0_g1	-2.3659	2.2814	0.0001	0.0010
DN1151_c0_g1	-3.2038	2.7867	0.0000	0.0003	DN5801_c0_g1	-2.1914	1.3573	0.0001	0.0009
DN11898_c0_g1	-2.1371	4.4910	0.0000	0.0003	DN6048_c0_g2	-2.0491	1.6333	0.0001	0.0010
DN1190_c0_g1	-2.1310	2.9561	0.0000	0.0003	DN6194_c0_g1	-3.5673	0.3537	0.0001	0.0008
DN1372_c0_g1	-2.0433	2.3208	0.0000	0.0004	DN6574_c0_g1	-3.7514	0.7794	0.0000	0.0004
DN1414_c0_g1	-2.1190	3.0637	0.0000	0.0003	DN6762_c0_g1	-4.6298	0.8517	0.0000	0.0004
DN14656_c0_g1	-2.6726	1.2331	0.0001	0.0008	DN6790_c0_g1	-2.6523	4.3212	0.0000	0.0003
DN15859_c0_g1	-3.9681	0.1050	0.0000	0.0005	DN6992_c0_g1	-5.6707	2.1438	0.0000	0.0003
DN16092_c0_g1	-2.9762	2.5389	0.0000	0.0005	DN7103_c0_g1	-2.1553	1.2664	0.0001	0.0007
DN1617_c0_g1	-2.0108	0.9761	0.0001	0.0010	DN7242_c0_g1	-3.3316	1.4429	0.0000	0.0006
DN1833_c0_g1	-2.5910	1.8577	0.0000	0.0003	DN7398_c0_g1	-3.3787	1.8590	0.0000	0.0003
DN1892_c0_g1	-2.0428	1.9668	0.0001	0.0006	DN807_c0_g1	-2.2809	1.8201	0.0000	0.0004
DN1927_c0_g2	-2.1232	1.2868	0.0001	0.0006	DN900_c0_g1	-2.6831	4.3255	0.0000	0.0003
DN1927_c0_g4	-0.3886	2.4207	0.0065	0.0176	DN9571_c0_g1	-3.4048	0.5610	0.0000	0.0006
DN193_c0_g1	-2.0707	4.4560	0.0000	0.0003	DN9982_c0_g1	-5.1440	0.4774	0.0000	0.0005
DN193_c1_g1	-0.0850	3.1196	0.2513	0.3176	DN9982_c0_g2	0.3363	0.2502	0.3745	0.4451
DN2026_c0_g1	-2.1619	3.6372	0.0000	0.0003	<b>tap53 vs IF down-regulated:</b>				
DN2026_c0_g2	-1.8561	0.6298	0.0002	0.0014	DN10076_c0_g1	2.4284	0.4898	0.0001	0.0010
DN2041_c0_g1	-3.3920	3.7768	0.0000	0.0003	DN10734_c0_g1	2.2010	5.1345	0.0000	0.0003
DN2230_c0_g2	-2.1069	2.1502	0.0000	0.0004	DN1427_c0_g1	2.4291	3.1888	0.0000	0.0006
DN2230_c0_g1	0.0860	-0.0032	0.6745	0.7298	DN1474_c0_g1	2.6037	3.6935	0.0000	0.0004
DN2234_c0_g1	-2.8868	3.3301	0.0000	0.0003	DN148_c0_g2	2.0424	4.0409	0.0000	0.0003
DN2262_c0_g1	-2.8071	2.5634	0.0000	0.0003	DN1692_c0_g1	2.1789	4.8821	0.0000	0.0003
DN2262_c0_g2	-2.5536	0.0853	0.0003	0.0020	DN2135_c0_g1	2.0561	2.0157	0.0001	0.0009
DN2316_c0_g1	-2.0388	2.6178	0.0001	0.0008	DN2257_c0_g1	2.8217	2.5499	0.0000	0.0005
DN2390_c0_g1	-2.8451	2.0833	0.0000	0.0004	DN2613_c0_g3	3.0836	5.0495	0.0000	0.0003
DN2390_c0_g2	-3.1993	-0.1175	0.0001	0.0011	DN329_c0_g1	3.5784	2.5133	0.0000	0.0004
DN2413_c0_g1	-2.5879	2.2904	0.0000	0.0003	DN3650_c0_g1	2.6883	1.7463	0.0000	0.0005
DN2416_c0_g1	-2.4166	3.2664	0.0000	0.0003	DN3674_c0_g1	2.9600	1.4825	0.0000	0.0004
DN2486_c0_g1	-2.4485	3.4264	0.0000	0.0003	DN4254_c0_g1	2.3917	5.2476	0.0000	0.0003
DN2516_c0_g1	-2.0222	2.6478	0.0001	0.0007	DN441_c0_g1	2.6301	2.8611	0.0000	0.0006
DN257_c0_g2	-3.0265	3.1359	0.0000	0.0003	DN473_c0_g1	3.8882	2.1512	0.0000	0.0004
DN257_c0_g1	-1.3075	6.3515	0.0000	0.0003	DN497_c0_g1	2.2796	3.1626	0.0000	0.0004
DN2585_c0_g1	-2.2906	2.8157	0.0000	0.0003	DN50882_c0_g1	2.3445	2.0176	0.0001	0.0009
DN2612_c0_g1	-2.0919	2.0987	0.0000	0.0006	DN5234_c0_g1	2.7761	2.4633	0.0000	0.0005
DN2637_c0_g1	-2.3554	2.3923	0.0000	0.0003	DN601_c0_g1	5.0211	6.8666	0.0000	0.0003
DN2654_c0_g4	-2.5254	2.7585	0.0000	0.0003	DN6609_c0_g1	2.7068	2.3523	0.0000	0.0005
DN2666_c0_g1	-5.4358	1.3392	0.0000	0.0003	DN6609_c0_g3	0.5102	0.4957	0.3879	0.4580
DN2666_c0_g2	-2.8974	0.8905	0.0000	0.0005	DN753_c2_g2	6.1503	2.3835	0.0000	0.0003
DN274_c0_g1	-6.1633	3.3148	0.0000	0.0003	DN753_c0_g1	1.1880	0.8426	0.0087	0.0217
DN275_c0_g1	-3.0607	2.6007	0.0000	0.0004	DN753_c1_g1	-0.9226	1.0733	0.0603	0.0985
DN276_c0_g1	-4.3002	4.6595	0.0000	0.0003	DN772_c0_g1	2.4891	5.9455	0.0000	0.0003
DN2900_c0_g1	-2.1370	3.9845	0.0000	0.0005	DN7739_c0_g1	2.4392	0.3484	0.0001	0.0010
DN2911_c0_g3	-2.6987	1.0679	0.0001	0.0007	DN7739_c0_g2	-1.0003	1.2817	0.0026	0.0089
DN296_c0_g1	-2.2520	3.4982	0.0000	0.0003	DN8053_c0_g1	2.9492	2.6234	0.0001	0.0006
DN3309_c0_g1	-2.6083	2.2388	0.0000	0.0003					
DN3342_c0_g1	-3.3102	2.6456	0.0000	0.0004					
DN3342_c0_g2	-2.6977	-0.4171	0.0003	0.0019					
DN3347_c0_g1	-2.4899	1.7446	0.0000	0.0004					
DN3377_c0_g1	-2.5272	2.2062	0.0000	0.0003					
DN356_c0_g1	-2.0589	3.7143	0.0000	0.0003					
DN3582_c0_g1	-2.5748	2.7171	0.0000	0.0003					
DN3621_c0_g3	-2.1030	2.0509	0.0000	0.0005					
DN3718_c0_g1	-6.3525	0.8521	0.0000	0.0003					
DN3829_c0_g1	-5.2723	1.6399	0.0000	0.0003					
DN3843_c0_g1	-3.6242	2.1728	0.0000	0.0004					
DN3895_c0_g1	-2.0433	2.1035	0.0000	0.0004					
DN3932_c0_g1	-2.6201	1.8230	0.0000	0.0003					
DN3932_c0_g2	0.6872	2.2232	0.0017	0.0065					
DN419_c0_g1	-3.6256	4.4647	0.0000	0.0003					
DN4246_c0_g1	-3.2899	1.4441	0.0001	0.0008					
DN4287_c0_g1	-2.1367	2.8496	0.0000	0.0004					
DN433_c0_g1	-2.1522	4.4814	0.0000	0.0003					
DN4366_c0_g1	-2.1974	2.6668	0.0000	0.0003					
DN455_c0_g1	-2.1357	2.1902	0.0001	0.0006					
DN45816_c0_g1	-5.4851	2.1502	0.0000	0.0003					
DN468_c1_g1	-2.0407	4.2479	0.0000	0.0004					
DN4750_c0_g1	-2.6850	2.0629	0.0000	0.0004					

## A. Appendix

**Table A1.7: Statistics on all differentially expressed genes after tap53 knockdown in a tap53 vs ITS comparison.**

Differential gene expression was performed on RSEM transcript quantifications with limma-voom in R. Transcripts were identified as differentially expressed by 4-fold changes and  $p < 0.05$ .

Trinity ID	logFC	logCPM	p-value	FDR	Trinity ID	logFC	logCPM	p-value	FDR
<b>tap53 vs ITS up-regulated:</b>					<b>tap53 vs ITS up-regulated:</b>				
DN1028_c0_g2	-2.5314	2.0340	0.0000	0.0003	DN6790_c0_g1	-2.1842	4.3893	0.0000	0.0001
DN1028_c0_g1	-1.1565	0.4846	0.0588	0.0938	DN6992_c0_g1	-5.5882	2.1394	0.0000	0.0001
DN10746_c0_g1	-4.1024	0.6251	0.0000	0.0002	DN7204_c0_g1	-3.1439	1.0197	0.0000	0.0004
DN108_c0_g1	-2.0297	4.3659	0.0000	0.0001	DN7242_c0_g1	-2.9321	1.4759	0.0001	0.0006
DN11018_c0_g1	-4.8170	0.0190	0.0000	0.0001	DN7474_c0_g1	-4.3885	1.2431	0.0000	0.0005
DN11018_c0_g2	0.1484	1.1057	0.3101	0.3787	DN7834_c0_g1	-2.3943	0.6588	0.0001	0.0010
DN1199_c0_g2	-2.1029	2.6376	0.0001	0.0010	DN807_c0_g1	-2.1927	1.7839	0.0000	0.0004
DN1199_c0_g1	-2.7464	-0.4500	0.0002	0.0013	DN8275_c0_g1	-2.5740	-0.2661	0.0001	0.0007
DN1199_c0_g3	-1.3730	1.4548	0.0036	0.0107	DN900_c0_g1	-2.5281	4.3118	0.0000	0.0001
DN1833_c0_g1	-2.6199	1.7989	0.0000	0.0003	DN9982_c0_g1	-5.0308	4.4706	0.0000	0.0005
DN1892_c0_g1	-2.0035	1.9119	0.0001	0.0008	DN9982_c0_g2	0.3810	0.1230	0.3213	0.3902
DN1995_c0_g1	-2.3353	1.4867	0.0001	0.0006	<b>tap53 vs ITS down-regulated:</b>				
DN2026_c0_g1	-2.1131	3.5879	0.0000	0.0002	DN10076_c0_g1	3.5635	1.3632	0.0000	0.0003
DN2026_c0_g2	-1.9701	0.5176	0.0002	0.0013	DN10734_c0_g1	2.8767	5.5616	0.0000	0.0001
DN2041_c0_g1	-3.1219	3.7869	0.0000	0.0001	DN1241_c0_g3	3.0830	3.1503	0.0000	0.0004
DN2116_c0_g1	-2.0000	2.7226	0.0000	0.0004	DN1241_c0_g1	2.1248	0.1395	0.0008	0.0037
DN2186_c0_g1	-2.6706	2.1015	0.0001	0.0006	DN1427_c0_g1	2.3421	2.9154	0.0000	0.0004
DN2186_c1_g1	0.0742	0.1555	0.7434	0.7855	DN1474_c0_g1	2.8515	3.7256	0.0000	0.0002
DN220_c0_g1	-2.1858	5.1189	0.0000	0.0001	DN148_c0_g2	2.5223	4.2836	0.0000	0.0001
DN2234_c0_g1	-2.4184	3.3904	0.0000	0.0003	DN1533_c0_g2	2.0933	6.6462	0.0000	0.0001
DN2262_c0_g1	-2.2953	2.6418	0.0001	0.0007	DN1533_c0_g1	1.4248	2.4952	0.0002	0.0013
DN2262_c0_g2	-2.3845	0.0717	0.0003	0.0017	DN1533_c0_g3	0.1893	2.2888	0.1746	0.2326
DN2316_c0_g1	-2.7879	2.3610	0.0000	0.0005	DN1692_c0_g1	2.3276	4.8276	0.0000	0.0001
DN2390_c0_g1	-2.8625	2.0353	0.0000	0.0003	DN2048_c0_g1	4.6281	3.2377	0.0000	0.0002
DN2390_c0_g2	-3.2572	-0.1581	0.0009	0.0039	DN2135_c0_g1	2.4691	2.1985	0.0001	0.0007
DN2413_c0_g1	-2.8833	2.1753	0.0000	0.0003	DN2257_c0_g1	2.9702	2.4896	0.0000	0.0004
DN2416_c0_g1	-2.7415	3.1365	0.0000	0.0005	DN2613_c0_g3	3.1143	4.8752	0.0000	0.0001
DN24347_c0_g1	-2.2895	2.4357	0.0000	0.0003	DN2633_c0_g2	2.0954	2.6003	0.0001	0.0006
DN2486_c0_g1	-2.2987	3.4090	0.0000	0.0001	DN2834_c0_g2	2.7280	1.0651	0.0001	0.0008
DN257_c0_g2	-2.4266	3.2224	0.0000	0.0003	DN2912_c0_g1	2.0346	2.3966	0.0001	0.0008
DN2585_c0_g1	-2.5243	2.6965	0.0000	0.0002	DN329_c0_g1	4.2485	2.9574	0.0000	0.0001
DN2612_c0_g1	-2.2249	1.9943	0.0000	0.0004	DN3650_c0_g1	2.4695	1.3500	0.0001	0.0009
DN2637_c0_g1	-2.1434	2.3924	0.0000	0.0004	DN3674_c0_g1	2.8593	1.1859	0.0000	0.0005
DN2666_c0_g1	-4.4589	1.3849	0.0000	0.0002	DN4110_c0_g1	2.4458	1.7640	0.0001	0.0007
DN2666_c0_g2	-2.3084	0.9816	0.0001	0.0006	DN4254_c0_g1	2.1964	4.8775	0.0000	0.0001
DN274_c0_g1	-5.3282	3.3372	0.0000	0.0001	DN441_c0_g1	2.5720	2.6131	0.0001	0.0007
DN275_c0_g1	-2.8792	2.5932	0.0000	0.0003	DN473_c0_g1	4.5605	2.6020	0.0000	0.0002
DN276_c0_g1	-3.2250	4.7684	0.0000	0.0001	DN497_c0_g1	2.6948	3.3486	0.0000	0.0002
DN2911_c0_g3	-2.7392	1.0096	0.0001	0.0006	DN50882_c0_g1	3.0605	2.4857	0.0000	0.0004
DN2929_c0_g1	-2.1771	2.7872	0.0000	0.0002	DN5234_c0_g1	3.0593	2.5316	0.0000	0.0005
DN2929_c0_g2	-2.0630	4.5982	0.0000	0.0002	DN5806_c0_g1	2.0174	2.9321	0.0001	0.0008
DN3124_c0_g1	-2.0850	5.8207	0.0000	0.0001	DN5806_c0_g2	1.7325	-0.0125	0.0034	0.0103
DN3309_c0_g1	-2.5948	2.1923	0.0000	0.0004	DN5806_c1_g1	-0.3599	1.8130	0.0260	0.0487
DN3342_c0_g1	-2.8167	2.7009	0.0001	0.0009	DN5806_c2_g1	0.4890	1.1125	0.0627	0.0988
DN3342_c0_g2	-2.6972	-0.4495	0.0014	0.0055	DN5806_c2_g2	-0.8623	0.8326	0.0646	0.1012
DN3347_c0_g1	-2.3737	1.7195	0.0000	0.0003	DN5816_c0_g1	2.3462	4.2347	0.0000	0.0003
DN3377_c0_g1	-2.5224	2.1535	0.0000	0.0003	DN5816_c1_g1	1.0476	1.1170	0.0071	0.0178
DN356_c0_g1	-2.0475	3.6516	0.0000	0.0003	DN601_c0_g1	5.7733	7.3993	0.0000	0.0001
DN3582_c0_g1	-2.3371	2.7233	0.0000	0.0005	DN6609_c0_g1	2.7151	2.1627	0.0000	0.0005
DN3621_c0_g3	-2.0269	2.0095	0.0001	0.0006	DN6609_c0_g3	1.3413	1.0055	0.1098	0.1578
DN3718_c0_g1	-4.2059	0.9504	0.0000	0.0003	DN753_c2_g2	7.1047	3.1253	0.0000	0.0001
DN3829_c0_g1	-3.7779	1.7451	0.0001	0.0008	DN753_c0_g1	1.2174	0.6888	0.0025	0.0083
DN3843_c0_g1	-3.3396	2.1837	0.0000	0.0005	DN753_c1_g1	-0.7281	1.0434	0.0605	0.0960
DN3932_c0_g1	-2.3473	1.8388	0.0000	0.0004	DN772_c0_g1	2.2701	5.5547	0.0000	0.0001
DN3932_c0_g2	0.8852	2.2126	0.0014	0.0054	DN7739_c0_g1	3.0122	0.6887	0.0000	0.0005
DN419_c0_g1	-3.6570	4.4326	0.0000	0.0001	DN7739_c0_g2	-0.8649	1.2426	0.0043	0.0123
DN4246_c0_g1	-3.5390	1.3709	0.0001	0.0006	DN8053_c0_g1	3.5302	2.9739	0.0000	0.0004
DN4250_c0_g1	-2.1523	1.4243	0.0001	0.0007					
DN4287_c0_g1	-2.2628	2.7517	0.0000	0.0004					
DN433_c0_g1	-2.2157	4.3997	0.0000	0.0003					
DN4366_c0_g1	-2.3379	2.5660	0.0000	0.0002					
DN45816_c0_g1	-4.3246	2.2093	0.0000	0.0001					
DN4750_c0_g1	-2.7581	1.9955	0.0000	0.0002					
DN4783_c0_g1	-2.5477	0.7757	0.0001	0.0007					
DN49535_c0_g1	-2.1215	5.0608	0.0000	0.0001					
DN5052_c0_g1	-2.3300	2.2288	0.0001	0.0009					
DN5511_c0_g1	-2.6026	2.4740	0.0000	0.0002					
DN6194_c0_g1	-3.6171	0.3118	0.0000	0.0003					
DN6194_c0_g2	0.9965	1.7486	0.0008	0.0038					

## A. Appendix

---

DN6478_c0_g1	-2.4984	1.0266	0.0001	0.0009
--------------	---------	--------	--------	--------

---

## A. Appendix

**Table A1.8: All identified proteins from differentially expressed genes after tap53 knockdown.**  
Proteins of differentially expressed genes were identified via BLASTp searches and domains were verified by HMMScan.

Organism	Name	Trinity ID	NCBI Acc. No.	Domain
<b>up-regulated genes:</b>				
<i>Trichoplax</i> sp. H2	hypothetical protein	DN1028	XP_002114860	MFS-type transporter SLC18B1, partial
<i>Trichoplax</i> sp. H2	BAG domain-containing protein Samui	DN10746	RDD40779	BAG domain
<i>Trichoplax</i> sp. H2	Equilibrative nucleoside transporter 3	DN1199	RDD43129	no domains found
<i>Trichoplax</i> sp. H2	N-acetyl-beta-glucosaminyl-glycoprotein	DN1833	RDD45506	4-beta-N-acetylgalactosaminyltransferase 1
<i>Trichoplax</i> sp. H2	Adhesion G protein-coupled receptor L3	DN1892	RDD40838	no domains found
<i>Trichoplax</i> sp. H2	Anoctamin-7	DN2026	RDD44260	Ca(2+)-dependent Cl(-) channels
<i>Trichoplax adhaerens</i>	hypothetical protein	DN2041	XP_002109144	Caspase recruitment domain (CARD)
<i>Trichoplax</i> sp. H2	Gamma-aminobutyric acid type B receptor subunit 2	DN2186	XP_002114343	no domains found
<i>Trichoplax</i> sp. H2	Serine palmitoyltransferase 1	DN2262	RDD38007	no domains found
<i>Trichoplax</i> sp. H2	Importin subunit beta	DN2316	RDD45158	beta-catenin-like repeats
<i>Trichoplax</i> sp. H2	Phosphatidyserine synthase 1	DN2390	RDD38981	no domains found
<i>Trichoplax</i> sp. H2	MAM and LDL-receptor	DN2413	RDD37230	MAM and LDL-receptor class A domain
<i>Trichoplax</i> sp. H2	hypothetical protein TrispH2_011036	DN2416	RDD37830	no domains found
<i>Trichoplax adhaerens</i>	hypothetical protein	DN2486	XP_002115250	Fatty acid desaturase
<i>Trichoplax</i> sp. H2	Leucine-rich repeat-containing protein 15	DN2585	RDD47304	no domains found
<i>Trichoplax adhaerens</i>	hypothetical protein	DN2612	XP_002114173	Fatty acid desaturase
<i>Trichoplax</i> sp. H2	Leucine-rich repeat-containing protein 15, partial	DN2585	RDD47304	no domains found
<i>Trichoplax adhaerens</i>	hypothetical protein	DN2612	XP_002114173	AMP-binding enzyme
<i>Trichoplax</i> sp. H2	Interleukin-1 receptor-associated kinase-like 2	DN2637	RDD46737	Protein tyrosine kinase
<i>Trichoplax</i> sp. H2	Tyrosine-protein phosphatase Lar	DN274	RDD37604	IgGfC binding protein
<i>Trichoplax adhaerens</i>	hypothetical protein	DN275	XP_002114710	GNS1/SUR4 family
<i>Trichoplax</i> sp. H2	predicted protein	DN276	RDD43554	no domains found
<i>Trichoplax</i> sp. H2	9-divinyl ether synthase	DN3309	RDD38701	Cytochrome P450
<i>Trichoplax</i> sp. H2	Neurotrypsin	DN3342	RDD37046	MAM domain
<i>Trichoplax</i> sp. H2	Apoptotic protease-activating factor 1 (APAF-1)	DN3347	RDD41288	NB-ARC domain, APAF-1 helical domain
<i>Trichoplax</i> sp. H2	putative cation-transporting ATPase 13A3	DN3377	RDD38190	E1-E2 ATPase.
<i>Trichoplax</i> sp. H2	Lysine-specific demethylase 6A	DN3621	RDD46064	Tetrapeptide repeat
<i>Trichoplax adhaerens</i>	predicted protein	DN3718	XP_002118410	no domain found
<i>Trichoplax adhaerens</i>	hypothetical protein	DN3829	XP_002114285	Hsp70
<i>Trichoplax</i> sp. H2	Dimethylaniline monooxygenase	DN3843	RDD37621	Flavin-binding monooxygenase-like
<i>Trichoplax adhaerens</i>	expressed protein	DN3932	XP_002113862	no domain found
<i>Trichoplax</i> sp. H2	hypothetical protein	DN419	RDD37812	von Willebrand factor type A domain
<i>Trichoplax</i> sp. H2	Endothelin-converting enzyme 1	DN4246	RDD40827	Peptidase family M13
<i>Trichoplax</i> sp. H2	UNC93-like protein MFS11	DN4287	RDD37497	no domain found
<i>Trichoplax</i> sp. H2	Transcription factor COE4	DN433	RDD42715	Transcription COE1 DNA-binding domain
<i>Trichoplax</i> sp. H2	hypothetical protein	DN4366	RDD46149	no domain found
<i>Trichoplax</i> sp. H2	Prostaglandin E synthase 3	DN45816	RDD40952	no domain found
<i>Trichoplax</i> sp. H2	Follistatin	DN4750	RDD45762	Kazal-type serine protease inhibitor domain
<i>Trichoplax</i> sp. H2	hypothetical protein	DN49535	RDD43554	no domain found
<i>Trichoplax</i> sp. H2	Nitric oxide synthase	DN5052	RDD42995	oxygenase domain
<i>Trichoplax</i> sp. H2	Extracellular calcium-sensing receptor	DN5511	RDD36948	Receptor family ligand binding region
<i>Trichoplax</i> sp. H2	Neuropeptide Y receptor type 6	DN6478	RDD36143	7 transmembrane receptor
<i>Trichoplax</i> sp. H2	Transcription factor Sox-9	DN6790	RDD36902	high mobility group box
<i>Trichoplax</i> sp. H2	hypothetical protein	DN6992	RDD36239	7 transmembrane receptor
<i>Trichoplax</i> sp. H2	hypothetical protein	DN7242	RDD41681	no domain found
<i>Trichoplax</i> sp. H2	Synaptic vesicle glycoprotein	DN7834	RDD36927	Major Facilitator Superfamily
<i>Trichoplax</i> sp. H2	Formimidoyltransferase-cyclodeaminase	DN7846	RDD40179	no domain found
<i>Trichoplax</i> sp. H2	Leucine-rich repeat-containing protein 15	DN807	RDD36975	no domain found
<i>Trichoplax</i> sp. H2	Ankyrin-3	DN9982	RDD41858	no domain found
<b>down-regulated genes:</b>				
<i>Trichoplax</i> sp. H2	hypothetical protein	DN10076	RDD41225	no pfam domain match
<i>Trichoplax adhaerens</i>	expressed protein	DN10734	XP_002110632	no pfam domain match
<i>Trichoplax</i> sp. H2	hypothetical protein	DN1474	RDD41298	no pfam domain match
<i>Trichoplax</i> sp. H2	hypothetical protein	DN148	RDD37032	NACHT domain
<i>Trichoplax</i> sp. H2	Deoxyribonuclease-1	DN1692	RDD44585	phosphatase family
<i>Trichoplax</i> sp. H2	Apoptotic protease-activating factor 1	DN2135	RDD41632	NB-ARC domain . APAF-1 helical domain
<i>Trichoplax</i> sp. H2	Adhesion G protein-coupled receptor L2	DN2257	RDD38518	7 transmembrane receptor (Secretin family)
<i>Trichoplax</i> sp. H2	Allene oxide synthase-lipoxygenase protein	DN2613	RDD45153	Lipoxygenase
<i>Trichoplax</i> sp. H2	Allene oxide synthase-lipoxygenase protein	DN329	RDD45153	Lipoxygenase
<i>Trichoplax adhaerens</i>	predicted protein	DN329	XP_002115553	NACHT domain
<i>Trichoplax adhaerens</i>	predicted protein	DN3650	XP_002111626	Helix-loop-helix DNA-binding domain
<i>Trichoplax</i> sp. H2	Serine/threonine-protein	DN3674	RDD36855	Ankyrin repeats (3 copies)
<i>Trichoplax</i> sp. H2	hypothetical protein	DN4254	RDD45022	Lipase (class 2)
<i>Trichoplax adhaerens</i>	predicted protein	DN473	XP_002118572	no pfam domain match

## A. Appendix

---

<i>Trichoplax</i> sp. H2	Patatin-like protein 2	DN497	RDD38737	Patatin-like phospholipase
<i>Trichoplax</i> sp. H2	hypothetical protein	DN50882	RDD45739	no pfam domain match
<i>Trichoplax</i> sp. H2	Plasminogen	DN5234	RDD38477	Kringle domain
<i>Trichoplax</i> sp. H2	hypothetical protein	DN601	RDD45804	no pfam domain match
<i>Trichoplax</i> sp. H2	Ecdysone-induced protein 74EF isoform B	DN6609	RDD37035	Ets-domain
<i>Trichoplax</i> sp. H2	hypothetical protein	DN753	RDD43027	GIY-YIG catalytic domain
<i>Trichoplax adhaerens</i>	phospholipase A21 precursor	DN772	XP_002116315	Phospholipase A2
<i>Trichoplax</i> sp. H2	Apelin receptor A	DN7739	RDD45467	rhodopsin family
<i>Trichoplax</i> sp. H2	hypothetical protein	DN8053	RDD36394	no pfam domain match

---

Unpublished sequencing data is deposited at the Institute of Animal Ecology, University of Veterinary Medicine Hannover, Foundation.



## A.2 New insights into the protein biochemistry of Myc and Max in the placozoan *Trichoplax adhaerens*. (Chapter IV)

**Table A2.1: Primer sequences for gene amplification and cloning into pET23a-YFP and pETDuet-1 plasmids.**

All sequences are listed in 5'/3' orientation and reverse primer sequences are defined in reverse complement direction. Enzyme restriction sites are highlighted in grey.

Gene	Primer name	Restriction site	Primer sequence
<i>tamyc</i>	myc_fw_BamHI	BamHI	GCGGATCCATGAAGCC
<i>tamyc</i>	myc_rv_XhoI	XhoI	GACTCGAGATTAATAA
<i>tamax</i>	max_fw_HindIII	HindIII	GCAAGCTTATAAGTAC
<i>tamax</i>	max_rv_NotI	NotI	GAGCGGCCGCTTAGT

**Table A2.2: 6His-taMax and 6His-YFP-taMyc amino acid sequences and protein information.**

Protein sequences of taMyc with a 6His-YFP tag and taMax with a 6His tag. Protein information about the molecular weight and theoretical pI was calculated by ExPASy.

### 6His-taMax:

MGSSHHHHHHSQDMSDEDKYLVDVIDSDDNGDTDKSTSGLTQADKRAHHNALERKRRDHKDC  
FFGLRDSVPTLQGEKASRAQILNKATDYIQFMKQKNQNHQSDIEDIRKENYQLELQLKTLERTRNN  
LTGTATSENIDSSTTTTTNSGRTRRNKAKRELQSDGNDEQKTDTKKVKAE

**Number of amino acids:** 179

**Molecular weight:** 20.482

**Theoretical pI:** 6.36

### 6His-YFP-taMyc:

MACTSHHHHHHHHGPVMVSKGEELFTGVVPILVELDGDVNGHKFSVSGEGEGDATYGKLTLLKFI  
CTTGKLPVPWPTLVTTFGYGLQCFARYPDHMKQHDFFKSAMPEGYVQERTIFFKDDGNYKTRAE  
VKFEGDTLVNRIELKIGIDFKEDGNILGHKLEYNYNSHNVYIMADKQKNGIKVNFKIRHNIEDGSVQL  
ADHYQQNTPIGDGPVLLPDNHLYSYQSALSQKDPNEKRDHMLLEFVTAAGITLGMDELVSGSGS  
MAVHAEAFSNKLDPEYGSYMGEDSEDDNIWVSLDIMPTPLSPARQQYITDTSSNYLADKLLQ  
VTENLDFDNALIDMVGDTNSIFNGGSKLRSLIQDCMWNAGICETDKKNLVNTNVSAFDTPCATP  
PRAEFISTSDCVDPIAVFPYTLSDQGGQQQFVEAQSDSEEEIDVVTVEKPNKRKLSIELPQQHKVTE  
DLQSPTKRAKSPQISTKGKEACSPKGGSLVQKPDIDNDVKRATHNVLERKRRNDLRYSFQTLRDQIP  
DLEDNERAPKVNILKSTYIKFLKEEESKLISMKETERERRKALLAKIDILKSKRN

**Number of amino acids:** 580

**Molecular weight:** 65.415

**Theoretical pI:** 5.55

## A. Appendix

**Table A2.3: Genetic distances of Myc and Max proteins and their conserved domains between human, chicken, *Hydra* and *Trichoplax*.** Genetic distances were calculated with Geneious v8.1.7. Sequences from Homo sapiens (Hs), Gallus gallus (Gg), Hydra vulgaris (Hv) and Trichoplax adhaerens (Ta) were obtained from NCBI. GenBank accession nos.: Hs c-Myc: NP\_002458.2, Gg Myc: NP\_001026123.1, Hv Myc1: GQ856263.1, Ta taMyc: XP\_002113957; Hs Max: NP\_002373.3, Gg Max: P52162.1, Hv Max: ACX32069.1, Ta taMax: XP\_002107861

	HsMyc	GgMyc	HvMyc	TaMyc
<b>Myc full-length</b>				
HsMyc				
GgMyc	63.38%			
HvMyc	23.89%	20.0%		
TaMyc	26.06%	27.73%	18.36%	
<b>Myc MBI</b>				
HsMyc				
GgMyc	100%			
HvMyc	35.00%	35.00%		
TaMyc	50.00%	50.00%	20.00%	
<b>Myc MBII</b>				
HsMyc				
GgMyc	100%			
HvMyc	41.18%	41.18%		
TaMyc	35.29%	35.29%	29.41%	
<b>Myc MBIIIa</b>				
HsMyc				
GgMyc	100%			
HvMyc	33.33%	33.33%		
TaMyc	66.67%	66.67%	16.67%	
<b>Myc MBIIIb</b>				
HsMyc				
GgMyc	46.15%			
HvMyc	38.46%	30.77%		
TaMyc	87.50%	62.50%	37.50%	
<b>Myc MBIV</b>				
HsMyc				
GgMyc	77.27%			
HvMyc	18.18%	13.64%		
TaMyc	25.00%	25.00%	10.00%	
<b>Myc bHLHZ</b>				
HsMyc				
GgMyc	81.18%			
HvMyc	46.43%	39.29%		
TaMyc	56.47%	54.12%	41.67%	
<b>Max full-length</b>				
HsMyc				
GgMyc	95.63%			
HvMyc	50.00%	49.43%		
TaMyc	43.53%	44.71%	43.18%	
<b>Max bHLHZ</b>				
HsMyc				
GgMyc	94.89%			
HvMyc	51.37%	50.68%		
TaMyc	47.48%	48.92%	43.45%	

## A. Appendix

**Table A2.4: Disorder probabilities of taMyc.**

The possibility of disorder for each amino acid of taMyc was calculated with PrDos. The residue number, amino acid, prediction and disorder probability are listed.

Resid. No.	aa	Pred.	Dis. Prob.	Resid. No.	aa	Pred.	Dis. Prob.	Resid. No.	aa	Pred.	Dis. Prob.
1	M	1	0.8923	71	D	-1	0.3276	141	D	-1	0.4751
2	A	1	0.9001	72	F	-1	0.3311	142	C	-1	0.4530
3	V	1	0.8617	73	D	-1	0.3289	143	V	-1	0.4218
4	H	1	0.9088	74	N	-1	0.3246	144	D	-1	0.3849
5	A	1	0.8641	75	A	-1	0.3125	145	P	-1	0.3539
6	E	1	0.8890	76	L	-1	0.3093	146	I	-1	0.3261
7	A	1	0.7563	77	I	-1	0.3028	147	A	-1	0.3166
8	F	1	0.7017	78	D	-1	0.2983	148	V	-1	0.3122
9	S	1	0.6301	79	M	-1	0.2988	149	F	-1	0.3175
10	N	1	0.5483	80	V	-1	0.3040	150	P	-1	0.3390
11	K	-1	0.4655	81	G	-1	0.3182	151	Y	-1	0.3779
12	L	-1	0.4178	82	D	-1	0.3317	152	T	-1	0.4310
13	D	-1	0.3915	83	T	-1	0.3431	153	L	-1	0.4881
14	F	-1	0.3656	84	N	-1	0.3579	154	S	1	0.5885
15	E	-1	0.3376	85	S	-1	0.3649	155	D	1	0.6720
16	P	-1	0.3148	86	I	-1	0.3676	156	Q	1	0.7333
17	Y	-1	0.3023	87	F	-1	0.3631	157	G	1	0.7799
18	G	-1	0.2987	88	N	-1	0.3582	158	Q	1	0.8176
19	S	-1	0.3102	89	G	-1	0.3441	159	Q	1	0.8412
20	Y	-1	0.3207	90	G	-1	0.3267	160	Q	1	0.8453
21	Y	-1	0.3214	91	S	-1	0.3011	161	F	1	0.8477
22	M	-1	0.3257	92	K	-1	0.2645	162	V	1	0.8424
23	G	-1	0.3278	93	L	-1	0.2255	163	E	1	0.8314
24	E	-1	0.3389	94	R	-1	0.1781	164	A	1	0.8213
25	D	-1	0.3461	95	S	-1	0.1366	165	Q	1	0.8045
26	S	-1	0.3362	96	S	-1	0.0976	166	S	1	0.7748
27	E	-1	0.3112	97	L	-1	0.0929	167	D	1	0.7345
28	D	-1	0.2854	98	I	-1	0.0855	168	S	1	0.6721
29	D	-1	0.2439	99	Q	-1	0.0835	169	E	1	0.6030
30	N	-1	0.1983	100	D	-1	0.0838	170	E	1	0.5388
31	I	-1	0.1611	101	C	-1	0.0912	171	E	-1	0.4583
32	W	-1	0.1273	102	M	-1	0.0994	172	I	-1	0.4106
33	S	-1	0.1073	103	W	-1	0.1461	173	D	-1	0.3795
34	C	-1	0.1025	104	N	-1	0.2026	174	V	-1	0.3614
35	L	-1	0.1056	105	A	-1	0.2644	175	V	-1	0.3594
36	D	-1	0.1253	106	G	-1	0.3212	176	T	-1	0.3739
37	I	-1	0.1506	107	I	-1	0.3734	177	V	-1	0.3876
38	M	-1	0.1748	108	C	-1	0.4075	178	E	-1	0.4095
39	P	-1	0.2016	109	E	-1	0.4345	179	K	-1	0.4262
40	T	-1	0.2381	110	T	-1	0.4511	180	P	-1	0.4367
41	P	-1	0.2602	111	D	-1	0.4556	181	N	-1	0.4515
42	P	-1	0.2902	112	K	-1	0.4596	182	K	-1	0.4642
43	L	-1	0.3282	113	K	-1	0.4740	183	R	-1	0.4651
44	S	-1	0.3713	114	N	-1	0.4830	184	K	-1	0.4666
45	P	-1	0.4137	115	L	-1	0.4858	185	L	-1	0.4773
46	A	-1	0.4579	116	V	1	0.5283	186	S	1	0.5108
47	R	1	0.5115	117	N	1	0.5713	187	S	1	0.5341
48	Q	1	0.5489	118	T	1	0.6111	188	I	1	0.5553
49	Q	1	0.5636	119	N	1	0.6468	189	E	1	0.5786
50	Y	1	0.5697	120	V	1	0.6718	190	L	1	0.6150
51	I	1	0.5840	121	S	1	0.6985	191	P	1	0.6404
52	T	1	0.6009	122	A	1	0.7078	192	Q	1	0.6646
53	D	1	0.6060	123	F	1	0.7122	193	Q	1	0.7006
54	T	1	0.6079	124	D	1	0.7198	194	H	1	0.7272
55	S	1	0.6151	125	T	1	0.7149	195	K	1	0.7483
56	S	1	0.6125	126	P	1	0.7002	196	V	1	0.7756
57	N	1	0.6053	127	C	1	0.6823	197	T	1	0.8087
58	Y	1	0.5945	128	A	1	0.6711	198	E	1	0.8429
59	L	1	0.5576	129	T	1	0.6709	199	D	1	0.8757
60	A	1	0.5100	130	P	1	0.6751	200	L	1	0.9087
61	D	-1	0.4457	131	P	1	0.6689	201	Q	1	0.9079
62	K	-1	0.4072	132	R	1	0.6594	202	S	1	0.9130
63	L	-1	0.3737	133	A	1	0.6559	203	P	1	0.9144
64	L	-1	0.3462	134	E	1	0.6390	204	T	1	0.9132
65	Q	-1	0.3236	135	E	1	0.6377	205	K	1	0.9145
66	V	-1	0.3100	136	F	1	0.6331	206	R	1	0.9148
67	T	-1	0.3060	137	I	1	0.6138	207	A	1	0.9158
68	E	-1	0.3035	138	S	1	0.5854	208	K	1	0.9168
69	N	-1	0.3127	139	T	1	0.5534	209	S	1	0.9190
70	L	-1	0.3233	140	S	1	0.5234	210	P	1	0.9212

## A. Appendix

Resid. No.	aa.	Pred.	Dis. Prob.	Resid. No.	aa.	Pred.	Dis. Prob.
211	Q	1	0.9247	281	S	-1	0.1209
212	I	1	0.9274	282	T	-1	0.1438
213	S	1	0.9297	283	E	-1	0.1606
214	T	1	0.9300	284	Y	-1	0.1750
215	K	1	0.9248	285	I	-1	0.1882
216	G	1	0.9195	286	K	-1	0.2097
217	K	1	0.9179	287	F	-1	0.2296
218	E	1	0.9142	288	L	-1	0.2539
219	A	1	0.9115	289	K	-1	0.2832
220	C	1	0.9110	290	E	-1	0.3155
221	S	1	0.9091	291	E	-1	0.3410
222	P	1	0.9077	292	E	-1	0.3666
223	K	1	0.9070	293	S	-1	0.3827
224	G	1	0.9043	294	K	-1	0.3834
225	G	1	0.9021	295	L	-1	0.3825
226	L	1	0.8938	296	I	-1	0.3807
227	S	1	0.8509	297	S	-1	0.3862
228	V	1	0.8247	298	M	-1	0.3921
229	K	1	0.8015	299	K	-1	0.3958
230	P	1	0.7713	300	E	-1	0.4014
231	D	1	0.7473	301	T	-1	0.4002
232	I	1	0.7253	302	E	-1	0.3905
233	D	1	0.7009	303	R	-1	0.3695
234	N	1	0.6818	304	E	-1	0.3556
235	D	1	0.6476	305	R	-1	0.3425
236	V	1	0.6114	306	R	-1	0.3261
237	K	1	0.5739	307	K	-1	0.3212
238	R	1	0.5179	308	A	-1	0.3227
239	A	-1	0.4512	309	L	-1	0.3403
240	T	-1	0.4195	310	L	-1	0.3604
241	H	-1	0.3847	311	A	-1	0.3984
242	N	-1	0.3461	312	K	-1	0.4452
243	V	-1	0.3188	313	I	1	0.5164
244	L	-1	0.3059	314	D	1	0.5846
245	E	-1	0.2998	315	I	1	0.6658
246	R	-1	0.2979	316	L	1	0.7758
247	K	-1	0.2981	317	K	1	0.8391
248	R	-1	0.3170	318	S	1	0.9024
249	R	-1	0.3317	319	K	1	0.9243
250	N	-1	0.3413	320	R	1	0.9497
251	D	-1	0.3403	321	N	1	0.9497
252	L	-1	0.3386				
253	R	-1	0.3173				
254	Y	-1	0.2855				
255	S	-1	0.2610				
256	F	-1	0.2364				
257	Q	-1	0.2107				
258	T	-1	0.1895				
259	L	-1	0.1737				
260	R	-1	0.1728				
261	D	-1	0.1734				
262	Q	-1	0.1943				
263	I	-1	0.2173				
264	P	-1	0.2430				
265	D	-1	0.2697				
266	L	-1	0.3005				
267	E	-1	0.3268				
268	D	-1	0.3342				
269	N	-1	0.3264				
270	E	-1	0.3029				
271	R	-1	0.2648				
272	A	-1	0.2189				
273	P	-1	0.1658				
274	K	-1	0.1232				
275	V	-1	0.0986				
276	N	-1	0.0912				
277	I	-1	0.0896				
278	L	-1	0.0923				
279	K	-1	0.0958				
280	K	-1	0.0940				

## A. Appendix

**Table A2.5: Disorder probabilities of 6His-YFP-taMyc.**

The possibility of disorder for each amino acid of 6His-YFP-taMyc was calculated with PrDos.

The residue number, amino acid, prediction and disorder probability are listed.

Resid. No.	aa	Pred.	Dis. Prob.	Resid. No.	aa	Pred.	Dis. Prob.	Resid. No.	aa	Pred.	Dis. Prob.
1	M	1	0.9121	71	P	-1	0.0987	141	E	-1	0.2111
2	A	1	0.9103	72	V	-1	0.0928	142	L	-1	0.2020
3	C	1	0.8506	73	P	-1	0.0883	143	K	-1	0.1981
4	T	1	0.8394	74	W	-1	0.0856	144	G	-1	0.2025
5	S	1	0.8255	75	P	-1	0.0857	145	I	-1	0.2130
6	H	1	0.8792	76	T	-1	0.0864	146	D	-1	0.2273
7	H	1	0.8601	77	L	-1	0.0874	147	F	-1	0.2487
8	H	1	0.8801	78	V	-1	0.0877	148	K	-1	0.2716
9	H	1	0.8858	79	T	-1	0.0906	149	E	-1	0.2973
10	H	1	0.8667	80	T	-1	0.0938	150	D	-1	0.3147
11	H	1	0.8342	81	F	-1	0.0981	151	G	-1	0.3385
12	H	1	0.8006	82	G	-1	0.0997	152	N	-1	0.3489
13	H	1	0.7652	83	Y	-1	0.0921	153	I	-1	0.3494
14	G	1	0.7295	84	G	-1	0.0913	154	L	-1	0.3430
15	P	1	0.6928	85	L	-1	0.0942	155	G	-1	0.3337
16	V	1	0.6691	86	Q	-1	0.1005	156	H	-1	0.3287
17	M	1	0.6495	87	C	-1	0.1071	157	K	-1	0.3250
18	V	1	0.6384	88	F	-1	0.1140	158	L	-1	0.3222
19	S	1	0.6299	89	A	-1	0.1295	159	E	-1	0.3292
20	K	1	0.6122	90	R	-1	0.1565	160	Y	-1	0.3344
21	G	1	0.5639	91	Y	-1	0.1879	161	N	-1	0.3438
22	E	-1	0.4889	92	P	-1	0.2162	162	Y	-1	0.3456
23	E	-1	0.4450	93	D	-1	0.2505	163	N	-1	0.3561
24	L	-1	0.4043	94	H	-1	0.2686	164	S	-1	0.3529
25	F	-1	0.3603	95	M	-1	0.2803	165	H	-1	0.3387
26	T	-1	0.3199	96	K	-1	0.2809	166	N	-1	0.3317
27	G	-1	0.2809	97	Q	-1	0.2908	167	V	-1	0.3233
28	V	-1	0.2487	98	H	-1	0.2990	168	Y	-1	0.3115
29	V	-1	0.2262	99	D	-1	0.2930	169	I	-1	0.3052
30	P	-1	0.2072	100	F	-1	0.2910	170	M	-1	0.3008
31	I	-1	0.1943	101	F	-1	0.2961	171	A	-1	0.2992
32	L	-1	0.1853	102	K	-1	0.3052	172	D	-1	0.3074
33	V	-1	0.1865	103	S	-1	0.3109	173	K	-1	0.3134
34	E	-1	0.1970	104	A	-1	0.3153	174	Q	-1	0.3191
35	L	-1	0.2150	105	M	-1	0.3127	175	K	-1	0.3219
36	D	-1	0.2379	106	P	-1	0.3117	176	N	-1	0.3136
37	G	-1	0.2607	107	E	-1	0.3052	177	G	-1	0.2940
38	D	-1	0.2795	108	G	-1	0.2890	178	I	-1	0.2764
39	V	-1	0.2863	109	Y	-1	0.2773	179	K	-1	0.2506
40	N	-1	0.2888	110	V	-1	0.2636	180	V	-1	0.2210
41	G	-1	0.2953	111	Q	-1	0.2394	181	N	-1	0.2105
42	H	-1	0.2955	112	E	-1	0.2233	182	F	-1	0.2094
43	K	-1	0.3067	113	R	-1	0.2112	183	K	-1	0.2095
44	F	-1	0.3236	114	T	-1	0.2069	184	I	-1	0.2289
45	S	-1	0.3473	115	I	-1	0.2141	185	R	-1	0.2471
46	V	-1	0.3748	116	F	-1	0.2299	186	H	-1	0.2755
47	S	-1	0.4037	117	F	-1	0.2531	187	N	-1	0.3052
48	G	-1	0.4300	118	K	-1	0.2882	188	I	-1	0.3345
49	E	-1	0.4516	119	D	-1	0.3157	189	E	-1	0.3570
50	G	-1	0.4681	120	D	-1	0.3326	190	D	-1	0.3704
51	E	-1	0.4635	121	G	-1	0.3455	191	G	-1	0.3728
52	G	-1	0.4472	122	N	-1	0.3419	192	S	-1	0.3688
53	D	-1	0.4363	123	Y	-1	0.3327	193	V	-1	0.3813
54	A	-1	0.4170	124	K	-1	0.3210	194	Q	-1	0.3838
55	T	-1	0.4098	125	T	-1	0.3049	195	L	-1	0.3788
56	Y	-1	0.3977	126	R	-1	0.2831	196	A	-1	0.3854
57	G	-1	0.3833	127	A	-1	0.2685	197	D	-1	0.3961
58	K	-1	0.3651	128	E	-1	0.2651	198	H	-1	0.4121
59	L	-1	0.3506	129	V	-1	0.2627	199	Y	-1	0.4353
60	T	-1	0.3343	130	K	-1	0.2547	200	Q	-1	0.4582
61	L	-1	0.3223	131	F	-1	0.2457	201	Q	-1	0.4772
62	K	-1	0.3105	132	E	-1	0.2389	202	N	-1	0.4794
63	F	-1	0.2930	133	G	-1	0.2364	203	T	-1	0.4850
64	I	-1	0.2735	134	D	-1	0.2315	204	P	-1	0.4808
65	C	-1	0.2613	135	T	-1	0.2303	205	I	-1	0.4816
66	T	-1	0.2348	136	L	-1	0.2297	206	G	-1	0.4602
67	T	-1	0.2126	137	V	-1	0.2250	207	D	-1	0.4245
68	G	-1	0.1834	138	N	-1	0.2152	208	G	-1	0.3882
69	K	-1	0.1492	139	R	-1	0.2180	209	P	-1	0.3472
70	L	-1	0.1127	140	I	-1	0.2145	210	V	-1	0.3033

## A. Appendix

Resid. No.	A. a.	Pred.	Dis. Prob.	Resid. No.	A. a.	Pred.	Dis. Prob.	Resid. No.	A. a.	Pred.	Dis. Prob.
211	L	-1	0.2680	281	M	-1	0.3467	351	K	-1	0.2578
212	L	-1	0.2333	282	G	-1	0.3494	352	L	-1	0.2299
213	P	-1	0.2088	283	E	-1	0.3601	353	R	-1	0.1950
214	D	-1	0.1988	284	D	-1	0.3742	354	S	-1	0.1677
215	N	-1	0.1971	285	S	-1	0.3869	355	S	-1	0.1449
216	H	-1	0.2042	286	E	-1	0.3868	356	L	-1	0.1256
217	Y	-1	0.2250	287	D	-1	0.3853	357	I	-1	0.1117
218	L	-1	0.2449	288	D	-1	0.3792	358	Q	-1	0.1154
219	S	-1	0.2621	289	N	-1	0.3720	359	D	-1	0.1215
220	Y	-1	0.2865	290	I	-1	0.3661	360	C	-1	0.1517
221	Q	-1	0.3046	291	W	-1	0.3608	361	M	-1	0.1880
222	S	-1	0.3266	292	S	-1	0.3592	362	W	-1	0.2237
223	A	-1	0.3535	293	C	-1	0.3559	363	N	-1	0.2649
224	L	-1	0.3819	294	L	-1	0.3548	364	A	-1	0.3074
225	S	-1	0.4114	295	D	-1	0.3576	365	G	-1	0.3487
226	K	-1	0.4368	296	I	-1	0.3675	366	I	-1	0.3913
227	D	-1	0.4514	297	M	-1	0.3788	367	C	-1	0.4195
228	P	-1	0.4593	298	P	-1	0.3870	368	E	-1	0.4459
229	N	-1	0.4636	299	T	-1	0.4082	369	T	-1	0.4625
230	E	-1	0.4592	300	P	-1	0.4263	370	D	-1	0.4693
231	K	-1	0.4495	301	P	-1	0.4566	371	K	-1	0.4739
232	R	-1	0.4333	302	L	1	0.5123	372	K	-1	0.4883
233	D	-1	0.4090	303	S	1	0.5605	373	N	1	0.5173
234	H	-1	0.3902	304	P	1	0.6063	374	L	1	0.5187
235	M	-1	0.3691	305	A	1	0.6475	375	V	1	0.5347
236	V	-1	0.3521	306	R	1	0.6800	376	N	1	0.5664
237	L	-1	0.3361	307	Q	1	0.7092	377	T	1	0.6010
238	L	-1	0.3267	308	Q	1	0.7224	378	N	1	0.6318
239	E	-1	0.3277	309	Y	1	0.7227	379	V	1	0.6522
240	F	-1	0.3340	310	I	1	0.7244	380	S	1	0.6740
241	V	-1	0.3438	311	T	1	0.7245	381	A	1	0.6787
242	T	-1	0.3629	312	D	1	0.7105	382	F	1	0.6817
243	A	-1	0.3815	313	T	1	0.6896	383	D	1	0.6873
244	A	-1	0.4033	314	S	1	0.6699	384	T	1	0.6867
245	G	-1	0.4294	315	S	1	0.6422	385	P	1	0.6795
246	I	-1	0.4567	316	N	1	0.6064	386	C	1	0.6734
247	T	-1	0.4815	317	Y	1	0.5684	387	A	1	0.6746
248	L	1	0.5297	318	L	1	0.5173	388	T	1	0.6852
249	G	1	0.5519	319	A	-1	0.4537	389	P	1	0.7013
250	M	1	0.5749	320	D	-1	0.4086	390	P	1	0.7073
251	D	1	0.5969	321	K	-1	0.3720	391	R	1	0.7032
252	E	1	0.6250	322	L	-1	0.3422	392	A	1	0.6961
253	L	1	0.6393	323	L	-1	0.3196	393	E	1	0.6772
254	Y	1	0.6533	324	Q	-1	0.2989	394	E	1	0.6664
255	S	1	0.6542	325	V	-1	0.2877	395	F	1	0.6517
256	G	1	0.6529	326	T	-1	0.2807	396	I	1	0.6214
257	S	1	0.6395	327	E	-1	0.2764	397	S	1	0.5840
258	G	1	0.6386	328	N	-1	0.2782	398	T	1	0.5463
259	S	1	0.6304	329	L	-1	0.2799	399	S	1	0.5134
260	M	1	0.6179	330	D	-1	0.2757	400	D	-1	0.4665
261	A	1	0.6039	331	F	-1	0.2697	401	C	-1	0.4447
262	V	1	0.5822	332	D	-1	0.2618	402	V	-1	0.4190
263	H	1	0.5636	333	N	-1	0.2561	403	D	-1	0.3861
264	A	1	0.5506	334	A	-1	0.2434	404	P	-1	0.3627
265	E	1	0.5296	335	L	-1	0.2443	405	I	-1	0.3479
266	A	-1	0.4845	336	I	-1	0.2435	406	A	-1	0.3461
267	F	-1	0.4647	337	D	-1	0.2472	407	V	-1	0.3538
268	S	-1	0.4449	338	M	-1	0.2572	408	F	-1	0.3681
269	N	-1	0.4291	339	V	-1	0.2749	409	P	-1	0.4019
270	K	-1	0.4272	340	G	-1	0.2956	410	Y	-1	0.4491
271	L	-1	0.4241	341	D	-1	0.3125	411	T	1	0.5363
272	D	-1	0.4324	342	T	-1	0.3243	412	L	1	0.6222
273	F	-1	0.4378	343	N	-1	0.3399	413	S	1	0.7166
274	E	-1	0.4346	344	S	-1	0.3457	414	D	1	0.8147
275	P	-1	0.4231	345	I	-1	0.3453	415	Q	1	0.8866
276	Y	-1	0.4111	346	F	-1	0.3378	416	G	1	0.9079
277	G	-1	0.3960	347	N	-1	0.3308	417	Q	1	0.9176
278	S	-1	0.3765	348	G	-1	0.3178	418	Q	1	0.9214
279	Y	-1	0.3611	349	G	-1	0.3019	419	Q	1	0.9216
280	Y	-1	0.3505	350	S	-1	0.2828	420	F	1	0.9201

## A. Appendix

Resid. No.	aa	Pred.	Dis. Prob.	Resid. No.	aa	Pred.	Dis. Prob.	Resid. No.	aa	Pred.	Dis. Prob.
421	V	1	0.9162	491	I	1	0.8046	561	E	1	0.5202
422	E	1	0.9102	492	D	1	0.7762	562	R	-1	0.4722
423	A	1	0.9038	493	N	1	0.7507	563	E	-1	0.4538
424	Q	1	0.8952	494	D	1	0.7147	564	R	-1	0.4402
425	S	1	0.8577	495	V	1	0.6804	565	R	-1	0.4295
426	D	1	0.8110	496	K	1	0.6387	566	K	-1	0.4305
427	S	1	0.7402	497	R	1	0.5971	567	A	-1	0.4347
428	E	1	0.6622	498	A	1	0.5450	568	L	-1	0.4543
429	E	1	0.5915	499	T	-1	0.4883	569	L	-1	0.4776
430	E	1	0.5173	500	H	-1	0.4653	570	A	1	0.5421
431	I	-1	0.4490	501	N	-1	0.4436	571	K	1	0.6003
432	D	-1	0.4143	502	V	-1	0.4243	572	I	1	0.6610
433	V	-1	0.3944	503	L	-1	0.4161	573	D	1	0.7216
434	V	-1	0.3917	504	E	-1	0.4168	574	I	1	0.7829
435	T	-1	0.4042	505	R	-1	0.4195	575	L	1	0.8647
436	V	-1	0.4201	506	K	-1	0.4249	576	K	1	0.9022
437	E	-1	0.4474	507	R	-1	0.4378	577	S	1	0.9192
438	K	-1	0.4713	508	R	-1	0.4474	578	K	1	0.9329
439	P	-1	0.4877	509	N	-1	0.4567	579	R	1	0.9481
440	N	1	0.5287	510	D	-1	0.4465	580	N	1	0.9474
441	K	1	0.5516	511	L	-1	0.4419				
442	R	1	0.5574	512	R	-1	0.4293				
443	K	1	0.5659	513	Y	-1	0.4089				
444	L	1	0.5822	514	S	-1	0.3868				
445	S	1	0.6032	515	F	-1	0.3699				
446	S	1	0.6223	516	Q	-1	0.3561				
447	I	1	0.6404	517	T	-1	0.3438				
448	E	1	0.6571	518	L	-1	0.3356				
449	L	1	0.6865	519	R	-1	0.3308				
450	P	1	0.6974	520	D	-1	0.3301				
451	Q	1	0.7045	521	Q	-1	0.3424				
452	Q	1	0.7134	522	I	-1	0.3539				
453	H	1	0.7197	523	P	-1	0.3694				
454	K	1	0.7173	524	D	-1	0.3854				
455	V	1	0.7242	525	L	-1	0.3998				
456	T	1	0.7374	526	E	-1	0.4067				
457	E	1	0.7539	527	D	-1	0.4056				
458	D	1	0.7652	528	N	-1	0.3978				
459	L	1	0.7841	529	E	-1	0.3764				
460	Q	1	0.8047	530	R	-1	0.3502				
461	S	1	0.8220	531	A	-1	0.3196				
462	P	1	0.8210	532	P	-1	0.2911				
463	T	1	0.8216	533	K	-1	0.2699				
464	K	1	0.8250	534	V	-1	0.2480				
465	R	1	0.8305	535	N	-1	0.2300				
466	A	1	0.8393	536	I	-1	0.2272				
467	K	1	0.8513	537	L	-1	0.2305				
468	S	1	0.8660	538	K	-1	0.2343				
469	P	1	0.8806	539	K	-1	0.2418				
470	Q	1	0.8953	540	S	-1	0.2575				
471	I	1	0.9081	541	T	-1	0.2658				
472	S	1	0.9024	542	E	-1	0.2772				
473	T	1	0.9054	543	Y	-1	0.2857				
474	K	1	0.9023	544	I	-1	0.2958				
475	G	1	0.9080	545	K	-1	0.3114				
476	K	1	0.9038	546	F	-1	0.3288				
477	E	1	0.8940	547	L	-1	0.3519				
478	A	1	0.8915	548	K	-1	0.3775				
479	C	1	0.8984	549	E	-1	0.4076				
480	S	1	0.9004	550	E	-1	0.4309				
481	P	1	0.9068	551	E	-1	0.4540				
482	K	1	0.9010	552	S	-1	0.4742				
483	G	1	0.9027	553	K	-1	0.4801				
484	G	1	0.9051	554	L	-1	0.4884				
485	L	1	0.9061	555	I	1	0.5100				
486	S	1	0.9099	556	S	1	0.5195				
487	V	1	0.8939	557	M	1	0.5276				
488	K	1	0.8765	558	K	1	0.5311				
489	P	1	0.8508	559	E	1	0.5355				
490	D	1	0.8297	560	T	1	0.5314				

## A. Appendix

**Table A2.6: Disorder probabilities of taMax.**

The possibility of disorder for each amino acid of taMax was calculated with PrDos. The residue number, amino acid, prediction and disorder probability are listed.

Resid. No.	aa	Pred.	Dis. Prob.	Resid. No.	aa	Pred.	Dis. Prob.	Resid. No.	aa	Pred.	Dis. Prob.
1	M	1	0.9234	71	I	-1	0.2097	141	R	1	0.7928
2	S	1	0.9209	72	L	-1	0.1830	142	N	1	0.7970
3	D	1	0.9293	73	N	-1	0.1628	143	K	1	0.7971
4	E	1	0.9047	74	K	-1	0.1486	144	A	1	0.8099
5	D	1	0.8551	75	A	-1	0.1475	145	K	1	0.8205
6	K	1	0.7856	76	T	-1	0.1452	146	R	1	0.8265
7	Y	1	0.7565	77	D	-1	0.1556	147	E	1	0.8341
8	L	1	0.7343	78	Y	-1	0.1704	148	L	1	0.8388
9	D	1	0.7159	79	I	-1	0.1910	149	Q	1	0.8470
10	V	1	0.7155	80	Q	-1	0.2170	150	S	1	0.8604
11	D	1	0.7180	81	F	-1	0.2492	151	D	1	0.8822
12	I	1	0.7253	82	M	-1	0.2859	152	G	1	0.9052
13	D	1	0.7369	83	K	-1	0.3235	153	N	1	0.9049
14	S	1	0.7570	84	Q	-1	0.3661	154	D	1	0.9111
15	D	1	0.7659	85	K	-1	0.4013	155	E	1	0.9154
16	D	1	0.7834	86	N	-1	0.4287	156	Q	1	0.9202
17	N	1	0.8005	87	Q	-1	0.4488	157	K	1	0.9228
18	G	1	0.8184	88	N	-1	0.4469	158	T	1	0.9235
19	D	1	0.8390	89	H	-1	0.4473	159	D	1	0.9227
20	T	1	0.8697	90	Q	-1	0.4426	160	T	1	0.9205
21	D	1	0.8894	91	S	-1	0.4374	161	K	1	0.9244
22	K	1	0.9029	92	D	-1	0.4254	162	K	1	0.9209
23	S	1	0.9058	93	I	-1	0.4130	163	V	1	0.9177
24	T	1	0.9022	94	E	-1	0.4045	164	K	1	0.9222
25	S	1	0.8871	95	D	-1	0.3961	165	A	1	0.9304
26	G	1	0.8636	96	I	-1	0.3938	166	E	1	0.9309
27	L	1	0.8224	97	R	-1	0.3902				
28	T	1	0.7866	98	K	-1	0.3840				
29	Q	1	0.7373	99	E	-1	0.3806				
30	A	1	0.6863	100	N	-1	0.3643				
31	D	1	0.6376	101	Y	-1	0.3540				
32	K	1	0.5946	102	Q	-1	0.3431				
33	R	1	0.5517	103	L	-1	0.3294				
34	A	-1	0.4823	104	E	-1	0.3129				
35	H	-1	0.4477	105	L	-1	0.3047				
36	H	-1	0.4127	106	Q	-1	0.3102				
37	N	-1	0.3728	107	L	-1	0.3167				
38	A	-1	0.3390	108	K	-1	0.3291				
39	L	-1	0.3155	109	T	-1	0.3577				
40	E	-1	0.2950	110	L	-1	0.3879				
41	R	-1	0.2872	111	E	-1	0.4244				
42	K	-1	0.2925	112	R	-1	0.4588				
43	R	-1	0.3049	113	T	1	0.5146				
44	R	-1	0.3158	114	R	1	0.5500				
45	D	-1	0.3103	115	N	1	0.5799				
46	H	-1	0.3039	116	N	1	0.6135				
47	I	-1	0.2869	117	L	1	0.6392				
48	K	-1	0.2640	118	T	1	0.6668				
49	D	-1	0.2381	119	G	1	0.6895				
50	C	-1	0.2189	120	T	1	0.7145				
51	F	-1	0.2016	121	A	1	0.7368				
52	F	-1	0.1827	122	T	1	0.7551				
53	G	-1	0.1814	123	S	1	0.7715				
54	L	-1	0.1867	124	E	1	0.7882				
55	R	-1	0.1890	125	N	1	0.7923				
56	D	-1	0.1953	126	I	1	0.7894				
57	S	-1	0.2032	127	D	1	0.7821				
58	V	-1	0.2279	128	S	1	0.7730				
59	P	-1	0.2519	129	S	1	0.7586				
60	T	-1	0.2806	130	T	1	0.7568				
61	L	-1	0.3096	131	T	1	0.7565				
62	Q	-1	0.3354	132	T	1	0.7639				
63	G	-1	0.3531	133	T	1	0.7726				
64	E	-1	0.3631	134	T	1	0.7855				
65	K	-1	0.3657	135	N	1	0.7930				
66	A	-1	0.3559	136	S	1	0.8045				
67	S	-1	0.3264	137	G	1	0.8114				
68	R	-1	0.2950	138	R	1	0.8086				
69	A	-1	0.2630	139	T	1	0.8037				
70	Q	-1	0.2344	140	T	1	0.7964				



## A. Appendix

**Table A2.7: Disorder probabilities of 6His-taMax.**

The possibility of disorder for each amino acid of 6His-taMyc was calculated with PrDos. The residue number, amino acid, prediction and disorder probability are listed.

Resid. No.	aa	Pred.	Dis. Prob.	Resid. No.	aa	Pred.	Dis. Prob.	Resid. No.	aa	Pred.	Dis. Prob.
1	M	1	0.9599	71	V	-1	0.2188	141	S	1	0.7745
2	G	1	0.9553	72	P	-1	0.2442	142	S	1	0.7601
3	S	1	0.9466	73	T	-1	0.2772	143	T	1	0.7564
4	S	1	0.9542	74	L	-1	0.3076	144	T	1	0.7573
5	H	1	0.9530	75	Q	-1	0.3318	145	T	1	0.7656
6	H	1	0.9633	76	G	-1	0.3472	146	T	1	0.7762
7	H	1	0.9538	77	E	-1	0.3555	147	T	1	0.7909
8	H	1	0.9555	78	K	-1	0.3553	148	N	1	0.8004
9	H	1	0.9539	79	A	-1	0.3431	149	S	1	0.8131
10	H	1	0.9473	80	S	-1	0.3109	150	G	1	0.8206
11	S	1	0.9403	81	R	-1	0.2768	151	R	1	0.8185
12	Q	1	0.9331	82	A	-1	0.2431	152	T	1	0.8138
13	D	1	0.9263	83	Q	-1	0.2154	153	T	1	0.8086
14	M	1	0.9174	84	I	-1	0.1938	154	R	1	0.8043
15	S	1	0.9064	85	L	-1	0.1745	155	N	1	0.8082
16	D	1	0.8807	86	N	-1	0.1629	156	K	1	0.8085
17	E	1	0.8308	87	K	-1	0.1590	157	A	1	0.8204
18	D	1	0.7714	88	A	-1	0.1680	158	K	1	0.8315
19	K	1	0.7213	89	T	-1	0.1741	159	R	1	0.8384
20	Y	1	0.6775	90	D	-1	0.1911	160	E	1	0.8447
21	L	1	0.6329	91	Y	-1	0.2111	161	L	1	0.8481
22	D	1	0.6032	92	I	-1	0.2326	162	Q	1	0.8546
23	V	1	0.5993	93	Q	-1	0.2550	163	S	1	0.8680
24	D	1	0.6134	94	F	-1	0.2814	164	D	1	0.8885
25	I	1	0.6367	95	M	-1	0.3100	165	G	1	0.9099
26	D	1	0.6721	96	K	-1	0.3407	166	N	1	0.9055
27	S	1	0.7126	97	Q	-1	0.3790	167	D	1	0.9113
28	D	1	0.7450	98	K	-1	0.4104	168	E	1	0.9146
29	D	1	0.7837	99	N	-1	0.4328	169	Q	1	0.9188
30	N	1	0.8128	100	Q	-1	0.4470	170	K	1	0.9210
31	G	1	0.8369	101	N	-1	0.4404	171	T	1	0.9217
32	D	1	0.8462	102	H	-1	0.4374	172	D	1	0.9204
33	T	1	0.8558	103	Q	-1	0.4306	173	T	1	0.9175
34	D	1	0.8677	104	S	-1	0.4232	174	K	1	0.9216
35	K	1	0.8739	105	D	-1	0.4101	175	K	1	0.9169
36	S	1	0.8692	106	I	-1	0.3980	176	V	1	0.9147
37	T	1	0.8580	107	E	-1	0.3916	177	K	1	0.9178
38	S	1	0.8382	108	D	-1	0.3880	178	A	1	0.9255
39	G	1	0.8113	109	I	-1	0.3899	179	E	1	0.9266
40	L	1	0.7715	110	R	-1	0.3884				
41	T	1	0.7373	111	K	-1	0.3826				
42	Q	1	0.6901	112	E	-1	0.3801				
43	A	1	0.6427	113	N	-1	0.3653				
44	D	1	0.5979	114	Y	-1	0.3563				
45	K	1	0.5563	115	Q	-1	0.3464				
46	R	1	0.5162	116	L	-1	0.3345				
47	A	-1	0.4571	117	E	-1	0.3206				
48	H	-1	0.4237	118	L	-1	0.3165				
49	H	-1	0.3897	119	Q	-1	0.3265				
50	N	-1	0.3511	120	L	-1	0.3379				
51	A	-1	0.3201	121	K	-1	0.3552				
52	L	-1	0.2973	122	T	-1	0.3878				
53	E	-1	0.2756	123	L	-1	0.4212				
54	R	-1	0.2685	124	E	-1	0.4596				
55	K	-1	0.2749	125	R	1	0.5153				
56	R	-1	0.2875	126	T	1	0.5592				
57	R	-1	0.2994	127	R	1	0.5921				
58	D	-1	0.2971	128	N	1	0.6180				
59	H	-1	0.2913	129	N	1	0.6475				
60	I	-1	0.2742	130	L	1	0.6699				
61	K	-1	0.2531	131	T	1	0.6922				
62	D	-1	0.2294	132	G	1	0.7117				
63	C	-1	0.2104	133	T	1	0.7340				
64	F	-1	0.1909	134	A	1	0.7530				
65	F	-1	0.1711	135	T	1	0.7674				
66	G	-1	0.1699	136	S	1	0.7811				
67	L	-1	0.1750	137	E	1	0.7952				
68	R	-1	0.1771	138	N	1	0.7983				
69	D	-1	0.1851	139	I	1	0.7938				
70	S	-1	0.1939	140	D	1	0.7829				

Raw data on microscale thermophoresis and analytical ultracentrifugation are provided in the digital appendix.

# Curriculum Vitae

Sarah Rolfes, M.Sc.

Am Graswege 27, 30169 Hannover, Germany, born 14<sup>th</sup> October 1987 in Vechta, Germany

## Education

since 03/2013	PhD student, Leibniz University Hannover, thesis title: 'Apoptosis and cell cycle regulation in a basal model system – Insights from the placozoan <i>Trichoplax adhaerens</i> '
10/2010 – 11/2012	M.Sc. in Animal Biology and Biomedical Sciences, University of Veterinary Medicine Hannover, thesis title: 'Mitochondrial genome analysis and functional studies on the p53 gene in the Placozoa',
10/2007 – 09/2010	B.Sc. in Biology, TU Braunschweig, thesis title: Tetrapyrrolbiosynthese in methanogenen Archaea: Reinigung und Charakterisierung der SAM-abhängigen Uroporphyrinogen III-Methyltransferase und der Precorrin-2-Dehydrogenase aus <i>Methanosarcina barkeri</i> ,
06/2007	General qualification of university entrance (Abitur), Liebfrauenschule Vechta

## Research Experiences and Field Work

01 – 04/2017	Research stay at UF Gainesville, Florida, USA, Prof. Dr. Andrew Berglund
09/2016	Research stay at UF Gainesville, Florida, USA, Prof. Dr. Andrew Berglund
02 – 05/2015	Field work in Australia, Madagascar and Seychelles
01 – 04/2014	Research stay at Duke University and NESCent, Durham, North Carolina, USA and the American Museum of Natural History, New York City, New York, USA
since 03/2013	PhD thesis, ITZ Ecology & Evolution, University of Veterinary Medicine Hannover, Prof. Dr. Bernd Schierwater
02 – 11/2012	Master thesis, ITZ Ecology & Evolution, University of Veterinary Medicine Hannover, Prof. Dr. Bernd Schierwater
04 – 06/2010	Bachelor thesis, Institute for Microbiology, TU Braunschweig, Prof. Dr. Gunhild Layer

## Teaching Experiences

Since 06/2013	Field assistant: 'Crau – Camargue – Mittelmeer', France, led by ITZ Ecology & Evolution, University of Veterinary Medicine Hannover
04/2013	Teaching assistant: Volker Schmid Training Course 'Experimental Developmental Biology of Marine Invertebrates', Station Biologique de Roscoff, France
Since 03/2013	Supervision of Bachelor- and Master theses, ITZ Ecology & Evolution, University of Veterinary Medicine Hannover
Since 12/2012	Supervision of practical courses: Molecular ecology and evolution, ITZ Ecology & Evolution, University of Veterinary Medicine Hannover

## Grants and Fellowships

01 – 06/2019	PhD Completion Grant, Equal Opportunities Office, Leibniz University Hannover
01 – 04/2017	Scholarship for a Research Stay Abroad, Graduate Academy, Leibniz University Hannover
06/2016	Conference Travel Grant, Graduate Academy, Leibniz University Hannover
01 – 04/2014	Short-term Visitor Fellowship NESCent, Duke University, Durham, NC, USA
06/2013 – 12/2018	Otto Bütschli PhD Fellowship, University of Veterinary Medicine Hannover

## Conferences

**Rolfes S.**, Tsiavaliaris G., Schierwater B. (2017). Evolution of the Myc/Max transcription factor network: Insights from *Trichoplax adhaerens*. Oral presentation at the International Workshop 'The diversification of early emerging metazoans: a window into animal evolution?', Tutzing, Germany.

**Rolfes S.**, Tsiavaliaris G., Schierwater B. (2016). Evolution of the Myc/Max transcription factor network: Insights from *Trichoplax adhaerens*. Oral presentation at the Evolution Meeting, Austin, TX, USA.

**Rolfes S.**, v.d.Chevalerie K., Schierwater B. (2015). Something to die for – Inhibition of the p53-Mdm2 interaction increases programmed cell death in the placozoan *Trichoplax adhaerens*. Oral presentation at the 108. Jahrestagung der Deutschen Zoologischen Gesellschaft, Graz, Austria.

## List of Publications

Storbeck, S., **Rolfes, S.**, Raux-Derry, E., Warren, M.J., Jahn, D., Layer, G. (2010). A novel pathway for the biosynthesis of heme in Archaea: genome-based bioinformatic predictions and experimental evidence, *Archaea*. 2010:175050

von der Chevallerie, K., **Rolfes, S.**, Schierwater, B. (2014). Inhibitors of the p53-Mdm2 interaction increase programmed cell death and produce abnormal phenotypes in the placozoon *Trichoplax adhaerens* (F.E. Schulze). *Dev Genes Evol* 224:79-85

Osigus, H.J., **Rolfes, S.**, Herzog, R., Kamm, K., Schierwater, B. (2019). *Polyplacotoma mediterranea* gen. nov., spec. nov. is a remarkably different placozoan species. *Curr Biol*. 29(5):R148-R149

Miyazawa, H., Osigus, H.J., **Rolfes, S.**, Kamm, K., Schierwater, B., Nakano, H. (in revision, *Genome Biology and Evolution*). Mitochondrial genome evolution of placozoans: gene rearrangements and repeat expansions.

## Acknowledgements

This thesis would not have been possible without the help and support of some people, which I very much appreciate and am grateful for.

First and foremost I would like to thank my supervisor Prof. Dr. Bernd Schierwater for giving me the opportunity to work on this exciting topic and for his guidance throughout the course of my thesis. He supported my scientific and personal growth by letting me gather experiences at international conferences, research stays abroad and field trips around the world.

I would further like to thank Prof. Dr. Dieter Steinhagen who kindly agreed to review this thesis, as well as Prof. Dr. Jutta Papenbrock for being part of the committee and chairing the disputation.

A special thanks goes to Rebecca Herzog. There would have been no better buddy to escaping angry baboons with, learn how to handle the 'mora mora' lifestyle but getting all work done before 8 am and feed ducks in (freezing) Central Park. For going through insanity of long lab nights and for your friendship during all the crazy ups and downs of life.

I am very grateful for my (former and present) colleagues and friends at the ITZ, with whom I have had a fantastic time and I deeply appreciate their help. Thanks to: Annkathrin Acktum, Nicole Bartkowiak, Nicole Bergjürgen, Dr. Tjard Bergmann, Jutta Bunnenberg, Dr. Sandra Damm, Felix David, Marco Dinter, Christiane Döhring, Dr. Wiebke Feindt, Kristin Fenske, PD Dr. Heike Hadrys, Sofia Haller, Dr. Eckhard Holtorf, Dr. Karolin Horn, Dr. Wolfgang Jakob, Marion Klein, Diana Knetsch, Nils Krause, Johannes Neumann, Ulrike Oberjatzas, Dr. Omid Paknia, Dr. Dasa Schleicherova, Björn Seegebarth, Moritz Schmidt, and Kathrin Wysocki.

I am especially thankful for the help from Dr. Kai Kamm and Dr. Haju Osigus. Es war mir eine Freude, wenn das Füllhorn eures Wissens auf mich herabregnete.

Arne Bielke, thank you for all your tireless help and the personal catering service.  
Verschoben bis zum Schluss!

Furthermore, I would like to thank Prof. Dr. Georgios Tsiavaliaris who kindly invited me to his lab and supported me during the protein characterization project.

Several members of the BPC helped me a lot and provided a pleasant atmosphere, thanks to present and past members of the AG Tsiavaliaris and AG Faix.

I have learned a lot through various international collaborations and research stays abroad. Therefore, I am thankful to Prof. Dr. Allen Rodrigo for inviting me to NESCent and Prof. Dr. Rob DeSalle for my short but fruitful and interesting stay at the AMNH. Thanks to Prof. Dr. Andy Berglund for inviting me to his lab at UF Gainesville and his encouraging scientific and financial support with the RNASeq experiments.

This thesis would not have been possible without the financial support from Prof. Dr. Bernd Schierwater and the University of Veterinary Medicine Hannover who provided me with an 'Otto Bütschli' scholarship. NESCent and the Graduate Academy of the Leibniz University Hannover endowed me with travel grants for research stays abroad and participation in international conferences. The Equal Opportunities Office of the Leibniz University Hannover further provided me with a PhD Completion Grant.

I am very grateful for my fantastic friends who were always supporting and patient and knew how to cheer me up.

Mein größter Dank gilt jedoch meiner Familie, meinen Brüdern Hanno und Lukas und ganze besonders meinen Eltern, Bärbel und Georg Rolfes. Ich danke euch von ganzem Herzen für eure Unterstützung und euer Verständnis. In guten und schweren Zeiten, wusste euch immer hinter mir und konnte mich auf euch verlassen. Danke!